Department of Health Science and Technology
Aalborg University
Fredrik Bajers Vej 7D2
DK-9220 Aalborg
Denmark

Title:
Linear model for deriving the posterior ECG leads V7-V12 in healthy subjects.

Project period:

01.09.2007-01.06.2008

Project group:

08gr1088h

Kartheeban Nagenthiraja

Supervisors:

Mads Peter Andersen

Johannes Struijk

Copies:

5

Synopsis

In this project we will developed a linear regression model to predict the posterior ECG lead V7-V12. A physiological interpretation of the regression coefficients is given. Furthermore we will evaluate different methods to obtain the regression coefficients and the precision of the point estimation.

Thirty-seven healthy persons without any history of heart diseases were included. In our investigation, we extended the standard 12-lead ECG with six posterior leads; three electrodes placed on the both side of the back. On each subject, 5 consecutive recordings of the 18-lead ECG were recorded.

In conclusion, we found the pooled method to be best performing, and segment wise estimation of the ECG signal improves the precision of the linear model further. Our results are promising in healthy subject, however it is difficult translate the results form this study to an assessment of the application of the model in AMI patients.

Preface

This report "*Linear model for deriving the posterior ECG leads V7-V12 in healthy subjects.*" is the result of the 10th semester project of Kartheeban Nagenthiraja at Department of Health Science and Technology at Aalborg University during the period 01.09.2007-01.06.2008. This documentation also includes a number of worksheets to document some the work that has been put into the project and the knowledge that forms the basis for these articles. The worksheets are independent documents and not supposed to be read in any particular order.

Matlab code as well as the report can be downloaded from the web:

www.hst.aau.dk/~knag03/Speciale

In this report following documents are enclosed:

- Linear model for deriving the posterior ECG leads V7-V12 in healthy subjects: Part1
- Linear model for deriving the posterior ECG leads V7-V12 in healthy subjects: Part 2
- Worksheets

Linear model for deriving the posterior ECG leads V7-V12 in healthy subjects: Part 1

Kartheeban Nagenthiraja

***Abstract*— In the present study, we develop a linear model to estimate the posterior ECG leads $V7$-$V12$ by means of the 8 independent ECG leads in healthy subjects.**

Thirty-seven healthy persons without any history of heart diseases were included. In our investigation, we extended the standard 12-lead ECG with six posterior leads; three electrodes placed on the both side of the back. On each subject, 5 consecutive recordings of the 18-lead ECG were recorded. The subjects were randomly divided into two groups; a training and a test group. The ECG recordings of the subjects in training group were merged to one large data set, and a regression model was determined. The model was validated by the ECG recordings in the test group.

The posterior leads $V7$-$V9$ were predominantly modeled by the electrical dipole in the horizontal lateral plane. Information of the electrical diploe in the horizontal anterior-posterior plane was attenuated in the regression model as a result of the transformation matrix and the intermediary steps of the best subset regression.

Modeling of the posterior leads $V10$-$V12$ by a linear regression model was possible in healthy subjects with acceptable accuracy by means of the standard 12-lead ECG. Likewise, the transformation of leads $V7$-$V9$, the information in the horizontal anterior-posterior plane, and in the vertical plane was also attenuated in the regression model for leads $V10$-$V12$.

The suppression of the information in the horizontal anterior-posterior plane in the regression model may question the models ability to transform possible information in the horizontal anterior-posterior recorded by the independent leads correctly to the posterior leads.

In conclusion the linear model developed in the present study on healthy subjects performed well on healthy subjects, but we expect this model yield a poor result when applied on patients with disturbed electrical pathways.

***Index Terms*— Regression matrix, minimum least square, dipole model, best subsets regression, 12-lead ECG**

I. Introduction

ST-elevation is one of the clinical findings of acute myocardial infarction (AMI) along with elevated blood troponin level and chest pain. ST-elevation does not appear in all AMI patients, despite elevated troponin level and chest pain, and these cases are termed non-STEMI. Appearance of ST-elevation highly depends on the location of the thrombus and the position of the ECG leads in relation to the area of ischemia. ST-elevation caused by occlusion of left circumflex artery (LCX) are under-represented compared to ST-elevation caused by occlusion of one of the two other main arteries; right coronary artery (RCA) and left anterior descending artery (LAD) [1].

Higher mortality rates have been reported among non-STEMI patients in proportion to STEMI patients [2]–[4], and this is a consequence of under-recognition and under-treatment of the non-STEMI patients [5].

Several studies have proposed an extension of the standard 12-lead ECG by three posterior leads [6], [7], to improve the sensitivity of diagnosis of non-STEMI patients. Evaluations of the standard 12-lead ECG versus 15-lead ECG have yielded a better sensitivity of diagnosing non-STEMI patients [8]–[12]. The 15-lead ECG is not a standard in health care system and the placement of the posterior leads in emergency situation may be impractical.

Mathematical models can be used to estimate the posterior ECG leads by means of the independent ECG leads. According to our literature review, only one publication exists concerning this field. In this study, they proposed a strategy to derive the posterior leads from the independent leads, for providing additional information in diagnosing AMI. The model was entirely based on healthy subjects, and they concluded the model to yield a satisfactory accuracy according to clinical criterions [13]. But they did not publish the regression matrix and their conclusions were mainly based on the output of the regression model and not based on the interpretation of the regression matrix. We consider these issues to be the main disadvantages of the study. Any considerations of how well their model will perform on non-healthy subjects e.g. patients with disturbance in the electrical pathways were not given either.

In this study, we develop a linear model to estimate the posterior ECG leads $V7$-$V12$ by means of the 8 independent ECG leads in healthy subjects. We publish the regression matrix and our conclusions are entirely based on interpretation of the regression matrix. We make a theoretical assessment of how well our model based on healthy subjects will perform on patients with AMI.

II. Methods & materials

A. Data acquisition

In this study ECG recordings from 37 healthy persons without any history of heart diseases were included. Twenty five subjects were males and 12 subjects were females. The healthy subjects were recruited from Institute of Health Science and Technology, Aalborg University and Aalborg Hospital.

In our investigation, we extended the standard 12-lead ECG with six posterior leads. Three electrodes were placed on both sides of the back. The 12 standard electrodes were placed according to existing standards [14] with the subject in supine position. The electrodes on the back were placed while the subjects were sitting, without support of the back.

	Training		Test		
Parameter	**Mean**	**SD**	**Mean**	**SD**	p**-Value**
Female	n = 6		n = 6		
Male	n = 13		n = 12		
Age	27.9 yr.	± 4.00	25.2 yr.	± 3.80	>0.05
Height	1.80 m	± 0.08	1.80 m	± 0.10	>0.05
Weight	77 kg	± 11.69	79 kg	± 16.49	>0.05
BMI	23.53 $\frac{kg}{m^2}$	± 2.40	24.17 $\frac{kg}{m^2}$	± 3.88	>0.05

TABLE I
SUMMARIZATION OF SUBJECTS CHARACTERISTICS

The posterior leads V_7-V_{12} were placed as follows; V_7: Left side of the back, over the posterior axillary line in same level as V_5. V_8: Left side of the back, over the midscapular line in same level as V_5. V_9: Left side of the back, half way between midscapular line and spine in same level as V_5. V_{10}: Right side of the back, over the posterior axillary line in same level as V_5. V_{11}: Right side of the back, over the midscapular line in same level as V_5. V_{12}: Right side of the back, half way between midscapular line and spine in same level as V_5).

All the recordings were performed with GE MAC 5000 (500 Hz sampling rate) with the subject in relaxing supine position and with a comfortable breath frequency. Five consecutive recordings of 10 seconds were acquired.

The data were converted to ascii format for further analysis. For each recording the ECG monitor provide a median beat of 1.2 sec duration.

B. Statistical model

In a linear regression of the standard leads to the posterior leads, the heart can be assumed as a dipole with a fixed location and variable orientation and magnitude. The surrounding tissue e.g. lungs, adipose tissue and bone together can be assumed as an infinite homogenous conductor [15].

$$y_j(t) = \beta_1 x_1(t) + \beta_2 x_2(t) + \beta_3 x_3(t) + \cdots + \beta_8 x_8(t) \quad (1)$$

where y_j is the vector of transformed posterior lead, and $j = 7, 8 \cdots, 12$. x_i is the independent leads, where $i = 1, 2 \cdots, 8$. β_i is the regression coefficients. For convenience the expression in 1 can be written in matrix notation

$$\mathbf{Y} = \mathbf{BX} \quad (2)$$

where matrix $\mathbf{Y}$ contains the posterior leads $V7$-$V12$. $\mathbf{B}$ is the regression coefficient matrix, and matrix $\mathbf{X}$ contains the independent leads. The coefficients of $\mathbf{B}$ are estimated by minimizing the error between the estimated output $\widehat{\mathbf{Y}}(n)$ and the recorded output $\mathbf{Y}(n)$, where n is the sample index.

$$min(\sum_{n=1}^{N}(\mathbf{Y}(n) - \widehat{\mathbf{Y}}(n))^2) \quad (3)$$

In expression 3 the intra-patient variation is neglected, and the data of subjects in the data base is assumed as a large data set [16].

The least square solution of the expression 2 is given by

$$\mathbf{B} = (\mathbf{X}'\mathbf{X})^{-1}\mathbf{X}'\mathbf{Y} \quad (4)$$

The coefficient of determination of the fit is given by

$$R^2 = 1 - \frac{SS_{error}}{SS_{total}} \quad (5)$$

where SS_{error} is the sums of squares of the difference between the estimated and the recorded signal, and SS_{total} is sums of squares of the difference between the recorded signal and the mean of the recorded signal.

C. Data analysis

The data analysis was performed in MATLAB (R2007a, The MathWorks, Inc.). The subjects in the data base were randomly divided into two groups; a training and a test group, respectively. The training group was used to develop the regression model and the test group was used to validate the regression model.The ECG recordings of all subjects in the training group were merged into one large data set and were considered as one data recording.

Prior to developing the regression model, we performed a pre-analysis of the ECG recordings of the training group. The pre-analysis contained an analysis of the correlation between the independent leads and an analysis of the correlation of the independent leads and the posterior leads.

The regression coefficients and the coefficients of determination (R^2) were calculated according to expression 4 and 5.

The stability of the regression coefficients were analyzed by step-wise adding more data to the model and determining the

	I	**II**	**V1**	**V2**	**V3**	**V4**	**V5**	**V6**
I	1							
II	0.7818	1						
V1	-0.4015	-0.5490	1					
V2	0.0264	-0.2589	0.8172	1				
V3	0.5752	0.2734	0.3863	0.7645	1			
V4	0.8755	0.7396	-0.2224	0.1610	0.7396	1		
V5	0.8845	0.9065	-0.5419	-0.2156	0.3808	0.8734	1	
V6	0.8380	0.9449	-0.6316	-0.3304	0.2331	0.7638	0.9718	1

TABLE II
CORRELATION COEFFICIENTS r OF THE INDEPENDENT LEADS

	β_I	β_{II}	β_{V1}	β_{V2}	β_{V3}	β_{V4}	β_{V5}	β_{V6}
V7	0.8004	0.9321	-0.7002	-0.4144	0.1362	0.6924	0.9338	0.9866
V8	0.7342	0.8952	-0.7568	-0.4988	0.0272	0.6072	0.8826	0.9567
V9	0.5287	0.7490	-0.8189	-0.6395	-0.2122	0.3715	0.7067	0.8231
V10	-0.6629	-0.4051	-0.2284	-0.5147	-0.7833	-0.7200	-0.5232	-0.3903
V11	-0.8485	-0.587	0.0360	-0.3439	-0.7496	-0.8363	-0.7140	-0.6099
V12	-0.8961	-0.5875	0.1595	-0.2484	-0.6878	-0.8292	-0.7419	-0.6488

TABLE III

CORRELATION COEFFICIENTS r OF THE INDEPENDENT LEADS AND THE DEPENDENT LEADS

regression coefficients for each step. In this particular analysis all subjects were included.

A best subset regression was performed to find the best subsets of independent leads which contribute with significant (p=0.01) amount of information in the regression model.

III. RESULTS

A. Characteristics of study group

In the training group 19 subjects were allocated; 6 females and 13 males. In the test group 18 subjects were allocated; 6 females and 12 males. The mean age in the training group was 28 years and the mean age in test group was 25 years (p>0.05). The mean height was equal in both group, while the mean weight was higher in test group then in the training group, 79 kg and 77 kg, respectively but not significantly (p>0.05). The higher mean weight in the test group is reflected in the body mass index (BMI), 24.17 kg/m^2 for the test group and 23.53 kg/m^2 for the training group (p>0.05), see table I.

B. Pre-analysis

In table II, the correlation coefficients of the independent leads are given. As expected, the neighboring precordial leads $V1$-$V6$ are well correlated ($r\approx$ 0.8), as well the limb leads I and II describing the horizontal lateral plane and the vertical plane respectively, are highly correlated (r>0.8) with the precordial leads $V5$ and $V6$.

In table III the correlation coefficients of the independent leads and the posterior leads are given. Leads $V7$ and $V8$ are highly correlated with lead II, $V5$ and $V6$. The posterior lead $V9$ is highly correlated with $V1$ and $V6$. Lead $V10$ is negatively correlated with all the independent leads, and the leads $V11$ and $V12$ are highly negatively correlated with leads I and $V4$. The correlation coefficients are depicted as bars in figure 1 for better graphical overview.

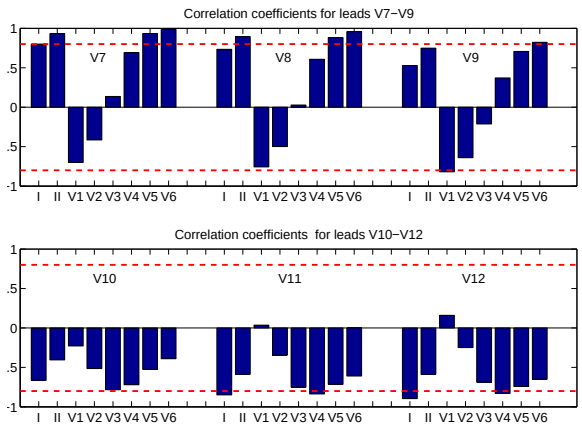

Fig. 1. Graphical presentation of the correlation coefficients of the independent leads and the dependent leads. The horizontal dashed red lines indicate r=0.8

C. Multiple regression model

Table IV shows the coefficients of the regression matrix for the multiple regression model. Each coefficients in the columns describes the weighting of the specific independent lead in the regression model to obtain the dependent leads (shown in the rows). To obtain the posterior leads $V7$-$V9$, the absolute value of the regression coefficients of leads $V5$ and $V6$ are of greatest magnitude. In determination of the posterior leads $V10$-$V12$, the absolute value of the regression coefficients of leads I, $V5$ and $V6$ are of greatest magnitude. The coefficients of the regression matrix are also plotted in figure 2 for better graphical overview.

The median coefficient of determination R^2 between the recorded and the estimated 6 dependent leads are given in table V. In column two and three the median and the interquartile

	I	**II**	**V1**	**V2**	**V3**	**V4**	**V5**	**V6**
V7	0.0580	0.0121	-0.0289	-0.0092	-0.0126	0.0344	-0.3500	1.0947
V8	0.0387	-0.0304	-0.0608	0.0123	-0.0755	0.1060	-0.5717	1.2764
V9	-0.0423	-0.1009	-0.0999	0.0271	-0.1008	0.1345	-0.7423	1.3453
V10	-0.2257	-0.0542	-0.0812	0.0139	-0.0647	0.0794	-0.4287	0.5339
V11	-0.2916	-0.0008	-0.0323	0.0046	-0.0469	0.0380	-0.2363	0.2661
V12	-0.3527	0.0582	0.0038	-0.0131	-0.0086	0.0061	-0.1355	0.1342

TABLE IV

REGRESSION MATRIX OF THE MULTIPLE REGRESSION MODEL

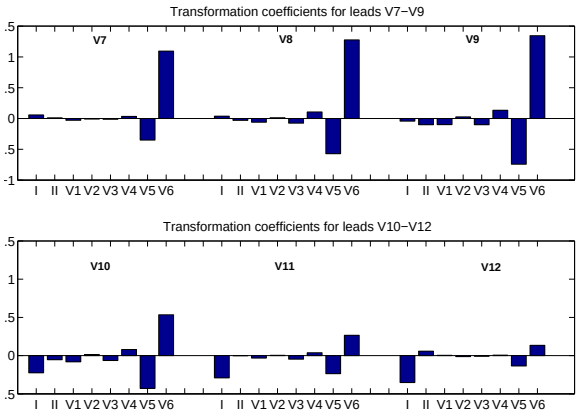

Fig. 2. Graphical presentation of the coefficients of regression matrix for multiple regression.

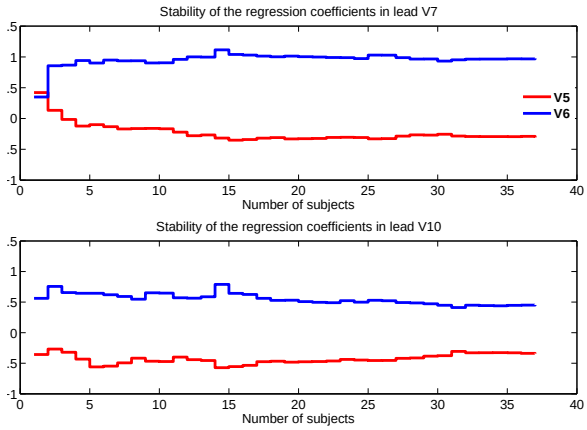

Fig. 3. The development of the regression coefficients of leads $V5$ and $V6$ for predicting leads $V7$ and $V10$.

range of R^2 for the training group are listed. In column four and five the same information is given for the test group. In both groups the highest R^2 is obtained for $V7$. R^2=0.98 for the training group and R^2=0.96 for the test group. R^2 is decreasing toward $V9$ in both group. For the leads $V10$-$V12$, R^2 is almost equal between the leads and also between the groups. The values given in the table are truncated values.

In figure 3 the development of the regression coefficients ($V5$ and $V6$) for the posterior leads $V7$ and $V10$ are given. The x-axis indicates the number of subject included to determine the particular regression coefficient. The subjects 1 to 19 is the subjects included in the training group and from 20 to 37 are the subjects from the test group. In the top row the development of the regression coefficients of the independent leads $V5$ (red) and $V6$ (blue) for regression model of lead $V7$ are depicted. The regression coefficients seem almost stable beyond subject number 15. In bottom row (lead $V10$) the regression coefficients converge beyond subject 19 and seem to become stable beyond subject 32. Only a limited range of the results form the analysis are given in figure 3.

The best subset regression method was performed on all posterior leads, and the summary of the best subset regression models is given in table VI. For lead $V7$ the best subset consist of leads $V1$, $V2$, $V3$ $V4$, $V5$ and $V6$. Addition of the limb leads did not yield a significant better model (p<0.01). For the leads $V8$, $V9$ and $V10$ the best subsets were II, $V1$, $V2$, $V3$, $V4$, $V5$, $V6$, where as lead I did not contribute significantly with more information to the model (p<0.01). The best subset for lead $V11$ was *II*, $V1$, $V3$, $V4$, $V5$, $V6$, adding leads I and $V2$ did not add significant more information (p<0.01). The best subset for lead $V12$ counted only four independent leads *II*, $V2$, $V5$, and $V6$ (p<0.01).

The graphical outcomes of applying the regression matrix, table IV on the independent leads are given in figure 4 and 5. Figure 4, shows cases of good modeling, where the R^2 for V7-V9 were $\approx$ 1 and for V10-V12 the R^2 were > 0.9. Figure 5, shows cases of poor modeling. For V7-V9 the R^2 were < 0.8 and for V10-V12 the R^2 were $\approx$ 0.

	Training		Test	
Lead	**Median**	**(Interq. range)**	**Median**	**(Interq. range)**
V7	0.98	(1.00-0.95)	0.96	(1.00-0.92)
V8	0.96	(0.99-0.92)	0.95	(1.00-0.87)
V9	0.95	(0.99-0.91)	0.92	(1.00-0.85)
V10	0.81	(0.90-0.71)	0.85	(0.96-0.73)
V11	0.82	(0.92-0.73)	0.86	(1.00-0.72)
V12	0.85	(0.93-0.77)	0.88	(0.98-0.78)

TABLE V

COEFFICIENTS OF DETERMINATION R^2 OF MULTIPLE REGRESSION MODEL

IV. DISCUSSION

Under-recognition and under-treatment of patients with posterior infarcts leads to higher mortality rates compared to other AMI patients. Several studies have reported better sensitivity by extension of the standard ECG leads with posterior leads. In this study, we developed a linear regression model to derive the posterior leads $V7$-$V12$ by means of the eight independent ECG leads. Our model is based on healthy males and females in the range of 21-37 year without any history of heart disorders.

Lead	**Best subset**	R^2	**F-stat**	**p-value**
V7	V1, V2, V3 V4,V5, V6	0.990	8.1	<0.01
V8	II, V1, V2, V3 V4, V5, V6	0.975	29.9	<0.01
V9	II, V1, V2, V3 V4, V5, V6	0.913	114.1	<0.01
V10	II, V1, V2, V3 V4, V5, V6	0.795	27.4	<0.01
V11	II, V1, V3, V4, V5, V6	0.862	164	<0.01
V12	II, V2, V5, V6	0.885	1661.4	<0.01

TABLE VI

SUMMARY OF BEST SUBSET REGRESSION

NOTE: THE CUT-OFF POINT FOR α=0.01 WITH NUMERATOR DEGREE OF FREEDOM OF ONE AND DENOMINATOR DEGREE OF FREEDOM OF ∞, $F_{1,\infty,0.01}$=6.63

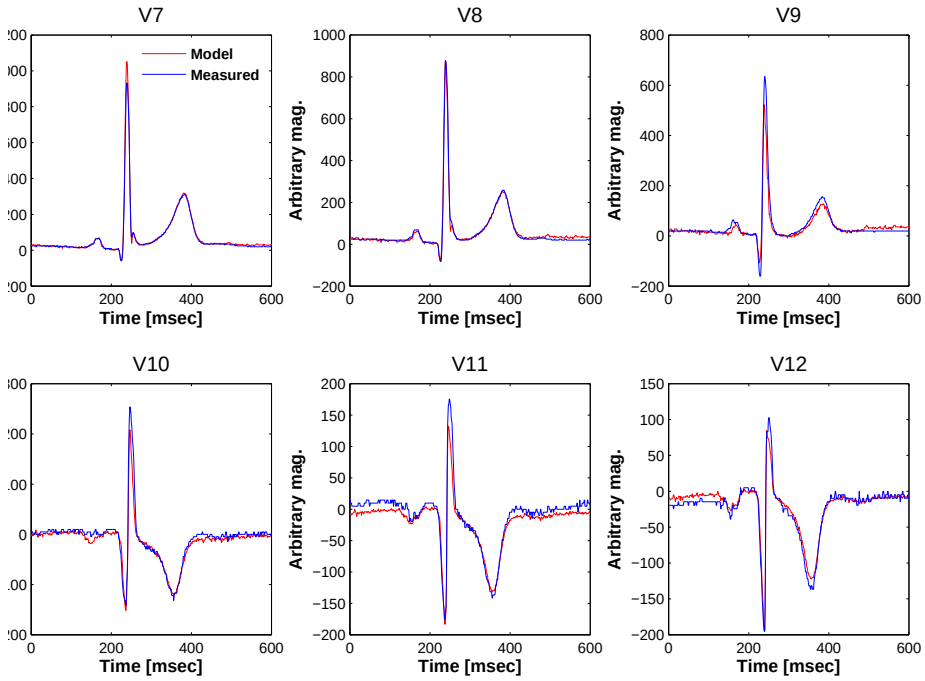

Fig. 4. Example of good modeling where the R^2 were > 0.9.

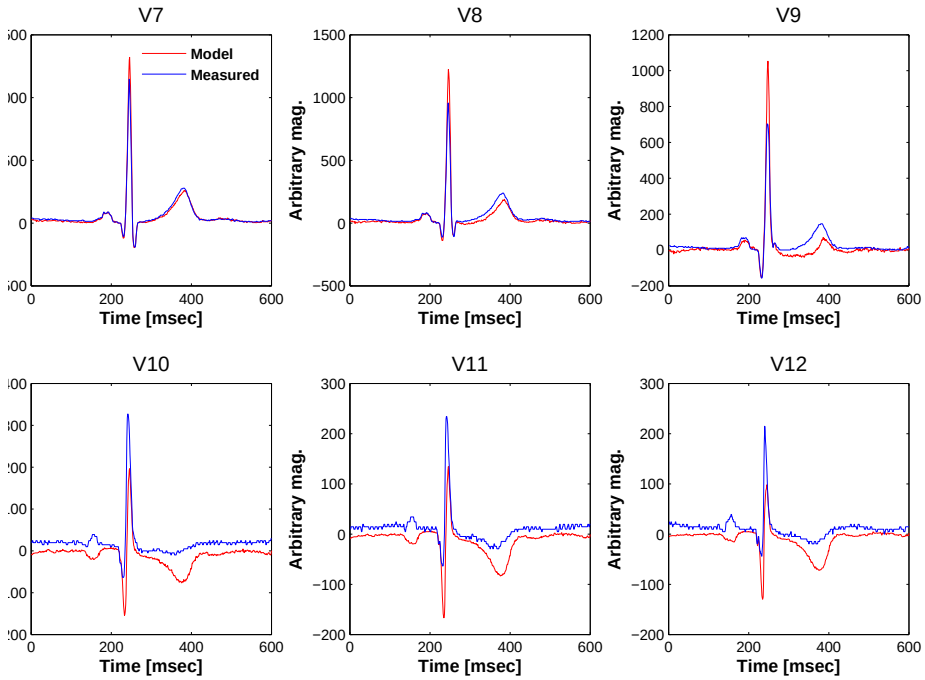

Fig. 5. Example of poor modeling where the R^2 were < 0.8.

A. Performance of the model

In the training and the test group the best median performance of R^2 for a single posterior lead was obtained for lead $V7$. This was expected as a result of the correlation coefficient matrix of the independent leads and the posterior leads, where lead $V7$ was highly correlated (r>0.8) with the independent leads I, II, $V5$ and $V6$, see table III. Lead $V7$ is highly correlated with leads $V5$ and $V6$ since the close anatomical placement between the leads. The lowest best median performance of R^2 was observed for lead $V10$ in both groups with R^2 = 0.81 for the training group and R^2 = 0.85 for the test group. According to figure 1, the posterior lead $V10$ was the only posterior lead which was not highly correlated with any of the independent leads, and this could be an explaining factors of the poor best median performance of lead $V10$. The stability of the regression coefficients may also have impact on the performance on the model, and in figure 3 we saw the regression coefficients of $V5$ and $V6$ predicting $V7$ were stable beyond subject 15. However the regression coefficients of $V5$ and $V6$ predicting $V10$ were converging beyond subject 19, i.e this particular model developed by means of the training group was maybe instable. In general the interquartile ranges of the test group are larger then of the training group. When the model was applied to a set of data, which was not used to develop the model, then the model performed with more extreme outcomes. We suppose this observable fact was attributed to the minimum least square method used to derive the expression of the coefficient matrix, expression 4.

In the regression model, expression 2, an intercept was not included. Figure 5 shows an example of poor modeling. We see the model is under estimated in order to the measured signal e.g. for lead $V10$. With implementation of an intercept in the regression model an improvement of the performance may be obtained, however a physiological interpretation of the intercept is meaningless and therefore not included in this study.

B. Interpretation of regression matrix

The regression coefficients of the multiple regression model yielded the magnitude and direction of the eight dimensions that described each single posterior lead. An intuitive interpretation of the eight coefficients simultaneously was not possible, whereas a stepwise and a pairwise interpretation of the coefficients would yield the resultant vector of a single posterior lead. As an example; consider the independent leads $V5$ and $V6$. In table III both leads are positively correlated with lead $V7$, however in the multiple regression model they appear with opposite signs. A geometrical interpretations of the coefficients for lead $V5$ and $V6$ are given in figure 6. The blue and the black vectors are the measured vectors of lead $V5$ and $V6$, respectively. The green vector is the measured vector of lead $V7$. The regression coefficient of lead $V6$ (see table IV) is $\approx$ 1.1 i.e. an extension of lead $V6$ in order to determine $V7$, depicted as a dashed black vector in figure 6. The regression coefficient of lead $V5$ is $\approx$ -0.4 i.e. a reduction of lead $V5$ in order to determine $V7$, depicted as a dashed blue vector. The resultant vector (green) of the blue and the black vector is the geometrical estimation of lead $V7$. The resultant vector is not identical with the measured vector in neither direction nor magnitude. Interpretation of the remaining leads in the same manner will yield a improved approximation of the measured posterior lead for each step.

The posterior lead $V10$ represented a reduced mirror image of all the independent leads while the posterior leads $V11$ and $V12$ also represented reduced mirror images of all the independent leads except lead $V1$. However, this fact was not directly interpretable from the regression coefficients (table IV), but it was obvious form the correlation coefficients in table III. In figure 4 bottom row, the P, QRS and T-waves are inverted. These results were in agreement with the theoretical assumption of how the electrical dipole of the heart acts on opposite placed electrodes.

C. Best subsets

In best subset regression, the independent lead I did not enter into any of the best subsets, see table VI, and furthermore the independent leads $V5$ and $V6$ were included in all the best subsets. Consider the correlation coefficients of the posterior lead $V7$ and the independent leads (figure 1), we find lead I to be better correlated with the lead $V7$ than the leads $V1$-$V3$. However these leads entered into the best subset of $V7$, while lead I did not. The geometrical interpretation of lead I is the electrical potential difference between the right arm and left arm (i.e. vector pointing toward left arm) in the horizontal plane. Consider the model in figure 6, the electrical potential difference from the right arm to the left arm in the horizontal lateral plane may already be represented in leads $V5$ and $V6$, and this supposition was supported by the results in table II. Lead I was highly correlated with leads $V5$ and $V6$ and, therefore lead I may not provide further information to the model in the horizontal lateral plane. The independent leads $V1$-$V3$ were poorly correlated with lead $V7$, however they described the electrical dipole of the heart in the horizontal anterior-posterior plane. Leads $V1$-$V3$ were therefore included in the best subset for lead $V7$ because they provided information in the horizontal anterior-posterior plane.

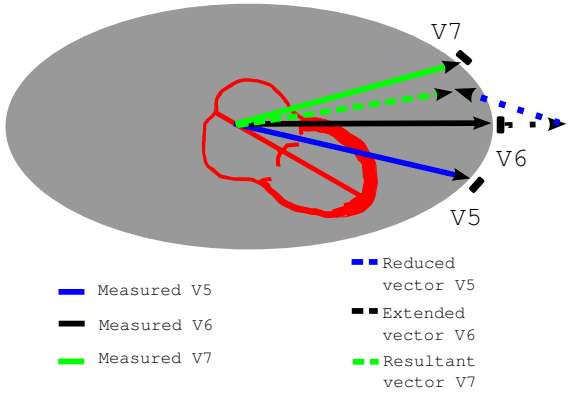

Fig. 6. Geometrical interpretation of regression coefficient of independent leads $V5$ and $V6$, in the horizontal plane.

D. Application of the model on AMI patients

The posterior leads $V7$-$V9$ were predominantly modeled by the electrical dipole in the horizontal lateral plane. Information of the electrical dipole in the horizontal anterior-posterior plane was attenuated in the regression model as a result of the regression matrix IV and the intermediary steps of the best subset regression (data not shown).
In clinical practice the independent leads *II*, $V3$ and $V4$ are used in the diagnosing procedure of posterior infarcts. Lead *II* is inspected for ST-elevation and leads $V3$ and $V4$ are inspected for ST-depression [17], [18]. Although appearance of ST-elevation/depression in these leads are not present in all patients with posterior infarcts, it is still a useful routine in clinical practice. The underlying cause of the ST-depression in $V3$ and $V4$ is a local dipole which is generated in the area of ischemia, see figure 7. This local dipole' anode is pointing toward $V7$-$V9$ and the cathode is pointing toward $V3$ and $V4$, causing the depression in the ST-segment of the independent leads. By the same way inferoposterior infarction can produce a downward angled (vertical) local dipole and cause ST-elevation in lead *II* [17]. The knowledge of ordinarily use of the independent leads *II*, $V3$ and $V4$ taken together with the interpretation of the regression matrix lead us to conclude that, any clinical valuable information concerning posterior infarction contained in the horizontal anterior-posterior plane and in the vertical plane are suppressed in the regression model. This may question if the use of a linear regression model developed on healthy subjects is suitable in patients with disturbed electrical pathways. The assumption we did about the heart as a fixed dipole, may be restricted when applied on AMI patients. In AMI patients presence of more than one dipole must be expected. A local dipole induced by the area of ischemia would appear, and then the single dipole model of the heart differs from the real property of the heart with ischemia. And the lacking publication of the regression matrices in similar studies makes it impossible, directly to compare the coefficients obtained in the different studies.

In this study, we extended the posterior ECG leads on the left side of the back with three additional leads on the right side of the back. According to our knowledge this has not been described earlier. Any posterior infarction will cause an elevation of the ST-segment in leads $V10$-$V12$, as a result of the mirror image effect, was hypothesized. The possibility of reconstructing the posterior leads $V10$-$V12$ with a linear model in healthy subjects with an acceptable accuracy was verified in this study. Likewise the regression of leads $V7$-$V9$ the information in the horizontal anterior-posterior plane and in the vertical plane was also attenuated in the regression model of leads $V10$-$V12$. The clinical value of these leads has not been evaluated elsewhere, hence it is not possible to assess the importance of these leads in clinical practice.

The concept of this study was to provide the physician in emergency departments with further information about the electrical conduction of the heart with existing standard ECG systems. The concept is simple, and the derived information has significant clinical value [8]–[12]. However, the model of the heart as a single dipole with a fixed location may not be adaptable in patients with AMI. To achieve the objective to reconstruct the posterior leads by means of the independent leads, we suggest a model with more then one dipole and variable location of the dipole. Our results intimate that assuming a heart with disturbed electrical pathways as a dipole with a fixed location and variable orientation and magnitude is too simplified. Including both healthy subjects and patients with AMI in the training group, may result in a more robust model for the posterior leads.

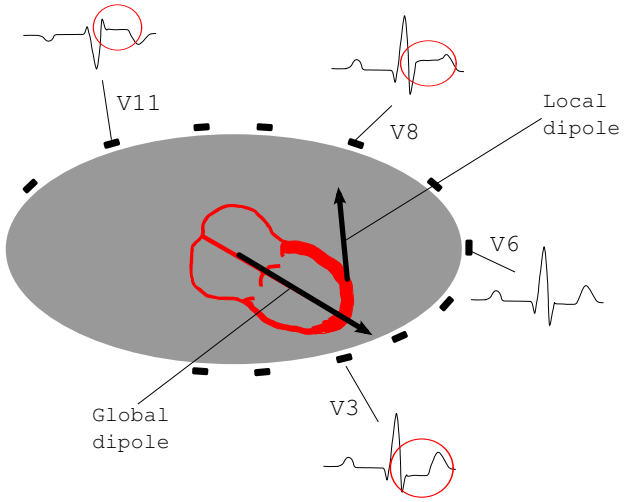

Fig. 7. Schematic presentation of the local dipole induced by ischemia and its impact on the posterior leads, in the horizontal plane

In conclusion, the linear model developed in the present study on healthy subjects performs well on healthy subjects, but we expect this model to yield a poor result when applied on patients with disturbed electrical pathways. The model assumed in this study, only fits persons without any electrical pathway disorders of the heart. More complex models are required to estimate the posterior leads in persons with electrical pathway disorders of the heart, by means of the standard 12-lead ECG.

V. Acknowledgements

We would like to thank Randi S. Berg for her untiring and enthusiastic help during the data acquisition. Furthermore we would like to thank Mette Vestergaard, secretary at Aalborg Hospital for providing location in Forskningens Hus, Aalborg Hospital for the data acquisition.

References

[1] C Berry, A Zalewski, R Kovach, M Savage, and S Goldberg. Surface electrocardiogram in the detection of transmural myocardial ischemia during coronary artery occlusion. *Am J Cardiol*, 63(1):21–6, 1989.

[2] Kjell C Nikus, Markku J Eskola, Vesa K Virtanen, Jarkko Harju, Heini Huhtala, Jussi Mikkelsson, Pekka J Karhunen, and Kari O Niemela. Mortality of patients with acute coronary syndromes still remains high: a follow-up study of 1188 consecutive patients admitted to a university hospital. *Ann Med*, 39(1):63–71, 2007.

[3] Kaes Al-Anee, Ahmed Al-Ani, Magne Henriksen, Bjorn Arild Halvorsen, and Per Anton Sirnes. [Mortality after acute coronary syndrome]. *Tidsskr Nor Laegeforen*, 127(12):1628–30, 2007.

[4] Christian Juhl Terkelsen, Jens Flensted Lassen, Bjarne Linde Norgaard, Jens Christian Gerdes, Tage Jensen, Liv Bjorn-Hansen Gotzsche, Torsten Toftegaard Nielsen, and Henning Rud Andersen. Mortality rates in patients with ST-elevation vs. non-ST-elevation acute myocardial infarction: observations from an unselected cohort. *Eur Heart J*, 26(1):18–26, 2005.

[5] J H Jr O'Keefe, K Sayed-Taha, W Gibson, T F Christian, T M Bateman, and R J Gibbons. Do patients with left circumflex coronary artery-related acute myocardial infarction without ST-segment elevation benefit from reperfusion therapy? *Am J Cardiol*, 75(10):718–20, 1995.

[6] M W Rich, M Imburgia, T R King, K C Fischer, and K L Kovach. Electrocardiographic diagnosis of remote posterior wall myocardial infarction using unipolar posterior lead V9. *Chest*, 96(3):489–93, 1989.

[7] R J Zalenski, D Cooke, R Rydman, E P Sloan, and D G Murphy. Assessing the diagnostic value of an ECG containing leads V4R, V8, and V9: the 15-lead ECG. *Ann Emerg Med*, 22(5):786–93, 1993.

[8] Michael P Somers, William J Brady, Devin C Bateman, Amal Mattu, and Andrew D Perron. Additional electrocardiographic leads in the ED chest pain patient: right ventricular and posterior leads. *Am J Emerg Med*, 21(7):563–73, 2003.

[9] J B Agarwal, K Khaw, F Aurignac, and A LoCurto. Importance of posterior chest leads in patients with suspected myocardial infarction, but nondiagnostic, routine 12-lead electrocardiogram. *Am J Cardiol*, 83(3):323–6, 1999.

[10] S Matetzky, D Freimark, M S Feinberg, I Novikov, S Rath, B Rabinowitz, E Kaplinsky, and H Hod. Acute myocardial infarction with isolated ST-segment elevation in posterior chest leads V7-9: "hidden" ST-segment elevations revealing acute posterior infarction. *J Am Coll Cardiol*, 34(3):748–53, 1999.

[11] L J Melendez, D T Jones, and J R Salcedo. Usefulness of three additional electrocardiographic chest leads (V7, V8, and V9) in the diagnosis of acute myocardial infarction. *Can Med Assoc J*, 119(7):745–8, 1978.

[12] A U Kulkarni, R Brown, M Ayoubi, and V S Banka. Clinical use of posterior electrocardiographic leads: a prospective electrocardiographic analysis during coronary occlusion. *Am Heart J*, 131(4):736–41, 1996.

[13] D. Wei. Derived electrocardiograms on the posterior leads from the 12-lead system: Method and evaluation. *Proccedings of the 25'th annual international conference of the IEEE*, pages 17–21, 2003.

[14] J. R. Hampton. *The ECG made easy*, chapter *. Churchill Livingstone, 6'st edition, 2003.

[15] J. Malmivuo and R. Plonsey. *Bioelectromagnetism*, chapter 7. Oxford University Press, 1995.

[16] C L Levkov. Orthogonal electrocardiogram derived from the limb and chest electrodes of the conventional 12-lead system. *Med Biol Eng Comput*, 25(2):155–64, 1987.

[17] Anton P. Gorgles, Domien J. Engelen, and Hein J. J. Wellens. *Hurst's The Heart*, chapter 53. McGRAW-HILL, 11th edition, 2004.

[18] C. J. Therkelsen. Personal communication with a cardiologist, October 2007.

Linear model for deriving the posterior ECG leads V7-V12 in healthy subjects: Part 2

Kartheeban Nagenthiraja

***Abstract*— In this study, we examined the effects of modelling the regression coefficients by two different methods. 1) The first method (average model) was based on patient-specific models and the regression coefficients were an average of the patient-specific models. 2) In the second method (pooled model) the regression coefficients were determined on pooled data. We also suggest a method to improve the accuracy of the point estimation of the posterior leads.**

The data used in this study contained 19 subjects. For each subject the standard 12-lead ECG and additional six posterior leads were recorded. For each subject an individual, regression model for predicting the posterior leads V7-V12 was determined. The regression coefficients of the average model were an average of the 19 individual regression models. The performance of the average model was determined and compared to the performance of the pooled model from our previous study. For the improvement of the point estimation the ECG data was segmented in three segments; P-wave, QRS-complex and T-wave, and partial regression models were developed.

For the average method the median R^2 for all the posterior leads are lower compared to the pooled method and the interquartile range are wider for the average method. In both methods the highest R^2 is obtained for $V7$. R^2 = 0.98 for the pooled and R^2 = 0.58 for the average method. The median residuals of the partial regression models are generally closer to 0 than for the global model. And the interquartile ranges of the partial models are narrower compared to the interquartile ranges of the global model.

In conclusion, the method of pooled data was less noise sensitive compared to the average method. Modelling the ECG in segments yield an improvement of the point estimation compared to the global regression model. With reference to our results it is not possible to reject the concept of using linear regression models to predict the posterior leads $V7$-$V12$ on AMI patients.

***Index Terms*— Average model, pooled model, reduced lead set, partial regression models**

I. Introduction

Studies have proposed linear regression models for predicting the posterior ECG leads $V7$-$V12$ by means of the standard leads [1], [2]; however the conclusions of the studies were not in agreement concerning the application of the models on AMI patients. Wei determined the regression model of the posterior leads $V7$-$V9$ as an average of 68 individual regression models of healthy subjects. We proposed a similar study based on ECG recordings from 37 healthy subjects, and besides the posterior leads $V7$-$V9$, we extended the ECG recordings with three additional leads on the right side of the back, termed $V10$-$V12$. Our regression model was based on pooled data. Both studies were proof of concept and despite the fact of two different methods, they both achieved acceptable accuracy between the estimated and the measured posterior leads $V7$-$V9$ ($V10$-$V12$). Wei declared a positive attitude for application of the regression model on AMI patients based on the similarity measurements of the estimated and the measured posterior leads in healthy subjects. Whereas our assessment of the application of the linear regression model in AMI patients was more sceptical, concerning the fact that the model considers the heart as a dipole, and this might not be the fact in AMI patients.

In this study, we will examine the two methods of modelling the regression coefficients mentioned above; 1) by averaging the patient-specific models and 2) by determining the regression model based on pooled data, with regard to the regression coefficients and the coefficient of determination (R^2).

The regression models developed in both studies mentioned above are based on the entire ECG signal including P-wave, QRS-complex and T-wave and the iso-electric line between the waves. Henceforward these models will be termed global regression models. By visual inspection differences in the P- and T-waves of the estimated and measured signals were observed, while the differences in QRS-complexes of the estimated and measured signals were insignificant, despite larger magnitude range in the QRS-complex. In the ECG signals the QRS-complexes are relative strong in magnitude compared to P- and T-waves, especially in leads I, II and $V4$-$V6$. The property of the minimum least square estimator is to find the best regression line in a given n dimensional space that minimizes the mean squared error. P- and T-waves may not be well described by the regression matrix because in order to minimize the mean squared error, the regression line is mainly fitted to the data points of QRS-complex. By modelling the three segments P-wave, QRS-complex and T-wave in three independent models may improve the point estimation of the posterior leads. These models are termed partial regression models.

In this study, we examined the effect of modelling the regression coefficients of method 1 and 2 in terms of the magnitude of the regression coefficients and R^2, and we suggest a method to improve the accuracy of the point estimation of the posterior leads.

II. Methods & materials

A. Data

The data used in this study contained 19 subjects of the 37 subjects initially enrolled in the ECG database. The subjects in the subset are randomly chosen and are identically with the training set used in [1]. The subset of 19 subjects was used for the purpose of being able to compare the results of

our previous study and the present study. Data acquisition and summarization of subject characteristics are described in [1]. For each subject the standard 12-lead ECG and additional six posterior leads were recorded. Three electrodes were placed on both sides of the back. In the modelling procedure only the pre-defined eight independent leads were used (I, II, $V1$-$V6$). The data analysis was performed in MATLAB (R2007a, The MathWorks, Inc.).

B. Average model

For each subject an individual regression model for predicting the posterior leads $V7$-$V12$ was determined. The final regression model was an average of the 19 individual models. Dispersion plots of the regression coefficients for the independent variables were generated for the purpose of analyzing the stability of the individual regression coefficients. For each recording of the six posterior leads the R^2 was determined and the median R^2 and the interquartile range of all R^2 were found.

To examine the noise sensitivity of the average method the number of independent variables was reduced from eight to three (these models will be termed "reduced average models"). In the example given in this study, we made two models to predict the posterior lead $V9$. The first model contained the independent variables; $V1$, $V5$ and $V6$. All the independent variables are highly correlated ($r > 0.8$) with $V9$, and the leads $V5$ and $V6$ are highly inter-correlated [1]. In the second model, the independent variables $V1$, $V4$ and $V6$ are non-correlated ($r < 0.8$), but they are highly correlated with the dependent variable $V9$ [1].

C. Global model vs. partial models

To obtain a better point estimation of the posterior leads, the ECG's of the subset were segmented into P-waves, QRS-complexes and T-waves, with respect to all leads. The segmentation algorithm is described in [3]. The P, QRS and T segments were pooled into large data sets, in correct subject order for the 14 leads. The improvements of the point estimation between the global model and the partial regression models were quantified by residuals. The residuals of the measured and the globally estimated posterior leads were determined for each segment and each lead. Likewise, the median residuals and the interquartile range of the residuals of the partial estimated posterior leads and the measured leads were found. The use of the residuals and not the R^2 to quantify the improvements will be discussed later. To test the equality of the residuals of the global regression model and the partial regression models, a Signed-Rank test was used.

III. Results

A. Average model

The regression coefficients of the average regression model are given in table I. The magnitudes of the coefficients are also depicted as bars in fig. 1. When predicting the posterior leads $V7$-$V9$, the absolute value of leads $V6$ is of the greatest magnitude, while the absolute magnitude of the other coefficients of the independent variables are considerably lower compared to the magnitude of coefficients of $V6$. When predicting the posterior leads $V10$-$V12$, the absolute magnitude of the regression coefficient of lead I is of the greatest magnitude.

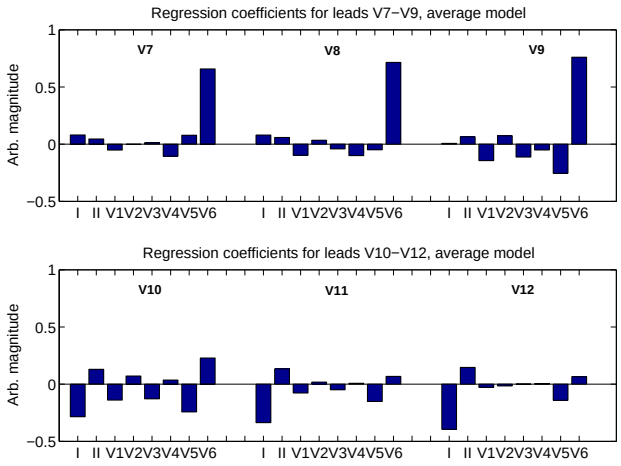

Fig. 1. The regression coefficients for the average model.

In fig. 2, the 19 different coefficients for the independent variables for predicting the posterior leads $V7$ and $V10$ are given. The highest dispersion of the coefficients is seen for the leads $V3$-$V6$. All coefficients for predicting the posterior lead $V7$, except for lead $V6$, are placed about zero and the coefficients can either be positive or negative. For predicting the posterior lead $V10$, all coefficients can be positive or negative.

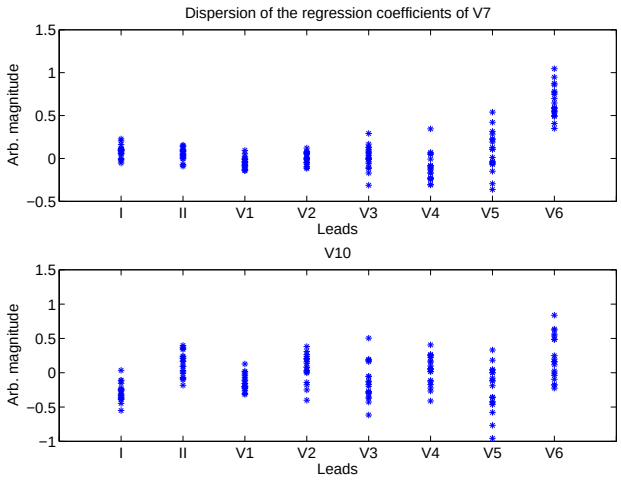

Fig. 2. The dispersion of the regression coefficients for predicting the posterior leads $V7$ and $V10$.

The median R^2 of the measured and the estimated posterior leads are given in table II. In column two and three the median and the interquartile range of R^2 from the pooled method are listed (data from [1]). In column four and five the same information is given for the average method. For the average method the median R^2 for all the posterior leads are lower

	β_I	β_{II}	β_{V1}	β_{V2}	β_{V3}	β_{V4}	β_{V5}	β_{V6}
V7	0.0811	0.0453	-0.0517	-0.0015	0.0128	-0.1048	0.0785	0.6580
V8	0.0797	0.0591	-0.0969	0.0345	-0.0416	-0.0999	-0.0489	0.7151
V9	0.0072	0.0643	-0.1438	0.0738	-0.1129	-0.0509	-0.2547	0.7611
V10	-0.2850	-0.1304	-0.1396	0.0712	-0.1280	0.0364	-0.2427	0.5339
V11	-0.3370	0.1343	-0.0774	0.0185	-0.0493	0.0081	-0.1512	0.0684
V12	-0.3936	0.1463	-0.0273	-0.0151	-0.0008	0.0037	-0.1411	0.0652

TABLE I

REGRESSION MATRIX, AVERAGE REGRESSION MODEL

compared to the pooled method and the interquartile range are wider for the average method. In both models the highest R^2 is obtained for $V7$. R^2 = 0.98 for the pooled and R^2 = 0.58 for the average method. The values given in the table are truncated values.

In fig. 3, the results of the analysis of reduced average models are presented. The first column presents the average regression coefficients and the dispersion of regression coefficients for the model including the independent variables $V1$, $V5$ and $V6$. The second column presents the results for the model including the independent variables $V1$, $V4$ and $V6$. In the model with non-correlated independent variables (second column), the magnitude of the regression coefficient for $V1$ and $V6$ are smaller and the dispersion of the regression coefficients is likewise smaller compared to the model with the correlated independent variables. For the model with correlated independent variables the median R^2 was 0.50 and the range was 0.87-0.13. In the model with non-correlated independent variables the median R^2 was 0.49 and the range was 0.83- 0.15. Both reduced average models were performing better than the average model, see table II.

	Pooled		**Average**	
Lead	**Median**	**(Interq. range)**	**Median**	**(Interq. range)**
V7	0.98	(1.00-0.95)	0.58	(0.97-0.19)
V8	0.96	(0.99-0.92)	0.52	(0.91-0.14)
V9	0.95	(0.99-0.91)	0.40	(0.75-0.05)
V10	0.81	(0.90-0.71)	0.32	(0.68-0.00)
V11	0.82	(0.92-0.73)	0.31	(0.66-0.00)
V12	0.85	(0.93-0.77)	0.30	(0.61-0.00)

TABLE II

R^2 OF THE POOLED AND THE AVERAGE METHOD.

In fig. 5, an example of estimating the posterior leads by the pooled method is given (data from [1]). In fig. 6 the same recording is estimated by the average method (coefficients of table I). The estimation by the average method is obviously poorer than the pooled method in fig. 5. Apart from the amplitude discrepancy, also the morphology of the ECG's is different. Especially the synchronization of the T-wave in the average method is poorer compared to the pooled method.

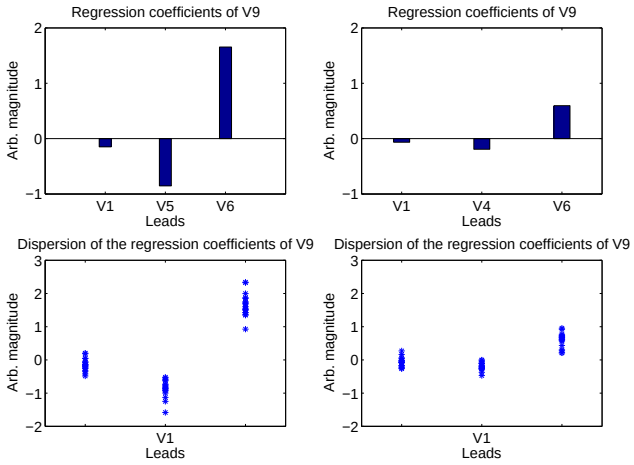

Fig. 3. The average magnitude of the regression coefficients and the dispersion of the regression coefficients of the reduced average models. In the left column the results of the model with correlated independent variables, and in the right column the model with non-correlated independent variables.

B. Global model vs. partial models

In fig. 4, the results of the simple regression of the leads $V5$ and $V7$ are given. The upper left subplot shows the output of lead $V5$ against the output of lead $V7$. The dashed line indicates the best model for the predicting $V7$. The three other subplots show the output of lead $V5$ against output of lead $V7$ when segmented. The dashed line indicates the model developed on the entire ECG's, and the solid lines indicate the models developed on the segments. For P- and T-wave the discrepancy between the partial model and the global model is noticeable, while for the QRS segment the two models appear to be similar. Only the results for $V5$ and $V7$ are shown.

In table III, median residuals and the interquartile ranges for the global regression model and the partial regression models are given. In column 3, the median residuals (global model) for the three segments with respect to the posterior leads are given, and in column 4 the corresponding interquartile ranges are given. In column 5-6, the same information for the partial models is given. The results of the Signed-Rank test, the test of equality of the distributions of the residuals from the global model and the partial models are given in column 7.

The results of table III are given in fig. 7 for better graphical overview. The median residuals of the partial models (solid lines) are generally closer to 0 than for the global model (given as dashed lines). The interquartile ranges of the partial models

		Pooled		Average		
Lead		**Median**	**(Range)**	**Median**	**(Range)**	p**-value**
	P	-10.24	(-26.91-6.43)	-0.13	(-3.67-3.40)	$p < 0.05$
V7	**QRS**	-10.32	(-124.79-104.14)	-1.54	(-11.55-8.48)	$p < 0.05$
	T	-24.68	(-59.23-9.85)	-0.68	(-6.24-4.88)	$p < 0.05$
	P	-9.61	(-26.48-7.25)	-0.20	(-3.98-3.58)	$p < 0.05$
V8	**QRS**	-11.82	(-115.96-92.31)	-4.60	(-20.63-11.43)	$p < 0.05$
	T	-11.91	(-36.77-12.93)	-2.29	(-9.28-4.69)	$p < 0.05$
	P	-3.07	(-15.65-9.50)	-0.54	(-5.54-4.46)	$p < 0.05$
V9	**QRS**	-2.68	(-94.96-89.59)	-4.34	(-26.81-18.13)	$p < 0.05$
	T	8.59	(-7.66-24.85)	-5.44	(-15.49-4.59)	$p < 0.05$
	P	-10.24	(-21.79-1.30)	1.49	(-5.14-8.14)	$p < 0.05$
V10	**QRS**	-4.27	(-53.94-45.39)	-1.38	(-24.67-21.90)	$p < 0.05$
	T	-3.70	(-15.75-8.35)	-1.82	(-10.71-7.06)	$p < 0.05$
	P	-4.42	(-16.11-7.27)	1.43	(-4.67-7.54)	$p < 0.05$
V11	**QRS**	-0.52	(-33.22-32.17)	-3.03	(-20.74-14.68)	$p < 0.05$
	T	-1.47	(-13.26-10.30)	-0.47	(-8.25-7.31)	$p < 0.05$
	P	-2.96	(-15.96-10.03)	-2.68	(-3.97-7.28)	$p < 0.05$
V12	**QRS**	-1.12	(-28.82-26.56)	-2.75	(-16.53-11.16)	$p < 0.05$
	T	-4.09	(-15.88-7.69)	-0.14	(-7.16-7.46)	$p < 0.05$

TABLE III

THE RESIDUALS OF THE GLOBAL MODEL AND THE PARTIAL MODELS.

are narrower compared to the interquartile ranges of the global model. The residuals of the global model and the residuals from the partial models were not form the same underlying distribution according to the Signed-Rank test.

An example of the improvement of the point estimation is shown in fig. 8. The depicted segments are derived from lead $V9$. The upper row shows an example of using the global model for estimating the three segments in lead $V9$, and the lower row shows an example of using the partial models for estimating the same data points. The blue curve indicates the measured signal and the red curve indicates the estimated signal. The P segment appears to be poorly estimated compared to the two other segments, however the resolution of the vertical axis are not identically in the subplot of the segments.

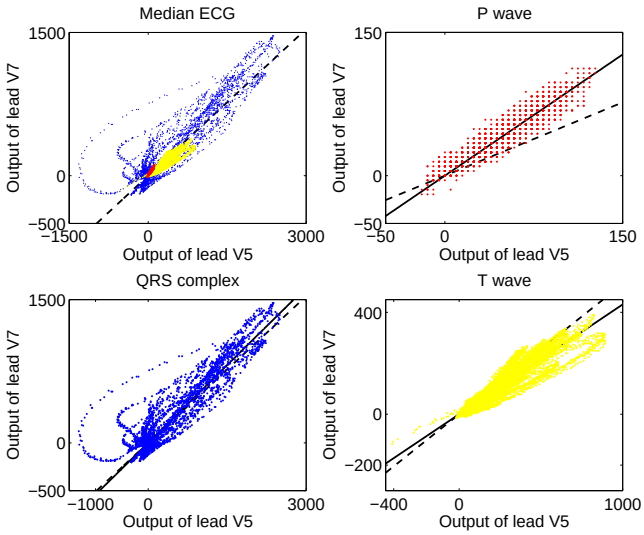

Fig. 4. The results of the simple regression of the leads $V5$ and $V7$. In the upper left subplot the output of leads $V5$ and $V7$ are given and the dashed line indicates the regression model. In the three other subplots the segments P, QRS and T are given, the solid line indicates the partial regression model.

IV. DISCUSSION

Studies have proposed linear regression models for predicting the posterior ECG leads by means of the standard leads. In our previous study [1], we presented a physiological interpretation of the regression coefficients. We suggest that an application of the model on AMI patients would yield poor results according to the assessment based on the interpretation of the regression coefficients. In this study, the aim was to examine two different methods of modelling the regression coefficients, and furthermore to improve the accuracy of the point estimation of the posterior leads by modelling the ECG signal in three segments; P-wave, QRS-complex and T-wave, respectively.

A. Average model

The best median R^2 performance of the average method was obtained for the posterior lead $V7$. The overall performance of the average method compared to the pooled method was poorer, according to the results of table II. By modelling the posterior leads by the average method, we performed a patient wise minimization of the error, and the final model was an average of the individual models, while in the pooled

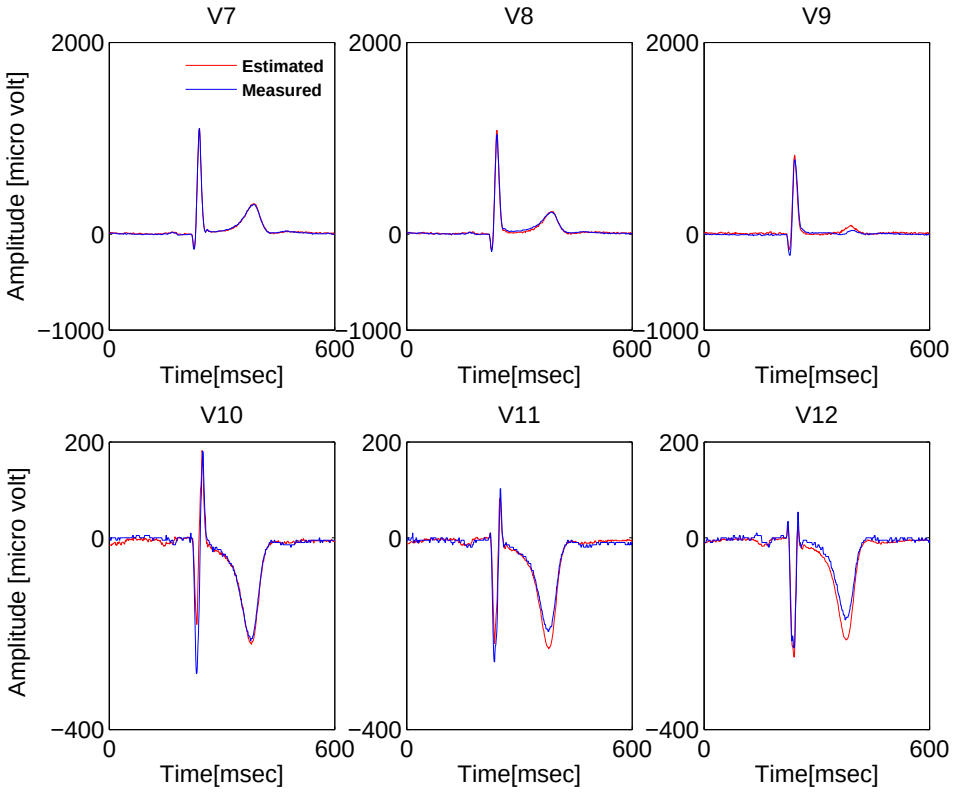

Fig. 5. An example of modelling the posterior leads by the pooled model.

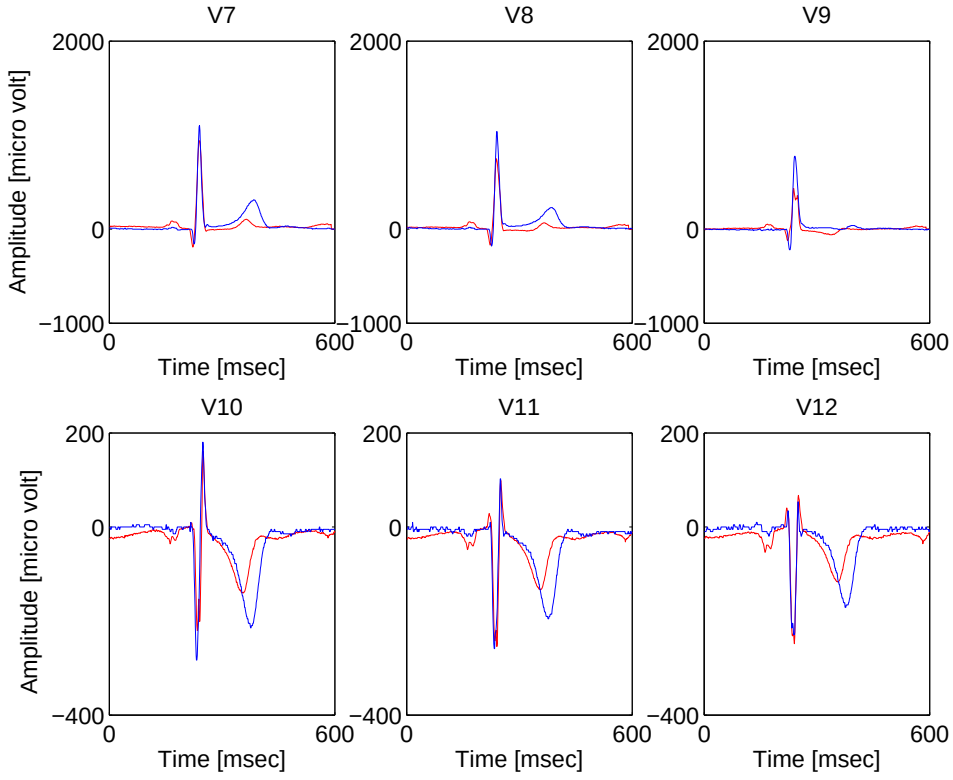

Fig. 6. An example of modelling the posterior leads by the average model.

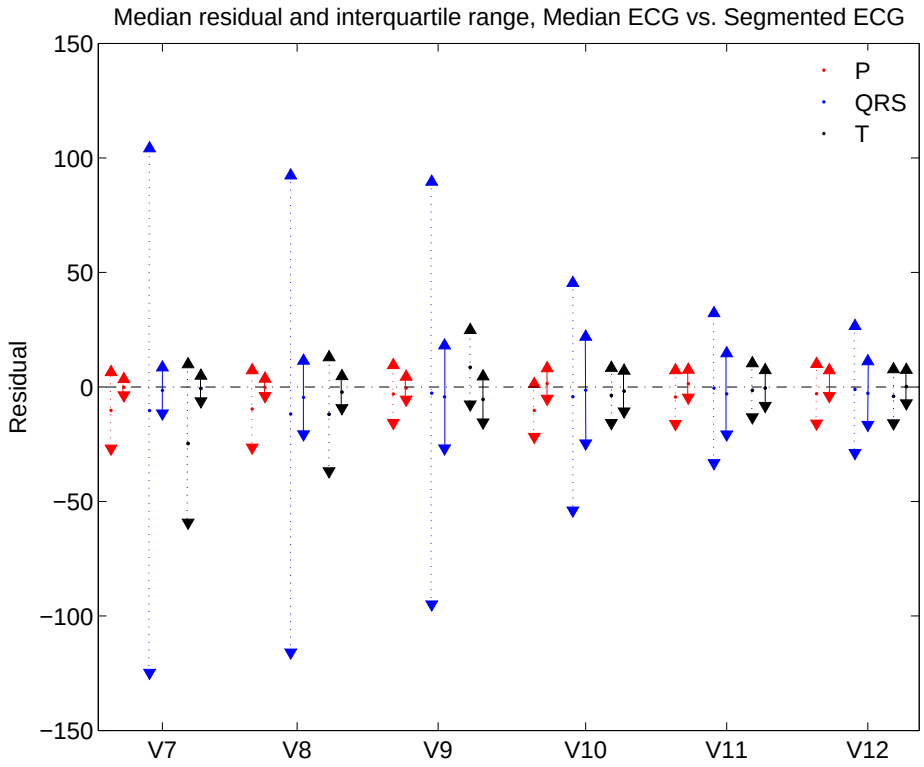

Fig. 7. The median residuals and the interquartile ranges of the three segments for leads V7-V12. The dashed lines indicate residuals from the global model and the solid lines indicate residuals form the partial models.

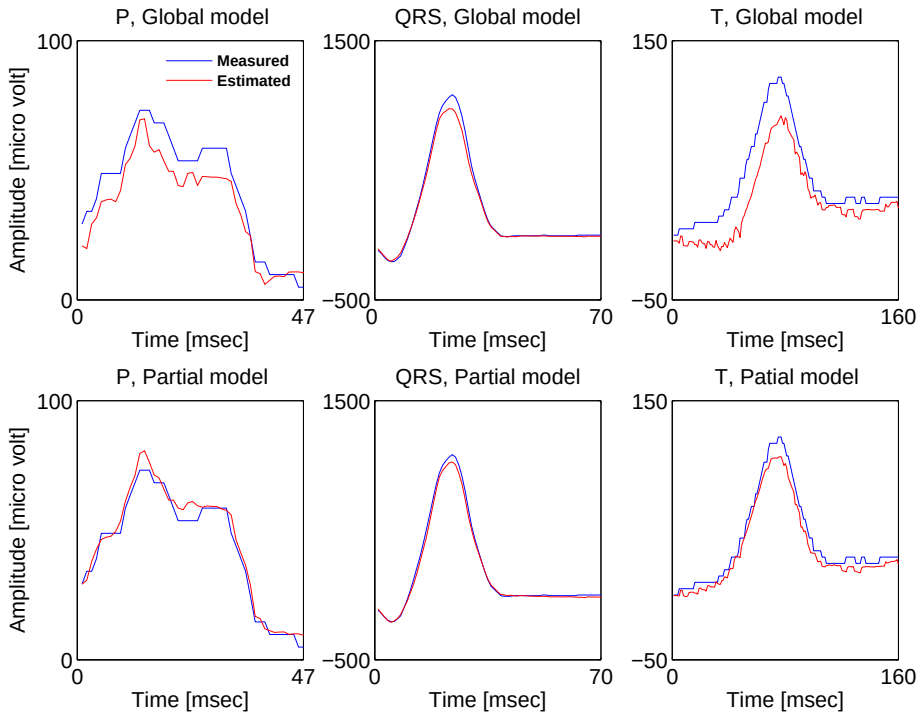

Fig. 8. An example of the segments P, QRS and T estimated by global model (upper row) and by the partial models (lower row) (leads $V9$). The blue line indicates the measured signal and the red line indicates the estimated signal.

method the minimization of the error was performed on the whole subject subset. In fig. 2, we see a large dispersion of the individual regression coefficients for the independent variables and this could be explained by the large number of independent variables and noise. The standard leads are highly correlated [1] and therefore the determination of the regression coefficients are depended on random noise in the standard leads.

As an attempt to limit the influence of the noise, we reduced the number of independent variables from eight to three. In the example shown in fig. 3, the posterior lead $V9$ is modeled by two different models. Model: A) including correlated independent variables and model B) including non-correlated independent variables. The performance of model A for $V9$ is better than the average method with regard to median R^2 and the interquartile range, see table II. However, we still observe a large dispersion of the regression coefficients of leads $V5$ and $V6$ (second row, first column, fig. 3), while the dispersion of the regression coefficients of lead $V1$ is limited. The correlation of lead $V5$ and $V6$ is almost equal 1, hence the determination of the magnitude of the regression coefficients of these two leads are still depended on contain of noise in the leads. By substituting the lead $V5$ with $V4$, we obtain a model with non-correlated independent variables (model B). The dispersion of the regression coefficients of model B is less than the dispersion of the regression coefficients of model A. The performance of the two models A and B are almost equal. The median R^2 for model A equals 0.50 and the median R^2 for model B equals 0.49. Our results indicate that, choosing highly correlated independent variables yield unstable regression models. We therefore believe that a physiologically interpretation of a regression model with highly correlated independent variables is complicated and it is not reliable to assess the performance of the regression model on AMI patients based on the interpretation of the regression coefficients.

The pooled method is less sensitive for noise than the average method, this is indicated by our results and we prefer the pooled method in future studies. The average method may be suitable in noise free recordings, but noise free ECG recordings are practically not obtainable.

We also suggest a reduction of the number of independent variables in the regression model for predicting the posterior leads. However issues as; number of standard leads and which standard leads, have to be considered. Theoretically, three leads describing the x,y,z-directions in the torso are enough to model the posterior leads, however which standard leads to be chosen for the model is more complicated to decide. The standard leads have to be highly correlated with the posterior leads and at the same time they must not be highly inter-correlated. The most obvious method to select the independent variables is the best subset regression method; though this method does not take in to account neither the direction of standard leads in the torso nor their inter-correlation.

B. Global model vs. partial models

The global regression model is predominantly determined on the data points of the QRS-complex; this is indicated by the results of simple regression models of the standard lead and the posterior lead, see fig. 4. This is explained by the property of the least square estimator which minimizes the mean squared error. The simple regression model is based on the entire ECG signal (the independent variables is $V5$ and the dependent variable is $V7$), and the model is depicted as a dashed line. The partial simple regression models are based on the three segments, depicted as solid lines. For the P and T segments, the dashed line is not centred with respect to the centroids in these subsets of data points. However, in the QRS segment, the dashed line and the solid line are almost identical and are centred with respect to the centroid. The different slopes of the solid lines in fig. 4 are a consequence of unequal manifestation of the three waves in the different leads. As an example, let us first consider the P segment. In lead $V5$ and in lead $V7$ the P segments are almost equally manifested (see fig. 4 upper right column) with respect to the magnitude, whereas the QRS segment is obviously not equally manifested in both leads (see fig. 4 lower left column). Therefore, partial models yield better results with respect to point estimation. The general tendency of the median residuals of the partial models is closer to zero compared to the global model. Furthermore, the interquartile ranges in the partial model are more narrow compared to the global model, this indicates a reduction of the number of extreme errors in the partial models compared to the global model, see fig. 7.

To quantify the improvements of modelling the ECG in partial models the residuals are used instead of coefficient of determination R^2. The R^2 is a ratio of the error when using the regression line and the error when not using the regression line for estimation. If the error of using the regression line is zero, then the R^2 = 1. In cases where the error using the regression line is greater than when not using the regression line then $R^2 < 0$, which is an invalid result. In some cases in the global model this occurred, and to avoid this problem of invalid results only the residual (or the error using the regression line) were used to quantify the improvements.

C. Perspectives

With reference to the new knowledge achieved in this study, it is not possible to reject the concept of using linear regression models to predict the posterior leads $V7$-$V12$ on AMI patients. In our previous study, we expected the linear regression model to be invalid in AMI patients as a consequence of relative small regression coefficients for specific leads. A physiological interpretation of the regression coefficients is complicated; this was acknowledged in the study. Hence assessing the performance of the regression model in AMI patients is not reliable. The method of pooled data to determine the regression coefficients was less sensitive to noise compared to the average method and therefore this method is preferable in future studies. Furthermore, a reduction of the number of highly correlated independent variables may yield stable and physiological interpretable regression model. To confirm the validity of linear regression models to predict the posterior leads on AMI patients, studies containing ECG recordings during ischemic periods must be conducted.

By segmentation of the ECG signal and performing partial linear regression models, we obtained improvements in the point estimation compared to the global model. Several studies have investigated the issue of minimal lead sets for reconstruction of the standard 12-lead ECG [4]. They are all conducted on the entire ECG signal and have obtained acceptable accuracy with reduced leads sets. Global linear regression models are mainly based on the data points of the QRS-complex, and therefore a poor estimation of the P- and T-waves was indicated by our results. This may question the accuracy of the estimated leads from the reduced lead sets.

In conclusion, the method of pooled data was less noise sensitive compared to the average method. Modelling the ECG in segments yield an improvement of the point estimation compared to the global regression model. With reference to our results it is not possible to reject the concept of using linear regression models to predict the posterior leads $V7$-$V12$ on AMI patients.

REFERENCES

[1] Kartheeban Nagenthiraja. Linear model for predicting the posterior ecg leads v7-v12 in healthy subjects: Part 1. Master's thesis, Department of Health Science and Technology, Aalborg University, 2007.

[2] D. Wei. Derived electrocardiograms on the posterior leads from the 12-lead system: Method and evaluation. *Proccedings of the 25'th annual international conference of the IEEE*, pages 17–21, 2003.

[3] Hnatkova K., Gang Y., Batchvarov V.N., and Malik M. Precision of qt interval measurement by advanced electrocardiographic equipment. *Pace-Pacing and Clinical Electrophysiology*, 29:1277–1284, 2006.

[4] S. P. Nelwan, J. A. Kors, and S. H. Meij. Minimal lead sets for reconstruction of 12-lead electrocardiograms. *Journal of electrocardiology*, 33, 2000.

Contents

Chapter 1

Introduction

This report is documentation of the solution within the problem of making an algorithm to detect ST-elevation myocardial infarction and Non-ST-elevation myocardial infarction. The project is carried out as a cooperation between Department of Health Science and Technology, Aalborg University and Department of Cardiology, Skejby Hospital.
The first five chapters are description of the different scientific fields concerning with the automatic diagnosis of acute myocardial infarction (AMI). Chapter six is concerning with statement of the problem.
For experienced readers in the field of ECG and AMI, the first five chapters are trivial, but for those who are not confident with these fields these chapters may be informative.
The chapters seven and eight are the documentation of the algorithm. And the last chapter is the synthesis.

Chapter 2

Epidemiology of acute myocardial infarction

Acute coronary syndromes is a general definition of several lethal conditions of the heart, and includes: unstable angina pectoris, ST-elevation myocardial infarction and non-ST-elevation myocardial infarction (ICD10 120-125) [1]. A medical definition of Acute Myocardial Infarction (AMI) is sudden onset of myocardial necrosis due to the formation of a thrombosis in the coronary arterial system obstructing arterial blood flow to the cardiac muscle [2].
The World Health Organization (WHO) estimates approximately 30 % of all deaths in 2004 were caused by cardiovascular disease corresponding to 7.2 million people worldwide. This makes cardiovascular disease as the most leading death cause in the world. [3]
The incidence rates of AMI in USA is reported to be approximately 40-50 cases per 10,000 persons [4,5]. In Europe, there are differences between the countries in the northern and the southern part of Europe. In the countries in the north the incidence rates are similar those in USA, while in countries in the southern part show lower incidence rates [6–8].
About 10 %-15 % of the incident cases of AMI die of disease in the north Europe [9–11]. In this per-cent interval also non-hospitalized cases of AMI are included. The hospitalized mortality rates are lower, due improved therapeutical and operational techniques.
There no clear consensus about the sex differences in mortality rates. According to WHO there are no distinct differences in deaths caused by ischemic heart disease among males and females [3], while some studies reports higher rates for women [8] and others reports lower mortality rates for females [12, 13].

2.1 Temporal changes in incidence and mortality of AMI

WHO conducted a study to clarify the temporal chances in cardiovascular disease in the period of 1979-2002. A total population of approximately 10 million peoples in 21 countries, makes this study to the largest study of temporal changes in incidence and mortality of AMI conducted yet [14]. The report by WHO and others conclude the incidence and mortality rates have been decreasing over the last decades [9, 14, 15]. The factors that may have the most impact on the decreasing incidence rates are improvements in life-style related factors such as food habits, smoking, physical activity etc. They also conclude the declining case-fatality rates are the main cause of the decreasing mortality rates. Declining case-fatality rates are due to improvements in medical interventions [9, 15–17]
Similar tendencies in decreasing incidence and mortality rates have been reported in Denmark in the period of 1985-2000 [18, 19]

2.2 The economical burden of AMI

The economical cost of diagnosis, treatment and rehabilitation of AMI, amounts to a significant portion of the total budget of the health care expenses. In Denmark expenses of AMI is in the range of 6.3 % - 7.5 % of the total health care expenses in the five regions [20]. In UK the expenses associated with AMI amounts to £7,06 billion, where the expenses for the disease, informal care and productivity loss were incorporated in the calculations [21]. AMI is the disease with the highest economical burden, in the UK [21].
Taylor et al. estimated the amount of the different economical issues (e.g. medication, operation etc.) in the treatment of a AMI [22]. They found the ward expenses account for more than 50 % of the total amount per patient in treatment [22]. They also found that countries with higher expenditure on patients tended to have lower case-fatality rates [22]. Despite the high economical expenses in treatment of AMI, the fact of the decreasing incidence rates may lead to a decrease in the total amount of expenses in the future [23].

Chapter 3

Anatomy and physiology

In this chapter there will be an short introduction to the anatomy of the heart. The action potential initiated in cardiac cells differ form the action potential in the muscle cells, a brief description on cellular level will be provided. Likewise the electrical conducting system of the heart which is the underlying cause of the electrical potentials measured by ECG will be introduced. Finally the etiology of AMI will be described.

3.1 Anatomy and the function of the heart

The heart is the organ that provides blood supply to the rest of the body. The heart is a muscle and therefore it consumes oxygen and produce waste products during the work.
The heart consist of four chambers see figure 3.1. The heart can be divided in to two parts; the right and the left part for convenience. In each part there is an atrium and a ventricle, which is separated by atrio-ventricular valves tricuspid valve (in the right part) and the mitral valve (in the left part). The right ventricle (RV) is connected to lungs by pulmonary artery and the left ventricle (LV) is connected to main arteries by aorta. [24]
In the right atrium the venous blood from superior and inferior vena cava is gathered and transported to the right ventricle during the diastole when the tricuspid valve opens. During the systole the heart squeezes the blood from the right ventricle through the pulmonary artery to lungs for the decarbondioxygenation and oxygenation processes. The oxygenated blood from the lungs enters the left atrium by pulmonary veins and is transported to left ventricle during the diastole when the mitral valve opens. During the systole the left ventricle squeezes the blood through aorta for distribution to the tissue. [24,25]

The walls of the heart consist of cardiac muscle cells, and these cells have different properties than skeletal muscle cells e.g. duration, initiation etc.

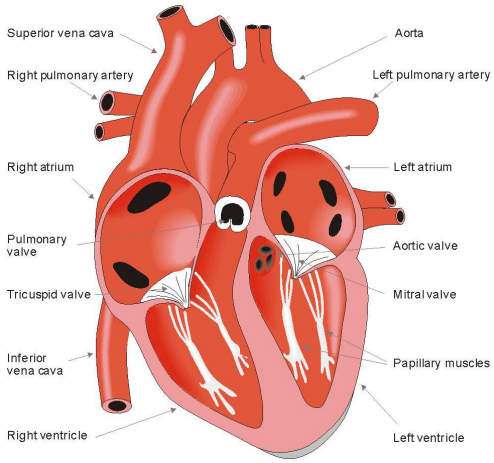

Figure 3.1: *Cross-sectional (frontal) view of the heart.* [26]

The muscle walls are oriented spirally and is divided into four groups, see figure 3.2. Two groups (top row) cover both ventricles on the outside and one group covers both ventricles (beneath) and finally the fourth group covers only the left ventricle (bottom row). [26]

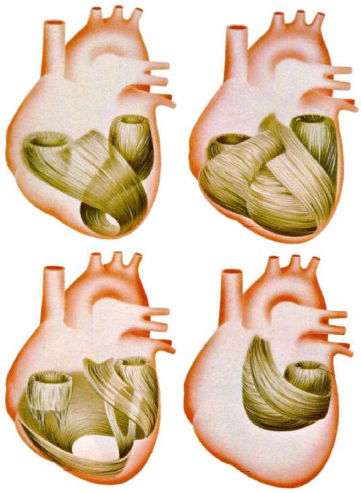

Figure 3.2: *Orientation of cardiac muscle fibers.* [26]

The blood supply to the heart is through three main arteries; right coronary artery (RCA), left anterior descending artery (LAD) and circumflex artery (LCX). Anatomically LAD and LCX are branches of left coronary artery (LCA), see figure 3.3. RCA and LCA originate from the trunk of ascending aorta. RCA supplies the anteroinferior and the medial posterior wall of

the heart. On figure 3.3 the posterior arteries are illustrated with white dotted borders. The LAD supplies the lateral anterior wall of the heart. The LCX supplies the lateral and lateroposterior wall of the heart. RCA, LAD and LCX are further branched in smaller arteries. The arteries innervate the cardiac muscle wall from the epicardium to the endocardium. In case of insufficient blood supply to the arteries, the will be a positive pressure gradient from the endocardium to the epicardium. As a consequence of the innervation direction the ischaemia commences as subendocardial and can in severe case develop as transmural ischemia.

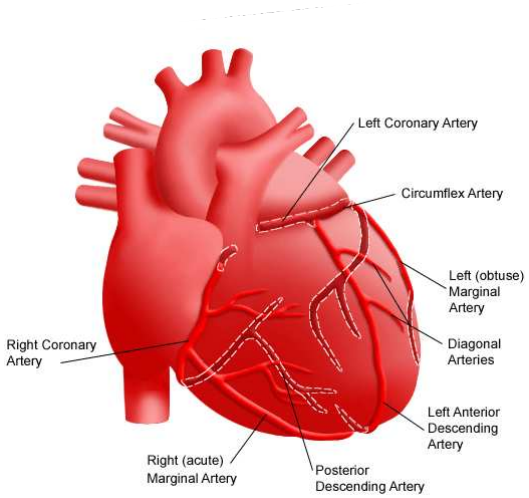

Figure 3.3: *The arteries of the heart. The arteries on the posterior wall of the heart are illustrated with white dotted borders.*

3.2 The electrical conduction system of the heart

In the right atrium a group of specialized cells called sinus node are placed. They are self-excitatory and generate the action potential (heart beat frequency). From sinus node the action potential propagates to the atrioventricular node and the bundle of His. From this point the signal pathway divides into two branches termed bundle of branches. The bundle of branches innervates both ventricles and ends in the purkinje fibers, see figure 3.4. The frequency of the heart is not only depended on the sinus node, but other regions in the heart are also self-excitatory and can generate action potential to keep the heart pumping, in case of malfunction of sinus node [25]. On figure 3.4 the different regions in the heart, where the cells are self-excitatory are marked with an arrow, and their self-excitatory frequency is given in beats per minute.

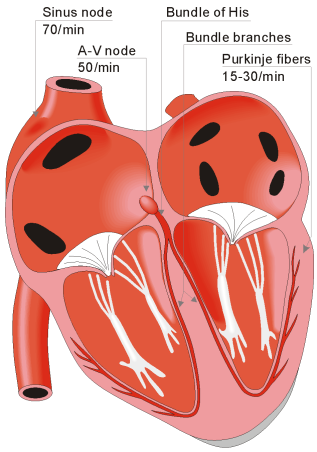

Figure 3.4: *The electrical conduction pathway in the heart. The self-excitatory regions in the heart are marked with an arrow, and the self-excitatory frequency is given in beats per minute.* [26]

3.3 The action potential in cardiac muscle cells

The action potential in a cardiac cell differ form a skeletal muscle cell in duration of the potential. The action potential in skeletal muscle is a short burst with a duration of few milliseconds (msec) [27], while the cardiac action potential has a duration of approximately 250 msec [24].
The cardiac action potential can be grouped in three phases; depolarization, plateau and repolarization, see figure 3.5.

Depolarization

The depolarization phase occur when the transmembrane potential (V_m) rises to -60 mV. When the V_m reach the threshold the membrane becomes permeable to Na^+. The result is rapid increase in the V_m to approximately $+30$ mV.

Plateau

At a V_m of $+30$ mV the Na^+-channels close, and the cell now actively transport the Na^+ out, meanwhile Ca^{2+}-channels open. As a consequence of the opposite transport the V_m remains about 0 mV for approximately 175 msec.

Repolarization

At the end of the plateau phase Ca^{2+}-channels close and K^{+}-channels open (efflux), and cause a decrease in the V_m to resting potential.

In skeletal muscles the action potential is initiated by motor nerves, while in cardiac muscles the action potentials are produced by it own (pacemaker cells) [25].

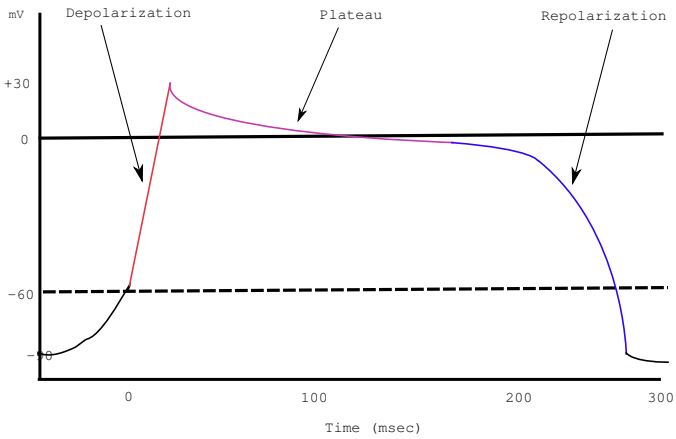

Figure 3.5: *Action potential in cardiac muscle cell. The action potential is grouped in three phases; depolarization, plateau and repolarization. For further description of the phases see the section above.*

In chapter 4 the link between the action potential in cardiac muscle cells and the recorded signal of the ECG will be clarified. This is an interesting concept to understand the origin of ECG.

3.4 Etiology of myocardial infarction

A medical definition of AMI is sudden onset of myocardial necrosis due to the formation of a thrombus in the coronary arterial system obstructing arterial blood flow to the cardiac muscle [2].
The underlaying causes of AMI can be grouped as; unstable angina (UA), non-ST-segment elevation AMI (non-STEMI) and ST-segment elevation AMI (STEMI). These three gruops refer to the clinical findings. UA is a result of reduced perfusion to the myocardium due to a non-occlusive thrombus, and no biochemical markers of necrosis are found. non-STEMI is a clinical condition similar to UA, however biochemical markers of myonecrosis are found and no elevation of the ST-segment of ECG occur. STEMI is the most lethal condition, and is secondary to a total occlusive thrombus in the coronary artery. [28, 29]
The formation of thrombus is caused by fatty deposit in the wall of coronary arteries [24]. The fatty deposit grows as cholesterol cults together in the

wall, and can narrow the passage and reduce the blood flow through the artery. In severe cases spasms in the artery walls can further reduce or stop the blood flow to the innervated regions of cardiac wall. This will immediate cause oxygen lack in the cell and can induce ischemia. Within 60 sec, loss of the myocardial contractility occurs, and within 20-40 min of total occlusion the loss of viability occurs. [24,25,30]
A narrowing of a coronary artery do not necessarily induce ischaemia, at resting or moderate work. While the cardiac oxygen demand rise e.g. when exercising, and the the blood supply is insufficient ischemia in the cardiac cells will be induced and can have fatal outcome [25].

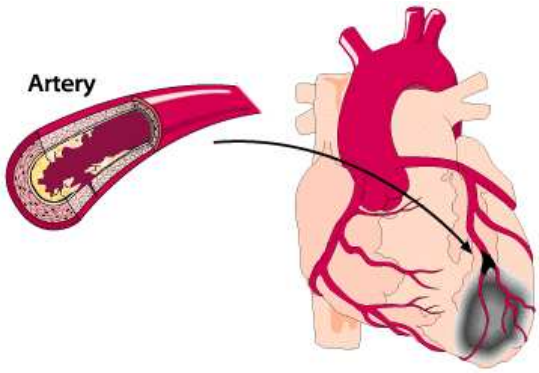

Figure 3.6: *Anterior view of the heart. Left; cross-sectional view of an arteriosclerotic LAD*

In ischemic tissue the electrical impulses are conduct slower than in well perfused tissue. The disturbance in the electrical pathway is reflected in the ECG, and will be further described in chapter 5.

Chapter 4

Symptoms, diagnosis and treatment of AMI

This chapter contains mainly medical related issues as; how to clarify the physical symptoms of the patient, and how to support the subjective statements with objective investigation methods and finally the treatments available at present.

4.1 Physical symptoms of AMI

The most evident sign of AMI is chest pain (angina pectoris). Often the origin of the pain is retrosternal, and is described by patients as tightness, squeezing or burning sensation in the chest region. The pain can radiate to left/right arm, ulnar, throat, neck, jaw and teeth. The intensity of pain vary between patients from mild discomfort to unbearable pain in the chest area. Some patients also report dyspnea. All these symptoms are not significant for AMI, and can be caused by e.g. extra cardiac conditions. Therefore the clinical findings must be supported by supplementary objective investigation methods. [31]

4.2 Diagnosis of AMI

UA, non-STEMI and STEMI have the same underlying physical condition, but are definitions of the severity of the physical condition. Therefore the diagnosis procedure is almost the same for all three conditions, and will be described as one diagnosis procedure. The complete diagnosis procedure consist of the following issue:

- History
- ECG

- Biochemical markers
- Imaging

History

As diagnosing any other diseased condition the history of the patient is important, and may exclude unnecessary diagnosis and encourage a rapid and adequate treatment. The history can provide useful information about drug intake, exercise level, smoking and life-style, which are all of importance for the physician to make a correct diagnosis.

ECG

In all patients complaining of angina pectoris an ECG will be performed. The ECG presents useful information for the physician about the electrical conductivity of the heart. In UA and non-STEMI patients a ST-segment depression during chest pain is a clinical finding for ischemia, but not a significant finding. If the ST-segment depression is presented in ECG during chest pain and in pain free periods, the diagnostic value of the findings are less specific. Often inverted T-wave occurs in the ECG of patients with UA or non-STEMI. ECG recorded during attack of chest pain have more diagnostic value than ECG recorded in pain free periods. In STEMI patients the frequent abnormality is elevation of the ST-segment, and subsequently Q wave occurs and the T wave is inverted. The elevation of ST-segment will return to the isoelectric line with time, usually within 48 hours. [29,29,32] The characteristics of ECG in patients with AMI will be further described in chapter 5.

Biochemical markers

Necrotic myocardial secrete macromolecules and enzymes and these substance are measurable in the blood [33]. Release of creatine kinase (CK) in the blood was proposed as marker of myocardial necrosis and it has been standard in emergency departments since 1980's [33,34]. The disadvantage of CK as marker is the CK release into the plasma do only occur in case of lost viability [35]. However the introduction of troponin T and I, has overcome this problem and now it is possible to detect necrosis before the state of viability [29,36].

Imaging

Imaging modalities are primarily not used as diagnostic tools to determine the presence of AMI. When the diagnosis of AMI is manifested then the imaging modalities are used to determine the location of the AMI and the severity. Modalities with advantages in the field of imaging the coronary arteries can be echocardiography, MRI, CT and coronary angiography (CAG). CAG is a technique, where the coronary arteries are illuminated by an imaging agent and the investigation of the arteries are supervised by x-ray, see figure 4.1. This is often used, but in contrast to the other modalities mentioned this is invasive and is linked with a risk of complication.

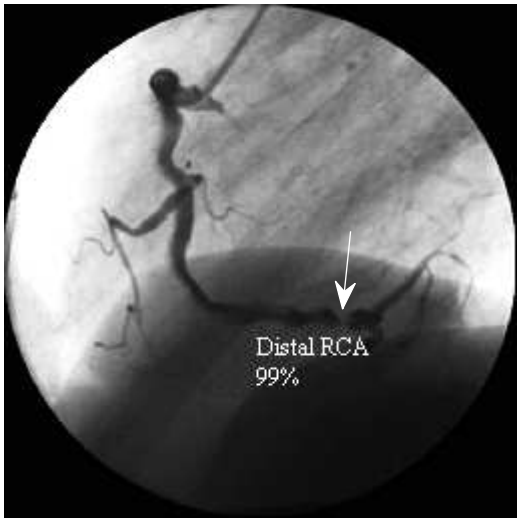

Figure 4.1: *X-ray of a chest anterior view. The occlusion is marked with a white arrow*

4.3 Treatment of AMI

Treatment of AMI can be therapeutical or operational or a combination of both. The aim of the treatment is to reduce symptoms, prevent future events of AMI and reestablishment of baseline hemodynamic parameters. [29,33]
Less severe case of AMI is often controlled therapeutical. The therapeutical agents consist of three main groups; vasodilators, antiplatelet and anticoagulant. [29,33]
The main effects of vasodilators are to reduce the oxygen demand of the heart and simultaneous increase the oxygen delivery to the heart. Agents in

this category is e.g. nitroglycerin and beta-adrenergic blockers. Antiplatelet are a group of agents to prevent thrombus formation in the blood. Antiplatelet are effective in artery circulation, while anticoagulant have the same antithrombotic effects as antiplatelet, but are most effective in venous circulation. Example of an agent in the antiplatelet group is aspirin, and an agent in the anticoagulant group is heparin. [29,33,37]
The aim of the operational procedures is to restore the blood supply to the ischemic areas of the heart. The mainly used methods are percutaneous transluminal coronary angioplasty (PTCA) or coronary artery bypass grafting (CABG). The PTCA is the method connect with less post-operational complications. A catheter is inserted in to one of the main arteries in body, and lead to the coronary artery of concern, see figure 4.2 left column. A balloon is inserted in the occluded area and inflated to restore normal flow across the occlusion, figure 4.2 middle column. During the withdrawal of the catheter a stent is placed in the dilated area to keep it open, figure 4.2 right column. [29,33,38]

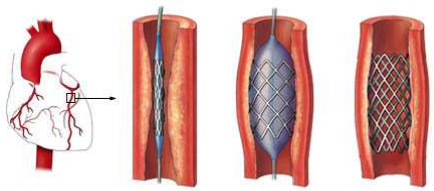

Figure 4.2: *An illustration of the PTCA step by step.*

The CABG method is more advanced and requires an surgical opening of the thorax. The blood flow through the total occluded area is bypassed with inserting an auto graft artery, often the mammary artery, see figure 4.3. [29,33,39]

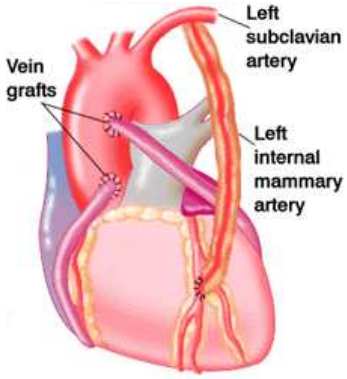

Figure 4.3: *An illustration of the concept of CABG*

Chapter 5

Electrocardiogram

The chapter is an overview of the basic technical concept of electrocardiogram (ECG). First section will contain short introduction to what the ECG is, how to obtain it and the 12 leads. A section will investigate the genesis of ECG, from intracellular action potentials to the electrical potentials measured on the precordium. Finally there will be a brief description of transformation of ECG (temporal information) data to vectorcardiography (VCG, spatial information).

5.1 The basics of ECG

In chapter 2 we dealt with the cardiac muscle contraction on cellular level. Every contraction of a cardiac muscle is associated with a depolarization of cardiac muscle cell. All these "individual" contraction can be measured as an electrical potential on the precordium by means of electrodes. [32]
The morphology of the ECG is illustrated in figure 5.1. The peaks and bottoms on the ECG are designated with the letters P, Q, R, S and T, and refer to different physiological events in the heart. The P wave corresponds to the depolarization of the cells in the atria. The complex QRS is the depolarization of the ventricles, and the amplitude of the QRS waves is larger than P wave due the larger mass of muscle in the ventricles. The T wave is the repolarization of the ventricles. [32]

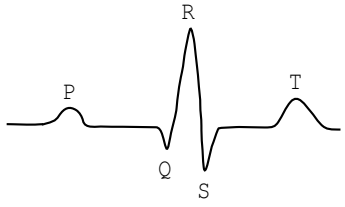

Figure 5.1: *The morphology of an ECG.*

The ECG is recorded by means of electrodes placed on the limbs and the precordium. The standard 12-lead ECG have three electrodes placed on the limbs (right arm, left arm and left leg), and six electrodes placed on the precordium, as shown in figure 5.2.

Figure 5.2: *The placement of the electrodes V1-V6 on precordium.*

By means of the nine electrodes 12 derivatives of the heart can be obtained. Six of the 12 derivatives depict the heart on the vertical plane, and the others depict the heart on the horizontal plane. The intra differences between the derivatives in the two planes are the angle where the electrical activity of the heart is depicted. On figure 5.3 the different planes and angles the derivatives "look" on the heart are shown (only schematic figure).

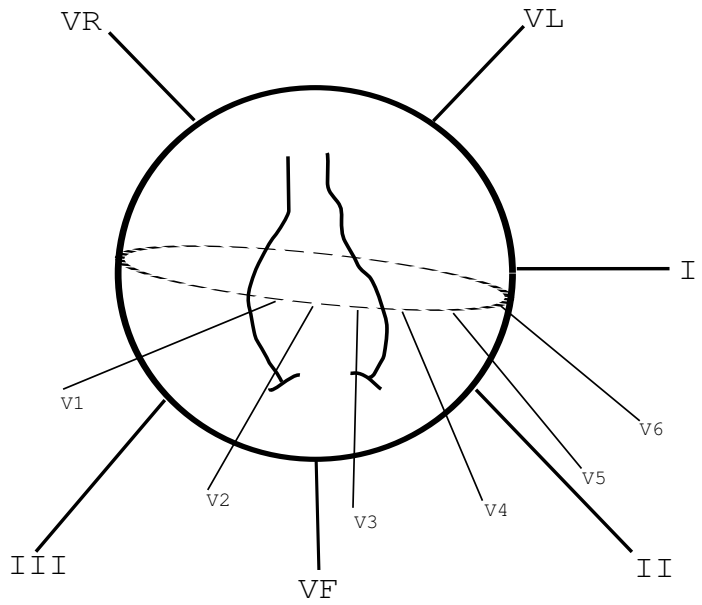

Figure 5.3: *A schematic illustration of the 12 derivatives of the electrical activity of the heart.*

To understand how it is possible to "look" on the heart from different angles, it is necessary to understand the fundamentals of electrode. Figure 5.4 shows the properties of the bioelectrical potential measured by means of electrodes. If the electrical resultant vector is perpendicular and toward the electrode, the amplitude will be positive and maximum (in order to calibration). If the electrical resultant vector is perpendicular but heading away from the electrode, the amplitude will be maximum but negative. In case of an oblique angle the amplitude will be lesser than in the cases of perpendicular angles. The final case is a parallel electrical resultant vector, which will cause no effect on the oscilloscope.

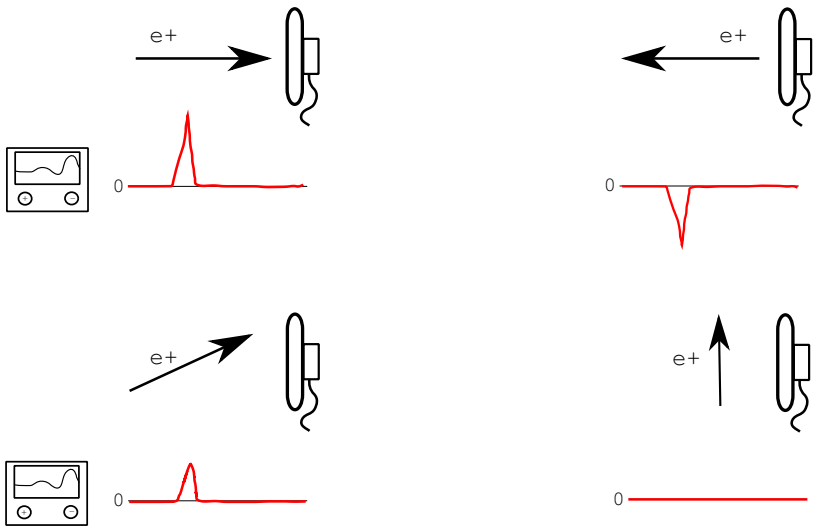

Figure 5.4: *A schematic illustration of the angle of the electrical resultant vector. A perpendicular resultant vector will result in a maximum effect, and a parallel vector will not have any effect.*

As described in chapter 2 the contraction of the heart starts in the atria and moves lateroinferior. The electrical resultant vector in the horizontal and vertical plane moves counter clockwise in an ellipse orbit, see figure 5.5. The figure illustrates the heart viewed in two different planes; horizontal and vertical, respectively. The green orbits indicate the location of the electrical resultant vector in different time instance. Actually there are two orbit; a big and and a small one indicating depolarization of atria and the ventricles. Further, which parts of the heart the different electrodes look on are also depicted as dotted arrows. By means of placing the electrodes in different positions it is possible to record the electrical resultant vector around the ellipse orbit. The leads I, II and VL look at the left lateral surface of the heart, III and VF look at the inferior surface, and VR looks at the right atrium. The precordial leads V1- and V2 look at the right ventricle, V3 and V4 look at the ventricular septum and the anterior wall of the left ventricle, and V5 and V6 look at the anterior and lateral walls of the left

ventricle. [32,40]

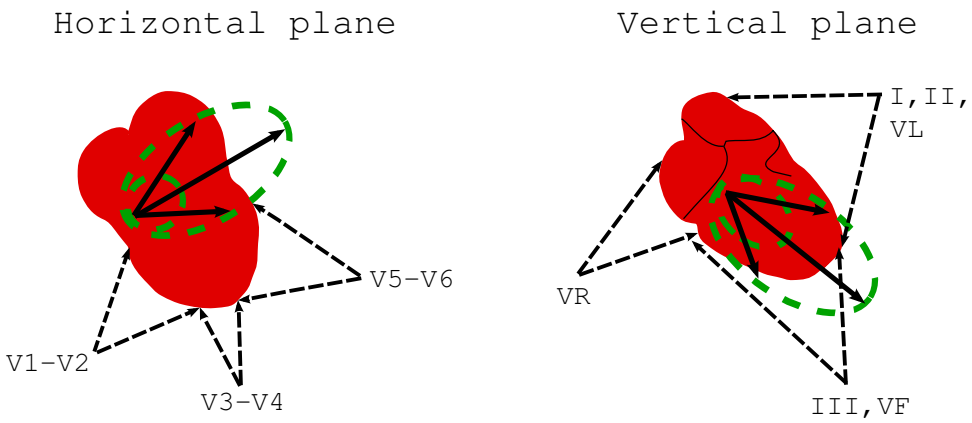

Figure 5.5: *A horizontal and vertical view of the heart.*

5.2 Origin of ECG

Chapter 2 provided a description of the generation of action potentials in cardiac muscle cells. In this section the link between the action potential and the potential measured at the precordium (or ECG) will be described. The description of the origin of ECG is a simplified model with to important assumptions. The first, the cardiac muscle cells are connected by low-resistance pathways. By means of this a cell can stimulate the following cell. The second, the action potential can only propagate in parallel direction to the wave front. [26,41]

Depolarization

A highly simplified model of the cardiac muscle cells is provided in figure 5.6 A and D. The cells are aligned parallel and the wave front is perpendicular to the direction of the cells. On left part of the model of the muscle the cells are in resting phase (they are not stimulated yet), on the right part of the model the cells are activated (they are stimulated). In the middle part of the model the wave front appears. In the vertical box the main mechanism causing the depolarization (influx of Na^+) or the repolarization (efflux of K^+) are depicted. On the outer-left side a measuring electrode is attached, and on the outer-right side a reference electrode is attached. The ECG is measured as the potential difference between these electrodes.
When the V_m reach -60 mV the influx of Na^+ begins and the V_m reach +30 mV rapidly, see figure 5.6 B. While the extracellular potential (P_o) decrease from 20 mV to -40 mV as a cause of decrease in the amount of Na^+ in extra cellular plasma. When the wave front is propagating from right to left, the

left side will be predominantly positive (resting phase), and the right side will be predominantly negative (activated phase). As the ECG is measuring the extra cellular potential difference a positive signal will appear, figure 5.6 C. [26, 41]

Repolarization

The repolarization is different form the depolarization, in two main points. The depolarization is a wave front where previous cell stimulates the next cell. The repolarization occur after a time instant, because the depolarization only appears in certain time interval. Therefore the repolarization is not stimulated by surrounding cell, but a cause of a intrinsic mechanism in the cell. As a consequence of this the cells that are depolarized first will also repolarize first. The duration of the repolarization is 100 ms (denoted DZ, depolarization zone or RZ, repolarization zone), while the depolarization only last 1 ms.
During the repolarization the situation in our muscle model is; on the left side the cells are activated (they are still stimulated), on the right side the cells are in resting phase (they are already repolarized), see figure 5.6 D. The efflux of K^+ will cause an decrease in V_m, form 30 mV to -80 mV. Opposite the P_o will increase, as a consequence of the increased amount of K^+ ions in the extra cellular plasma, figure 5.6 E. Therefore the left side of the model is predominantly negative and the right side is predominantly positive. As the electrical resultant vector is pointing away from the measuring electrode (in this idealized case also perpendicular on the electrode) a negative ECG signal will appear. [26, 41]

5.3 Converting ECG data to vectorcardiography

Vectorcardiography (VCG) is a technique used rarely in clinical situations. In 1970's the novel technique was popular and foretold a huge clinical impact, but the VCG has never gain a footing in clinic. The VCG is said to be superior to ECG in e.g. to detect ischemia.
As aforementioned VCG is depiction of the electrical field produced by the heart during a heart cycle. When consider a VCG we assume the heart as a point generator of electromotive forces, and the body (thorax) as a volume conductor. For every time instance the point generator (heart) produce a vector, with a magnitude corresponding to the strength of the electromotive forces and a direction of the force. By joining all these instantaneous vectors, we obtain a VCG. [41, 42]
VCG can be recorded by means of vectorcardiograph, but it is also possible to convert ECG to VCG by a transformation matrix. The transformation is

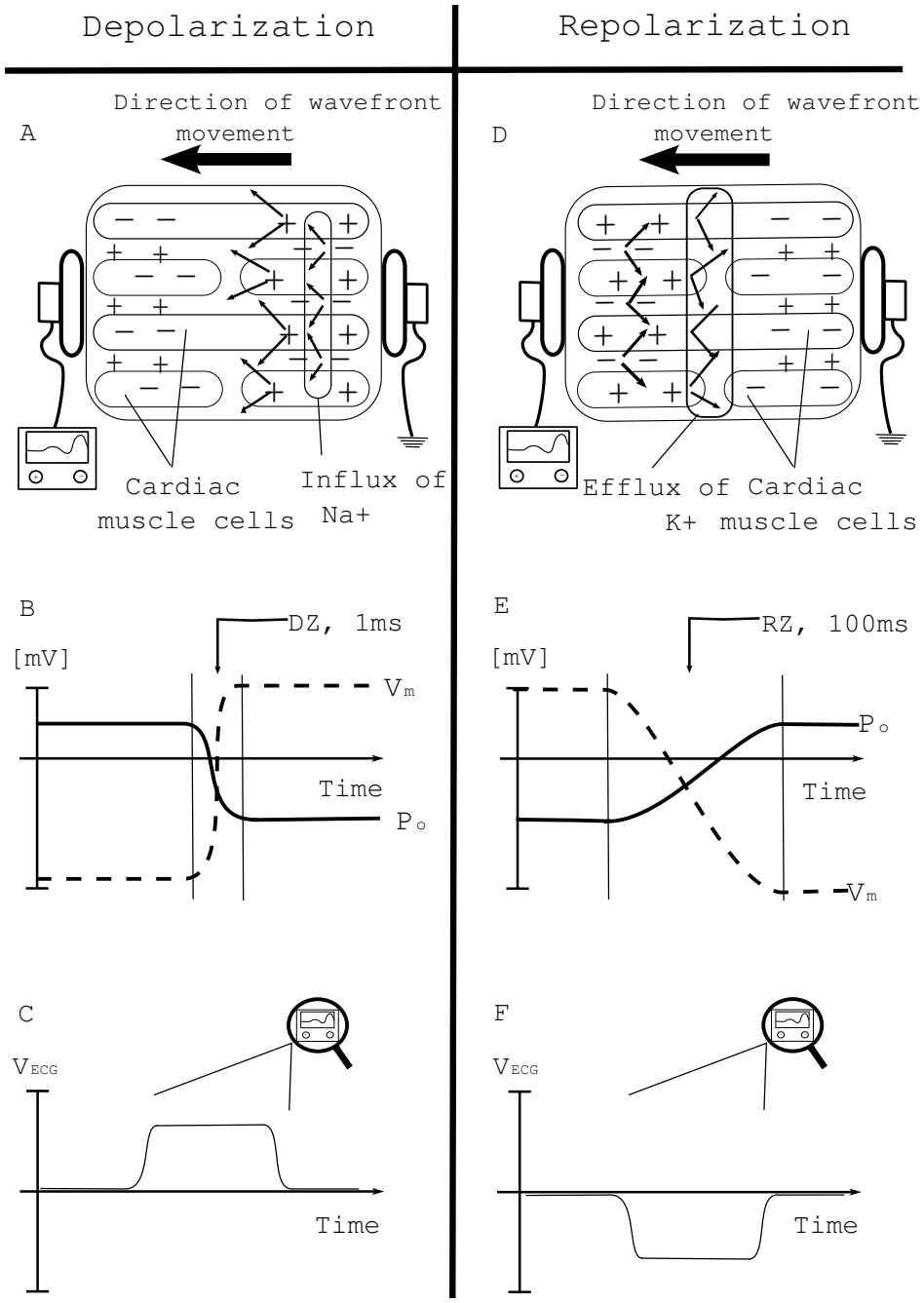

Figure 5.6: *A schematic illustration of the origin of ECG. Left column shows the depolarization phase and the right column shows the repolarization phase. The three rows show; the model of the cardiac cells, the changes in the extra cellular potential (P_o) and the transmembrane potential (V_m) and the ECG recorded by means of electrodes, respectively. Notice the time axes are not comparable. Simplified by inspiration of [26].*

given by:

$$\begin{bmatrix} x \\ y \\ z \end{bmatrix} = T_{ID} \begin{bmatrix} I \\ II \\ \vdots \\ V_5 \\ V_6 \end{bmatrix} \tag{5.1}$$

where the left side is the three dimensional coordinates of the VCG. The matrix on the right side contains the ECG leads. The matrix T_{ID} is e.g. Inverse Dower transformation matrix [43], which contains data yielding the linear transformation of the ECG data from temporal to spatial information. By plotting the x, y, z-coordinates in the space yields a VCG as shown in figure 5.7. [41, 42] The VCG consist of three loops (ellipses); QRS, P and T respectively. The main axis of the ellipses are directed toward the largest amount of muscle (left ventricle). The largest loop is the ORS-loop corresponding to the depolarization of the left ventricle.

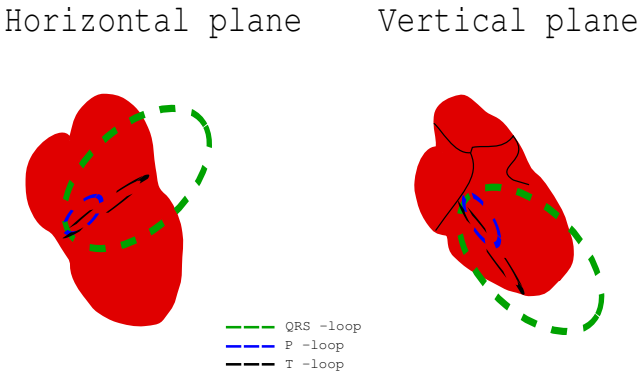

Figure 5.7: *Normal VCG in horizontal and vertical plane.*

Chapter 6

ECG as a tool for diagnosis

In this chapter the aim is to investigate the options of ECG in clinical practice. The last chapter was technically, this chapter is more clinically. The first section is how a AMI look like on an ECG. And how it is possible to locate the area of occlusion by analysis of an ECG. Several studies has showed an early diagnosis of AMI has a positive impact on the outcome. The last section of this chapter is a review of the present literature on this issue.

6.1 The ECG in AMI

As aforementioned the RCA supplies the right ventricle, LAD supplies the anterior, lateral, septal and inferoapical parts of the left ventricle. LCX supplies the posterior, lateral and inferior parts of the left ventricle. Occlusions in RCA and LAD appear in the ECG as ST-elevation in the different leads, according to the location of the thrombosis. Occlusions in LCX are often difficult to find in standard 12-lead ECG, because they often appear without ST-elevation in the ECG. [44]

Anterior wall infarction

Typically an occlusion in the anterior wall will cause ST-elevation in the precordial leads V_2, V_3 and V_4. However elevation in other leads occur, in accordance with the specific branch of LAD where the occlusion is. [44]

Proximal occlusion of LAD, see figure 6.1 arrow 1, will hinder perfusion of the diagonal and 1. septal branch and cause ischemia in left ventricle and the septal wall. In the vertical plane ST-elevation occur in I, V_R and V_L, and ST-depression in V_F. In horizontal plane ST-elevation in V_1, V_2 and V_3, and ST-depression in V_5 and V_6.

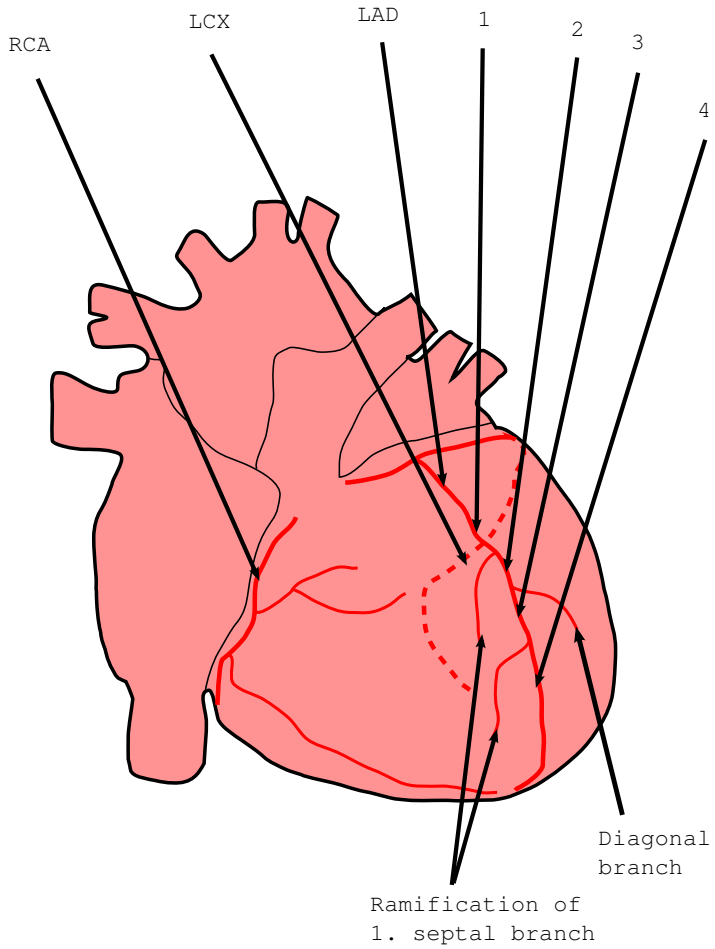

Figure 6.1: *frontal view of the heart. The coronary arteries; RCA, LAD and LCX and their main branches are depicted. The numbers indicate different locations of occlusion in LAD.*

Distal occlusion of LAD, see figure 6.1 arrow 4, will obstruct perfusion to the inferoapical area and induce ischemia. In the vertical plane ST-depression is seen in V_R, and in the horizontal plane ST-elevation is seen in V_2-V_5. [44]
The last two cases described is an inter-patient difference of ramification of the 1. septal branch. The ramification of septal branch can either be proximal or distal to the diagonal branch, see figure 6.1 arrow 2 and 3. [44]
If the 1. septal branch is located distal to the diagonal branch, and an occlusion occur intermediate of these branch (arrow 3 in figure 6.1), ischemia in the septal-apical area will be induced. In the vertical plane ST-depression in lead V_L, and in the horizontal plane ST-elevation is in the leads V_1-V_4. [44]
In patients where the 1. septal branch is located proximal to the diagonal branch (arrow 2 in figure 6.1), an intermediate occlusion will induce ischemia in the inferoapical area. In the vertical plane ST-depression in leads III and V_R. In the horizontal plane ST-elevation in leads V_2-V_6. [44]

Inferoposterior wall infarction

Occlusion in the RCA results in inferoseptal ischemia, and are reflected as elevations in the vertical plane in leads II and III. Since the ST-segment vector is directed toward lead III, the elevation is more pronounced in lead III than lead II, and also causing ST-depression in lead I and V_L. [44]
Occlusions in LCX, cause ischemia in posterolateral area, and the ST-segment vector is pointing toward lead II. The ST-elevation is therefore more pronounced in lead II than lead III, but often occlusions in LCX do not show any ST-elevation on ECG.
All the different patterns in ST-elevation/depression in different location of the occlusions in vertical and horizontal planes are summarized in table 6.1 for convenience. [44]

	Anterior wall				Inferoposterior wall	
	Prox.(1)	Dis.(4)	Sep.(3)	Sep.(2)	RCA	LCX
I	↑				↓	
II					↑	↑ II>III
III				↓	↑ III>II	↑
VR	↑	↓		↓		
VL	↑		↓		↓ VL>I	
VF	↓			↑		
V1	↑		↑			
V2	↑	↑	↑	↑		
V3	↑	↑	↑	↑		↓
V4		↑	↑	↑		↓
V5	↓	↑		↑		
V6	↓			↑		

6.2 The impact of early diagnosis of AMI

Early diagnosis of AMI is recommended by the American Heart Association and others [45–47]. The recommendation is based on several studies investigating the impact of early diagnosis of AMI on the outcome of the treatment. To encourage early diagnosis, pre-hospital ECG components are often used. These are integrated in existing devices in ambulance e.g. defibrillators. The ECG is acquired on the spot with least possible delay, and provides an strong diagnostic tool. The ECG can be interpreted by special trained paramedic [48, 49] or transmitted by electronic communication line to a cardiologist for analysis [50]. During the transportation to the hospital, the cardiologist can decide a proper treatment or require further investigation of the patient to comply with the most suitable treatment. The pre-hospital ECG has shown equal precision as ECG obtained in hospital [51–53].

An work group in the National Heart Attack Alert Program recommended, benchmarks on the treatment of AMI from the onset of symptoms to initial treatment of the patient. They recommended reperfusion treatment within 60 min of symptoms onset or within 30 min of the arrival at hospital. [54]
These benchmarks are based on studies investigating the impact of early diagnosis of AMI for the outcome of the treatment. The studies had reported an early diagnosis of AMI improved the outcome of the treatment [55–60]. The results of Boersma et. al showed the mortality rates can be lowered with 6.5 % if the reperfusion is initiated within the first hour. By prolonging the time to reperfusion increases the mortality rate and after 12 hours of the symptom onset the reperfusion therapy is no longer effective [58]. And DeLuca showed the one-year mortality is increased by 7.5 % for each half an hour of delay before initial treatment [59].
An effective way of reducing the initial treatment time is by letting the paramedics analyze the pre-hospital ECG on the spot, and decide the most suitable hospital center for treatment. The so called door-to-balloon time (entering hospital to PCI) was reduced form 112 min to 58 min by letting the paramedics analyze the ECG [56]. The mortality rate was 0 % in MI patients identified by paramedics and in the compared group of MI patients, the mortality rate was 4.3 % [57].

Chapter 7

Discussion

7.1 Summary of analysis

Acute Myocardial Infarction (AMI) is sudden onset of myocardial necrosis due to the formation of a thrombosis in the coronary arterial system, obstructing arterial blood flow to the cardiac muscle [2].
The incidence rates of AMI in USA is reported to be approximately 40-50 cases per 10,000 persons [4,5] and in northern Europe similar rates have been reported [8].
The economical cost of diagnosis, treatment and rehabilitation of AMI, amounts to a significant portion of the total budget of the health care expenses. In Denmark expenses of AMI is in the range of 6.3 % - 7.5 % of the total health care expenses in the five regions [20].
The ECG is a strong diagnostic tool and presents useful information for the physician about the electrical conductivity of the heart. An occlusion of one of the coronary arteries is reflected in an ECG, as an elevation of the isoelectric ST-segment. In order to the location of the occlusion, ST-elevation will appear in different leads on the ECG.
Early diagnosis of AMI is recommended by the American Heart Association and others [45–47], and is based on several studies. Boersma et. al showed the mortality rates can be lowered with 6.5 % if the reperfusion is initiated within the first hour [58], and DeLuca showed the one-year mortality is increased by 7.5 % for each half an hour of delay before initial treatment [59].
The main hindrance of an early diagnosis of AMI is the presence of a specialist to correct interpret the ECG in the initial state of symptom onset. Therefore are algorithms to automatic detect AMI in an early state been developed.

7.2 Review of previous work on automatic detection algorithm for AMI

Several study groups have dealt with automatic detection algorithm for AMI, with varying success. Some groups are succeed with commercializing there algorithm, but without widely acceptance in the clinical practice. This review includes some of the main publication, and the purpose with the review is to identify the limitation of the previous studies in this field.
The previous work in the field of automatic detection of AMI can be roughly sub-divided in three groups:

Decision support Decision support system relying on quantitative and qualitative parameters.

Body surface mapping Mapping the electrical potentials on the surface, in high resolution.

Morphology Systems based on ECG morphology analysis.

Decision support

The algorithms in this group are mainly based on neural network, probability models or regression models [61–64].
Xue et al. developed a neural network model, where the input parameters were different features of the ECG and VCG and qualitative parameters as age and gender. They compared the emergency physicians ability to diagnose AMI correct with the assistance of the system and without the assistance of the system. With the assistance of the system the emergency physicians improved their sensitivity by 50 %. [61] Other decision support systems rely on parameters such as biochemical markers, and qualitative parameters as age gender and symptoms. The strength of decision support systems are they include both quantitative and qualitative parameters, which is may assumed to be non-correlated. The main limitation of these systems is the number of input parameter and the easiness of obtaining the parameters. E.g. some of the systems include biochemical markers [62–64], and the determination of the concentration of different biochemical markers in the blood is only possible after the arrival to the hospital. The critical time interval from the symptom onset is therefore wasted on transportation only, without attempting to diagnose the AMI.

Body surface mapping

Body surface mapping (BSM) is a technique where the standard 12-lead ECG is replaced with a electrode grid with e.g. 80 electrodes or more. By

applying an electrode grid on the thorax (anterior) and on the back (posterior) high resolution mapping of the surface electrical potentials is possible. Owens et al. developed a algorithm based on BSM [65]. The input parameters in their model were features derived for the BSM. The performance of their model was compared with the performance of the physician. The sensitivity/specificity for the physicians were 60 %/ 99 %, respectively and the sensitivity/specificity for the algorithm 77 % / 99 %, respectively. By letting the physicians make the diagnosis supported by the developed algorithm, the sensitivity increased to 85 %, and they concluded the model is suitable for diagnosing patients with non-diagnostic ECG in particular. [65] The strength of the BSM is the advantages of the high resolution mapping of the electrical potentials, and the concept is evaluated and found better in diagnosing AMI [65–68], than standard 12-lead ECG. However the limitation of the concept of BSM is too cumbersome in clinical practice, and has never gained acceptance [69].

ECG morphology analysis

ECG morphology analysis is based on the technical fields of signal processing and pattern recognition.

Different approaches to morphology analysis of ECG have been tested. One study analyzed the temporal changes in ST-segment, to detect known periods of coronary occlusion. By means of sampling continuously ECG, they defined three time points to evaluate ST-segment changes in the ECG. With at set up of simplified rules for the ST-segment changes they classified the patients in three groups; occluded, indeterminate and patent. The performance of their algorithm was very well, but they concluded that the selection of the lead of interest was done manually, and the lead of interest varied over the precordium with the artery occluded. [70, 71]

Similar study was set up by Fiol et al., however their aim was to differentiate between occlusion in the RCA and LCX in contrary to [70, 71]. Further Fiol et al. made predefinition of the leads of interest included in the morphology analysis. The leads included were I, II, III, V_1-V_3 and aVF. They concluded the performance of their algorithm yield a good sensitivity and specificity but only for occlusion in RCA. [72]

Lehmann et al. conducted a more comprehensive study [73], where they extended the standard 12-lead ECG with the right precordial leads V_3R-V_6R and the posterior leads V_7-V_9. In the statistical analysis of the ECG morphology, ST-elevation/depression, presence of Q-wave, presence of positive or negative T-wave and R-wave were taken into account. The true classification of occlusion in LAD, RCA and LCX was 84 %, 74 % and 71 %, respectively. However they did only include patients with angiographically confirmed AMI in this study, and therefore were not able to test the speci-

ficity of the algorithm. Based on their own results and another study [74], they concluded the detection of an occlusion in LAD was the least cumbersome, and the differentiation was more complicated when RCA and LCX were involved. An review of the literature on the issue of differentiating between RCA and LCX reveal no consensus about the ECG morphology parameters to include in the statistical calculations. No robust algorithm to detect both inferior and posterior infarctions has yet been developed, and is the main disadvantage of these studies [75–79]. By means of the 12 standard leads it is possible to automatic detect occlusion in LAD, but to differentiate between occlusion in RCA and LCX several studies have proved the necessity of posterior leads [76, 80–86]. But the application of the posterior leads in the clinical practice is cumbersome and have not gained acceptance, therefore algorithms including measured posterior leads are not desired in clinical practice. Therefore the most suitable solution will may be an algorithm based on the standard 12-lead ECG, where the posterior leads can be derived and analyzed for differentiating between occlusion in RCA and LCX.

7.3 Aim

The aim of the study is to develop an algorithm to automatic detection of AMI, based on 12-lead ECG. The first intermediate aim is to develop a linear model to derive the posterior leads by means of the precordial leads. The second intermediate aim is develop an algorithm based on the 12-lead ECG and the derived posterior leads to automatic locate the presence or an absence of an occlusion in LAD, RCA and LCX.

Chapter 8

Method

8.1 Mathematical consideration of transformation matrix

The linear transformation of the standard leads to the posterior leads is only possible if the heart is assumed as a dipole with a fixed location and variable orientation and magnitude. The surrounding tissue e.g. lungs, adipose tissue and bone together is assumed as a infinite homogenous conductor [87].
The recorded leads are a projection of the electrical resultant vector of the heart on the lead vector formed by the location of the electrodes.

The electrical resultant vector of the heart is depicted as an yellow arrow, on figure 8.10, top. The lead vectors are depicted as blue vectors in the frontal plane, bottom. The projections on leads I, II and III are marked with red arrows. In matrix convention the projection is given as

$$\mathbf{v} = \mathbf{l}^T \mathbf{R}_e \tag{8.1}$$

where $\mathbf{v}$ is the matrix containing the recorded potentials, $\mathbf{l}$ is the denotation of the lead vectors and is constant. $\mathbf{R}_e$ is the electrical resultant vector of the heart and is time dependant.

X, Y, Z-transformation

The transformation of the standard 12-lead ECG to X, Y, Z-signal is used as a control step before transforming 12-lead ECG to posterior leads, see figure 8.2.

The transformation of 12-lead ECG to X, Y, Z-signal is a reduction of redundant data. The transformation is given by

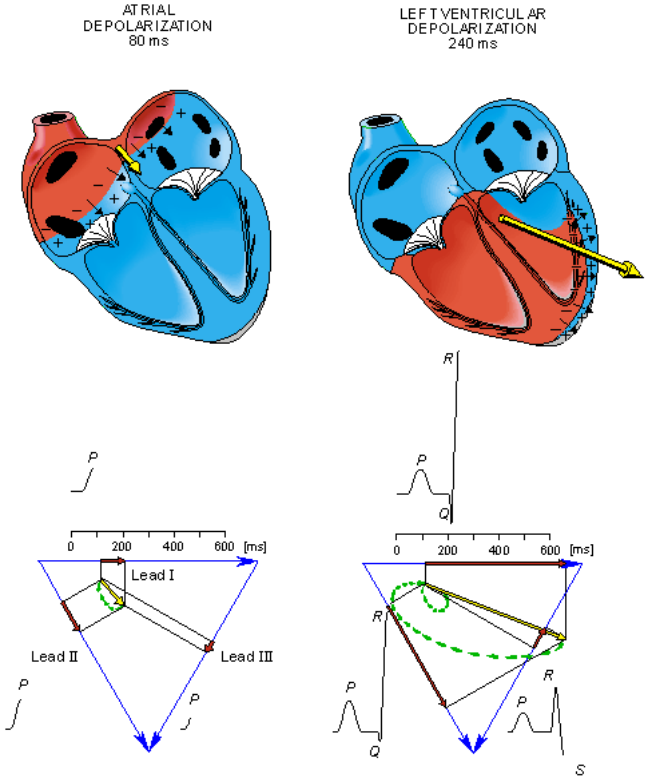

Figure 8.1: *Schematic illustration of projection of the electrical resultant vector of the heart on the lead vector I, II and III. [40]*

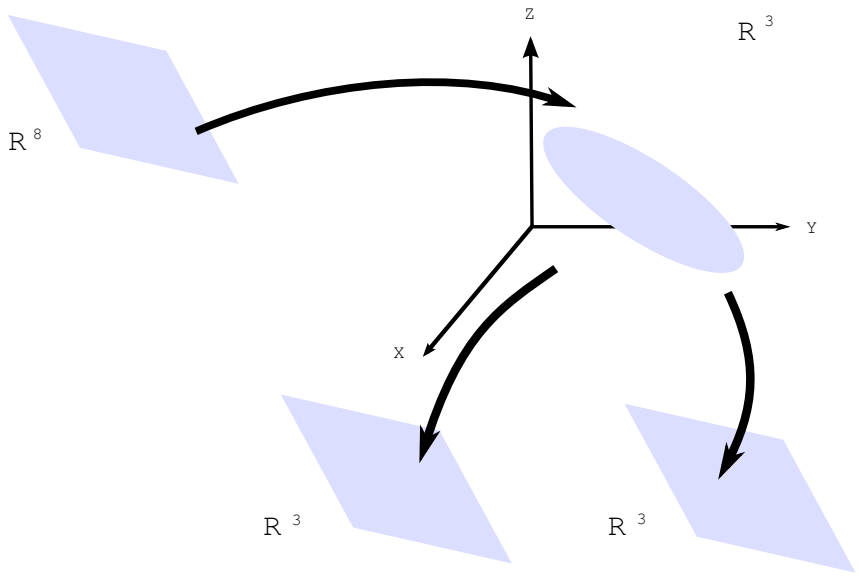

Figure 8.2: *The figure illustrates the steps of transformations. The standard leads can be assumed as matrix with eight time dimensions. It is transformed in to a 3-dimensional space also termed X,Y,Z-signal. The X,Y,Z-signal is further transformed (back) into two separate three time dimensions. This figure shows two final time space, while we chose to derive the posterior leads $V7$-$V12$ in two different trials.*

$$\mathbf{V_{xyz}} = \mathbf{T_{inv}}\mathbf{V}_s \tag{8.2}$$

where $\mathbf{V_{xyz}}$ containing the 3-dimensional coordinates of the vector loops ($3xn$ matrix). $\mathbf{T_{inv}}$ is the improved inverse transformation matrix, described in [61] ($3x8$ matrix). And $\mathbf{V}_s$ is the matrix containing the eight measured standard leads ($8xn$ matrix).
In ischemic conditions the heart will not perform as homogeneous dipole model, and this will cause disturbed vector loops.

Posterior-transformation

Since the $\mathbf{R}_e$ is the underlying cause of the potentials measured on the surface, determination of $\mathbf{R}_e$ is required for deriving the posterior leads. By means of three independent leads, it is possible to determine the magnitude of $\mathbf{R}_e$ for different time instance. Given that the vector $\mathbf{l}$ is column vector with three elements, $\mathbf{R}_e$ is given by

$$\mathbf{R}_e = (\mathbf{L}^T)^{-1}\mathbf{V} \tag{8.3}$$

where $L = (l_I, l_{II}, l_{III})$ and $V = (v_I, v_{II}, v_{III})^T$. In fact lead III is not independent but derived from leads I andIII. For convenience in this section we a assume III is independent. By substituting $\mathbf{R}_e$ in equation 8.26 with

equation 8.27

$$\mathbf{v} = \mathbf{l}^T(\mathbf{L}^T)^{-1}\mathbf{V} \tag{8.4}$$

$\Updownarrow$

$$\mathbf{v} = \mathbf{aV} \tag{8.5}$$

In standard ECG only eight of the 12 leads are independent (I, II, $V1$, ... $V6$). Transforming this fact in to $\mathbf{a}$ in equation 8.29 yields

$$\mathbf{a} = \mathbf{l}^T(\mathbf{L}\mathbf{L}^T)^{-1}\mathbf{L} \tag{8.6}$$

Determination of $\mathbf{a}$ can be performed by measuring the standard leads. However in our case we use the derived X, Y, Z-signal from equation 8.2. Transforming formula 8.29 to a computational equation containing X, Y, Z-signal yields

$$\mathbf{V}_p = \mathbf{A}\mathbf{V}_{xyz} \tag{8.7}$$

where p and xyz refer to the derived posterior leads and X, Y, Z-signal, respectively. The unknown $\mathbf{A}$ contains the coefficients of transformation.

$$\mathbf{A} = (\mathbf{V}_{xyz}\mathbf{V}_{xyz}^T)^{-1}\mathbf{V}_{xyz}^T\mathbf{V}_p \tag{8.8}$$

Statement of the matrix dimension

We expect the dimension of the matrix $\mathbf{A}$ must be 3x3, because we have three independent leads (X, Y, Z) and desire to determine three unknown leads.
Let us assume that the $\mathbf{V}_{xyz}$ is of dimension $nx3$, where n is the number of samples and the three coordinates i space. $\mathbf{V}_p$ is of dimension $nx3$, the three posterior leads. $\mathbf{V}_{xyz}^T$ is $3xn$. Therefore the dimension of statement in parentheses $(\mathbf{V}_{xyz}^T\mathbf{V}_{xyz})^{-1}$ is $3x8$. Dimension of $\mathbf{V}_{xyz}^T\mathbf{V}_p$ is $3x3$. Then the dimension of the matrix $\mathbf{A}$ in equation 8.33 is $3x3 \cdot 3x3 = 3x3$.

The deviation of the model

The evaluation of the transformation matrix, was made by a comparison of the measured posterior leads and the derived posterior leads. The difference between the measured and derived is calculated for each sample, and then averaged by the total number of samples. The average error of the derived posterior leads is given by

$$E_{ave} = \frac{1}{n}\sum_{i=1}^{n}(|V_i^{measured} - V_i^{derived}|) \tag{8.9}$$

If $Error_{ave} = 0$ then the model is ideal.

8.2 Computational considerations

When computing the regression model all the ECG's measured were merged together in three matrices containing $[I, II, V1 \dots V6]$, $[V7 \dots V9]$ and $[V10 \dots V12]$, respectively. By merging the data we assumed all the data is recorded under same surrounding conditions. The data is given in matrix notation

$$V_s = \begin{bmatrix} I_{1,1} & II_{1,1} & V1_{1,1} & \dots & V6_{1,1} \\ \vdots & \dots & \dots & \dots & \vdots \\ I_{5,1} & II_{5,1} & V1_{5,1} & \dots & V6_{5,1} \\ \vdots & \dots & \dots & \dots & \vdots \\ I_{1,j} & II_{1,j} & V1_{1,j} & \dots & V6_{1,j} \\ \vdots & \dots & \dots & \dots & \vdots \\ I_{5,j} & II_{5,j} & V1_{5,j} & \dots & V6_{5,j} \end{bmatrix}$$

$$V_{7-9} = \begin{bmatrix} V7_{1,1} & V8_{1,1} & V9_{1,1} \\ \vdots & \dots & \vdots \\ V7_{5,1} & V8_{5,1} & V9_{5,1} \\ \vdots & \dots & \vdots \\ V7_{1,j} & V8_{1,j} & V9_{1,j} \\ \vdots & \dots & \vdots \\ V7_{5,j} & V8_{5,j} & V9_{5,j} \end{bmatrix}$$

where j denotes the total number of subjects included in the regression model. The notation for the leads V_{10-12} are trivial and are not shown.
When merging data, edge distortion will appear, see figure **??**.

But in our study this was not of concern, because we were only interested in the correlation between a certain data point in the independent variable and the corresponding data points in the dependant variables. The edge distortion should be of concern if some spectral analysis of the merged signal were performed.

8.3 Post-processing of the derived signal

The transformation described above is actually a reduction or compression of the signal in the time domain. In frequency domain the signal is low-

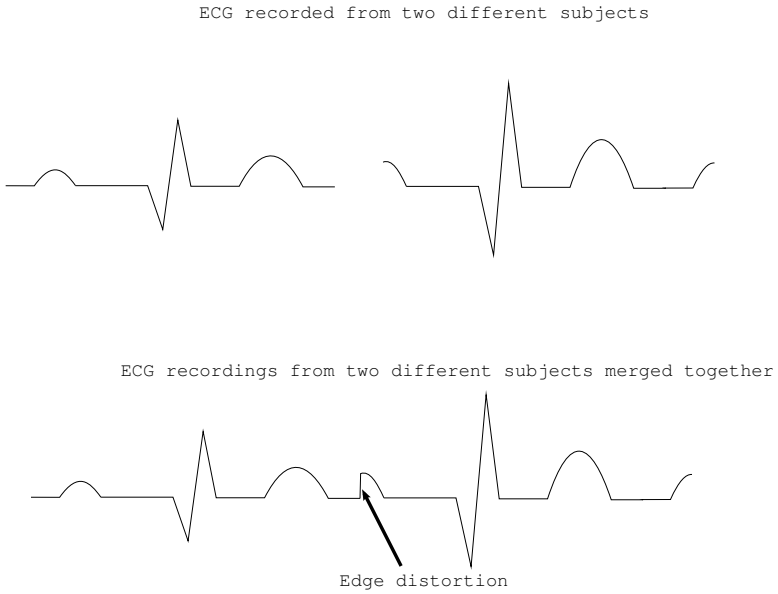

Figure 8.3: *Edge distortion can appear when data is merged.*

pass filtered, and applicable information in the signal may be removed. To restore the high frequency component we applied a frequency domain filter to restore the derived signal.

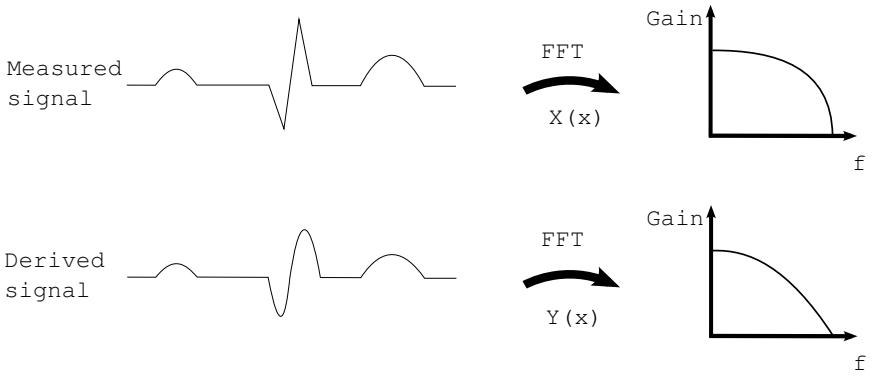

Figure 8.4: *The difference in the frequency components of the derived and measured signal.*

The derived signal has a sharper attenuation in the higher frequency band then the measured signal, for schematic illustration see figure 8.4. Since we assume the system as a linear time invariant system following relationship exist

$$Y(x) = H(z)X(z) \tag{8.10}$$

where the $Y(z)$ is the fourier transform of the derived signal, $X(z)$ is the fourier transform of the measured signal and $H(z)$ is the transfer function.

By determining the transfer function and applying to the derived signal, we were able to restore the high frequency components of the signal.

$$H(z) = Y(z)^{-1}_{derived} X(z)_{measured} \tag{8.11}$$

$$X(z)^{restored}_{derived} = H(z)^{-1} Y(z)_{derived} \tag{8.12}$$

8.4 Least square estimator

The linear transformation of the standard leads to the posterior leads is only possible if the heart is assumed as a dipole with a fixed location and variable orientation and magnitude. The surrounding tissue e.g. lungs, adipose tissue and bone together is assumed as a infinite homogenous conductor [87].
The recorded leads are a projection of the electrical resultant vector of the heart on the lead vector formed by the location of the electrodes.

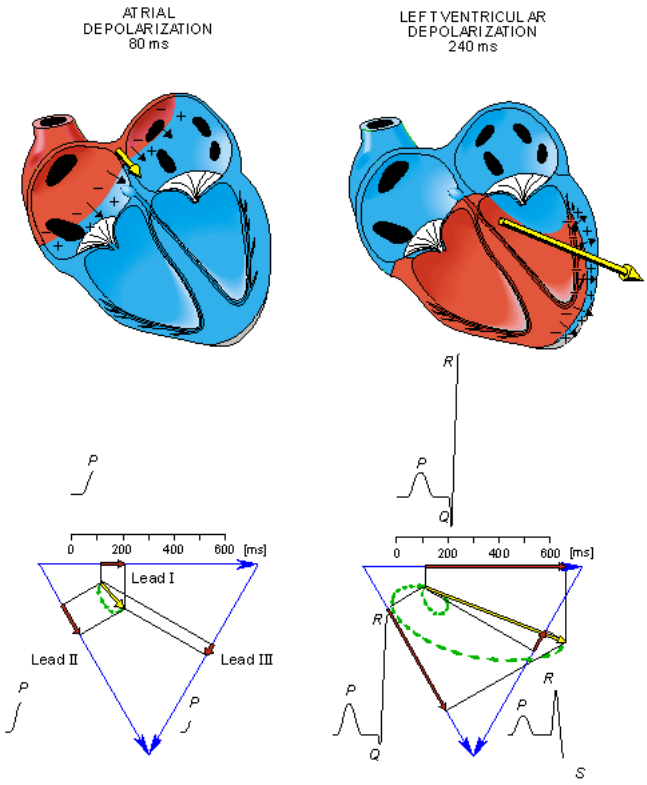

Figure 8.5: *Schematic illustration of projection of the electrical resultant vector of the heart on the lead vector I, II and III. [40]*

The electrical resultant vector of the heart is depicted as an yellow arrow, on figure 8.10, top. The lead vectors are depicted as blue vectors in the frontal plane, bottom. The projections on leads I, II and III are marked with red arrows. In matrix convention the projection is given as

$$\mathbf{x}_i = \mathbf{l}_i^T \mathbf{r}_e \tag{8.13}$$

where $\mathbf{x}_i$ is the vector containing the recorded potentials (i, refers to the lead of interest), $\mathbf{l}$ is the denotation of the lead vector and is constant. $\mathbf{r}_e$ is the electrical resultant vector of the heart and is time dependant.

Least square estimators

By the model showed in figure 8.6, the output $Y(t)$ (the posterior leads) is determined by weighting the measured standard leads $x_1(t)$-$x_8(t)$.

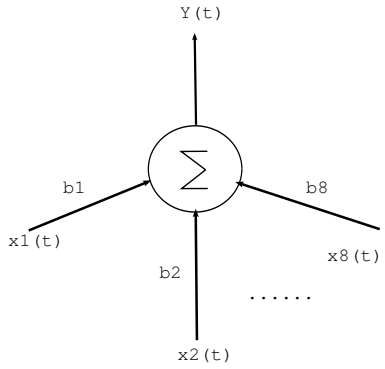

Figure 8.6: *Schematic illustration of the concept of multiple linear regression. [Inspired by the simplicity of Johannes J. Struijk' way of thinking☺]*

The relationship can be expressed algebraic

$$Y(t) = B\mathbf{X}(t) \tag{8.14}$$

The coefficients of B are estimated by minimizing the error between the calculated output $\widehat{Y}(t)$ and the measured output $Y(t)$. The sum of squares of error is

$$SSE = \sum_{p=1}^{k} \sum_{t=1}^{n} (Y_p(t) - \widehat{Y}_p(t))^2 \tag{8.15}$$

⇕

$$SSE = \sum_{p=1}^{k}\sum_{t=1}^{n}(Y_p(t) - B_0 + B_1 x_{p,1}(t) + B_2 x_{p,2}(t) \ldots + B_8 x_{p,8}(t))^2 \quad (8.16)$$

Where t denotes the time and $(p, \#)$ denotes the patient and the number of lead. To minimize the SSE, the partial derivatives of equation 8.16 with respect to B_0-B_8 is found and the derivatives are solved equal to 0. [88]

$$\frac{\delta SSE}{\delta B_0} = \sum_{p=1}^{k}\sum_{t=1}^{n}(Y_p(t) - B_0 + B_1 x_{p,1}(t) + B_2 x_{p,2}(t) \ldots + B_8 x_{p,8}(t)) \quad (8.17)$$

$$\vdots$$

$$\frac{\delta SSE}{\delta B_8} = \sum_{p=1}^{k}\sum_{t=1}^{n} x_{p,8}(t)(Y_p(t) - B_0 + B_1 x_{p,1}(t) + B_2 x_{p,2}(t) \ldots + B_8 x_{p,8}(t))$$

Rewriting the partial derivatives yields

$$\sum_{p=1}^{k}\sum_{t=1}^{n} Y_p(t) = knB_0 + B_1 \sum_{p=1}^{k}\sum_{t=1}^{n} x_{p,1}(t) + \ldots B_8 \sum_{p=1}^{k}\sum_{t=1}^{n} x_{p,8}(t) \quad (8.18)$$

$$\vdots$$

$$\sum_{p=1}^{k}\sum_{t=1}^{n} x_{p,8}(t)Y_p(t) = B_0 \sum_{p=1}^{k}\sum_{t=1}^{n} x_{p,8}(t) + B_1 \sum_{p=1}^{k}\sum_{t=1}^{n} x_{p,8}(t)x_{p,1}(t) + \ldots B_8 \sum_{p=1}^{k}\sum_{t=1}^{n} x_{p,8}^2(t)$$

For convenience the equations 8.18 can be written in matrix notation. The general linear relationship is given by

$$\mathbf{Y} = \mathbf{BX} \quad (8.19)$$

When incorporating the time variable and the patient variable, the matrices $\mathbf{Y}$ (single column matrix), $\mathbf{B}$ (single column matrix) will be three dimensional matrices. While matrix $\mathbf{X}$ is a nine dimensional matrix. In figure 8.7 this concept is illustrated schematically. The axis represent the time dimension, the patient dimension and the lead dimension. Notice the lead dimension is a non-figurative axe. Actually it represents eight dimension on one axe, unlike the time and patient dimension which represents only one dimension on each axis.

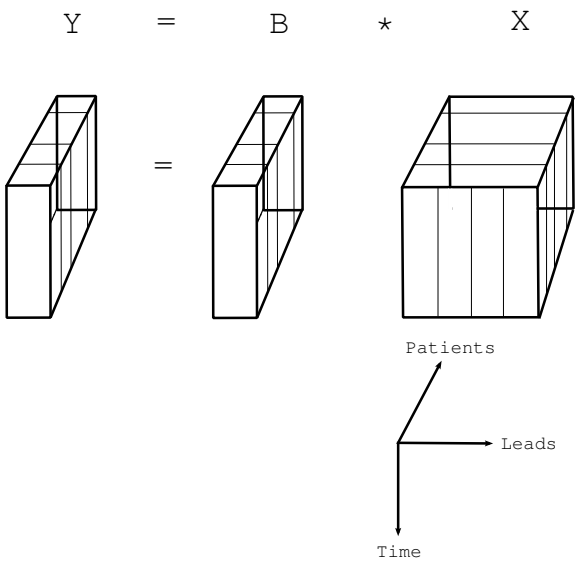

Figure 8.7: *Illustration of the dimensions of the matrices.*

The equations in 8.18 written in matrix notation

$$\mathbf{X}'\mathbf{Y} = \mathbf{X}'\mathbf{X}\mathbf{B} \tag{8.20}$$

Assuming that $(\mathbf{X}'\mathbf{X})^{-1}$ is invertible, then

$$\mathbf{B} = (\mathbf{X}'\mathbf{X})^{-1}\mathbf{X}'\mathbf{Y} \tag{8.21}$$

The expression in 8.21 is actually the same as an Wiener filter. The nominator is the cross-correlation of the signal $\mathbf{X}$ and $\mathbf{Y}$ and the denominator is the auto-correlation of the signal $\mathbf{X}$. [89]
Let us assume the formula 8.21, is presenting the way to determine the coefficient matrix $\mathbf{B}_p$ with respect to intra-patient variation. Then the determination of the coefficient matrix $\overline{\mathbf{B}}$ with respect to inter-patient variation is

$$\overline{\mathbf{B}} = \frac{1}{k}\sum_{p=1}^{k}\mathbf{B}_p = \frac{1}{k}\sum_{p=1}^{k}(\mathbf{X}_p'\mathbf{X}_p)^{-1}\mathbf{X}_p'\mathbf{Y}_p \tag{8.22}$$

The goodness of fit can be determined by the coefficient of determination R^2

$$R^2 = \frac{SST}{SSR} = \frac{\sum_p\sum_t(\widehat{Y}_p(t) - \overline{Y}_p)^2}{\sum_p\sum_t(Y_p(t) - \overline{Y}_p)^2} \tag{8.23}$$

8.5 Significance test of independent variables

The question of adding independent variables to the regression model yields more information to our model is important to reduce redundant or noise in the model. To test the significance of the added variable a F-test is conducted.
The null hypothesis:

$H_0 : \beta_{a1} = \beta_{a2} \ldots = \beta_{aP}$

And the alternative hypothesis:

H_1 : At least one $\beta \neq 0$

At significance level α the H_0 is rejected if:

$$\frac{\frac{SSE' - SSE}{P_1}}{\frac{SSE}{n-P-1}} > F_{K_1, n-K-1, \alpha} \tag{8.24}$$

8.6 Segmentation

The aim of this analysis was to investigate the regression coefficients in a segment wise regression of the median beat consisting of P-, QRS-, and T-wave.
The analysis was divided into three parts; determination of the mean duration of P-, QRS-, and T-waves, segmentation of ECG and finally calculation of the regression coefficients.

Segment duration

The segmentation of ECG did not require exact segmentation of the waves, but the most important issue was to make algorithm to detect the waves and exclusion of intermediary signals between the waves were not highly desired. The mean signal of the independent leads were determined to detect the time index of the peaks of P-, QRS-, and Twave for each person and each measurements.
The QRS-segment was defined as 70 milliseconds before and after the maximum value in the median beat. One sample corresponds to 2.4 milliseconds. The start point of the ST-T segment was defined as the end point of QRS-segment plus one sample. And the end point was defined as 192 milliseconds after the maximum of T-wave.

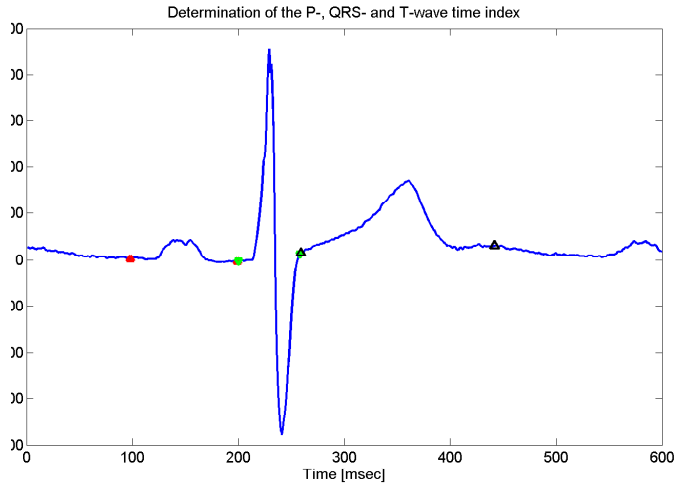

Figure 8.8: Figure shows an example of the time indexes of the independent mean beat is given. Red upward triangles indicate the P-segment, green downward triangles indicate the QRS-segment and the black upward triangles indicate the ST-T-segment.

The start point of P-wave was defined as 108 milliseconds before the maximum of P-wave. The end point of P-wave was defined as the start point of QRS-wave minus one sample. In figure 8.8 an example of the time indexes of the independent mean beat is given. Red upward triangles indicate the P-segment, green downward triangles indicate the QRS-segment and the black upward triangles indicate the ST-T-segment.

Segmentation of ECG

For each person and each measurements the time indexes of the P-, QRS-, and T-wave were used to segment the independent leads, and an example of the segmentation is shown in figure 8.9

Determination of regression coefficients

Regression coefficients for each posterior lead and for each segment was determined i.e. 18 sets of regression coefficients. The regression coefficients were determined according to expression 8.21.

Analysis of the magnitude range and segmentation

The ECG recordings of all subjects in the subset were merged into one large data set and were considered as one data recording. The maximum and minimum magnitude value of the pooled data set was found and graphically depicted as ranges for all measured leads. Q-Q plots of the ECG data from the 14 leads were generated and analyzed. To obtain a better approxima-

tion to the normal distribution, the ECG's of the subset were segmented into P-waves, QRS-complexes and T-waves, with respect to all leads. The segmentation algorithm is described in citeandersen. The P, QRS and T segments were pooled into large data sets, in correct subject order for the 14 leads. New Q-Q plots were generated and a better approximation to the normal distribution was achieved. The means and the standard deviations of the segments for the standardization procedure were determined.

Standardized beta coefficients

Standardized beta coefficients (SBC) are useful when comparisons of the independent variables in the regression model are of interest. The SBC are determined in the same matter as the regressions coefficients derived in formula 4, see [90]. However in the SBC model, the independent variables are standardized in order to their mean and their standard deviation, as follows:

$$z_{i,n} = (x_n - \mu_i)/\sigma_i \tag{8.25}$$

,where i denotes the number of the lead, and n the sample index. Next to the standardization, partial regression models for each posterior lead and for each segment were determined.

8.7 Data acquisition protocol

Background

Acute myocardial infarction (AMI) is one of the main leading causes of death in the western countries [3]. AMI is a occlusion of the coronary arteries by a thrombus, which cause necrosis due lack of blood perfusion. The main symptom of AMI is severe pain in the chest region with radiation to the upper limbs and neck [31].
The electrocardiogram (ECG) is a strong diagnostic tool in diagnosing AMI. An occlusion of one of the coronary arteries is reflected in an ECG, as an elevation of the isoelectric ST-segment. In order to the location of the occlusion, ST-elevation will appear in different leads on the ECG. Simplified the occlusion can occur in; the left anterior descending branch (LAD), the right coronary artery (RCA) or the left circumflex artery (LCX). Table 8.1 shows in which leads the ST-elevation will appear in order to the different locations of the thrombus.

According to the table 8.1, the presence of a thrombus in RCA or LCX will cause a ST-elevation in the standard leads II and III. To differentiate

	Occlusion in		
	LAD	RCA	LCX
ST-Elev./Dep.	V_2	II	II
	V_3	III	III
	V_4		

Table 8.1: The table is a simplified representation of the occurrence of ST-elevation in different leads in order to the location of the thrombus. In an occlusion of RCA the ST-elevation is mostly represented in lead III. In an occlusion of LCX the ST-elevation is mostly represented in lead II. [44]

between the two locations, it necessary compare the magnitude of the elevation in the two leads. For an occlusion in RCA, the ST-elevation will be most pronounced in lead II. For an occlusion in LCX, the ST-elevation will be most pronounced in lead III. Less than 50 % of the patients with AMI in LCX, present ST-elevation in ECG, therefore is ST-elevation in the lead III not a clinically significant finding of an occlusion of LCX [91,92]. Although in clinical practice posterior leads are not used as standard.

The precordial leads V_1-V_6 are sensitive to diagnose an occlusion in LAD and RCA, while an occlusion in LCX is insensitive to diagnose with the precordial leads [93–95]. Several studies had proposed extension of the standard 12 ECG with further three leads (V_7, V_8 and V_9) to obtain better assessment of the electrical activity of the posterior wall [80,96]. Additional posterior leads are generally accepted as an improvement of the ECG as a diagnostic tool for posterior wall infarction, as a consequence of the results from several studies investigating the impact of adding posterior leads to improve the sensitive of diagnosing occlusion in LCX [75,82–84,97]. As a lack insufficient mapping (with 12-lead EGC) of the electrical activity of the posterior wall, some cardiologists analyze possible ST-depression (indirect/inverse reflection) in the precordial leads V_3 and V_4 [98]. This indirect use of V_3 and V_4 may indicate further extension of the 15-lead ECG to 18-lead ECG, where the three new electrodes (V_{10}, V_{11} V_{12}) are placed on the right lateral side of the back.

Despite the fact that the extended 15-lead (or further) ECG is more sensitive to diagnose posterior wall infarction, only few ECG apparatus are dimensioned for this purpose, and further there are some practical issues concerning placement of the three additional electrodes on the back of a patient.

The aim of the study is to develop a mathematical model to derive the posterior leads V_7-V_{12} form a standard 12-lead ECG.

Method

Sample size

In this study ECG's from a group of 30 healthy persons without any history of heart diseases are included. The sample of the 30 persons must reflect the variation in the population in order to different kind of body shape, age and gender. The persons included are students and employees at Institute of Health Science and Technology, at Aalborg University.

Data acquisition

Before placement of the electrodes, cleaning of the skin with alcohol is required for better adhesion of the electrode. If the person is very hairy, shaving the area may be necessary. Placement of the posterior electrodes is done with the person standing. The placement of the precordial electrodes is in supine position. The anatomical placement of the 8 standard electrodes and the three additional posterior electrodes are listed below.

Right arm (RA) On right arm distal on radius.

Left arm (LA) On left arm distal on radius.

Left foot (LF) On left leg over lateral malleolus.

V1 Fourth intercostal space to the right of the sternum.

V2 Fourth intercostal space to the Left of the sternum.

V3 Directly between leads V_2 and V_4.

V4 Fifth intercostal space at midclavicular line.

V5 Level with V_4 at left anterior axillary line.

V6 Level with V_5 at left midaxillary line.

V7 Left lateral side of the back, over the posterior axillary line. (Same level as V_5)

V8 Left lateral side of the back, over the midscapular line. (Same level as V_5)

V9 Left lateral side of the back, half way between midscapular line and spine. (Same level as V_5)

V10 Right lateral side of the back, over the posterior axillary line. (Same level as V_5)

V11 Right lateral side of the back, over the midscapular line. (Same level as V_5)

V12 Right lateral side of the back, half way between midscapular line and spine. (Same level as V_5)

The ECG monitor (Brand, sampling, resolution??) used in this study is dimensioned for 12 channels, therefore only 15-lead ECG are available at each recording. Since the desire is to derive the three posterior lead (V_7-V_9) and the additional posterior leads (V_{10}-V_{12}) on the right side of the back, the recording procedure is conducted in two trials. In the first trial leads V_1-V_9 are measured. In second trial the leads V_7-V_9 are moved form the left side of the back to the right side of the back, and the leads recorded are now V_1-V_6 and V_{10}-VR_{12}. For each trial, 10 recordings of 10 seconds are acquired. During the recording the person is in a supine position, and can breath normally, but no movements of the body are allowed to avoid noise for the surrounding muscles.
Beside the recorded ECG, personal information as gender, birth day, weight and height are registered.

Determination of the transformation matrix for the posterior leads V_7-V_{12}

The linear transformation of the standard leads to the posterior leads is only possible if the heart is assumed as a dipole with a fixed location and variable orientation and magnitude. The surrounding tissue e.g. lungs, adipose tissue and bone together can be assumed as a infinite homogenous conductor [87]. The recorded leads are a projection of the electrical resultant vector of the heart on the lead vector formed by the location of the electrodes.

The electrical resultant vector of the heart is depicted as an yellow arrow, on figure 8.10 top. The lead vectors are depicted as blue vector in the frontal plane, bottom. The projections on leads I, II and III are marked with red arrows. In matrix convention the projection is given as

$$\mathbf{v} = \mathbf{l}^T \mathbf{R}_e \tag{8.26}$$

where $\mathbf{V}$ is the matrix containing the recorded potentials, $\mathbf{l}$ is the denotation of the lead vectors and are constant. $\mathbf{R}_e$ is the electrical resultant vector of the heart and is time dependant.
Since the $\mathbf{R}_e$ is the underlying cause of the potentials measured on the surface, it is valuable to determine $\mathbf{R}_e$ for further calculations. By means of three independent leads, it is possible to determine the magnitude of $\mathbf{R}_e$

for different time instance. Given that the $\mathbf{l}$ is column vector with three elements, the $\mathbf{R}_e$ is given by

$$\mathbf{R}_e = (\mathbf{L}^T)^{-1}\mathbf{V} \tag{8.27}$$

where $L = (l_I, l_{II}, l_{III})$ and $V = (v_I, v_{II}, v_{III})^T$. By substituting $\mathbf{R}_e$ in equation 8.26 with equation 8.27

$$\mathbf{v} = \mathbf{l}^T(\mathbf{L}^T)^{-1}\mathbf{V} \tag{8.28}$$

$$\Updownarrow$$

$$\mathbf{v} = \mathbf{a}\mathbf{V} \tag{8.29}$$

In standard ECG only eight of the 12 leads are independent (I, II, $V1$, ... $V6$). Transforming this fact in to $\mathbf{a}$ in equation 8.29 yields

$$\mathbf{a} = \mathbf{l}^T(\mathbf{L}\mathbf{L}^T)^{-1}\mathbf{L} \tag{8.30}$$

Determination of $\mathbf{a}$ can be performed by measuring the standard leads and in our case the posterior leads $V7$,...,$V12$. Transforming formula 8.29 to a computational equation yields

$$\mathbf{V}_p = \mathbf{A}\mathbf{V}_s \tag{8.31}$$

where p and s refers to the posterior leads and standard leads, respectively, and $\mathbf{A}$ contains the coefficients of transformation. The only unknown in equation 8.31 is $\mathbf{a}_{p,s}$.

$$\mathbf{A} = (\mathbf{V}_s^T\mathbf{V}_s)^{-1}\mathbf{V}_s^T\mathbf{V}_p \tag{8.32}$$

Statement of the matrix dimension

We expect the dimension of the matrix $\mathbf{A}$ must be 8x3, because we have eight independent leads and desire to determine three unknown leads.
Let us assume that the $\mathbf{V}_s$ is of dimension $nx8$, where n is the number of samples and the eight independent leads. $\mathbf{V}_p$ is of dimension $nx3$, the three posterior leads. $\mathbf{V}_s^T$ is $8xn$. Therefore the dimension of statement in parentheses $(\mathbf{V}_s^T\mathbf{V}_s)^{-1}$ is $8x8$, dimension of $\mathbf{V}_{standard}^T\mathbf{V}_p$ is $8x3$. Then the dimension of the matrix $\mathbf{A}$ in equation 8.33 is $8x8 \cdot 8x3 = 8x3$.

The deviation of the model

The evaluation of the transformation matrix, is made by a comparison of the measured posterior leads and the derived posterior leads. For the measured

posterior leads the average amplitude is determined. The average error of the derived posterior leads is given by

$$Error_{ave} = \frac{1}{n} \sum (V_{measured} - V_{derived}) \tag{8.33}$$

The average deviation is given as percentage error in order to the average amplitude of the measured posterior leads. If $Error_{ave} = 0$ then the model is ideal.

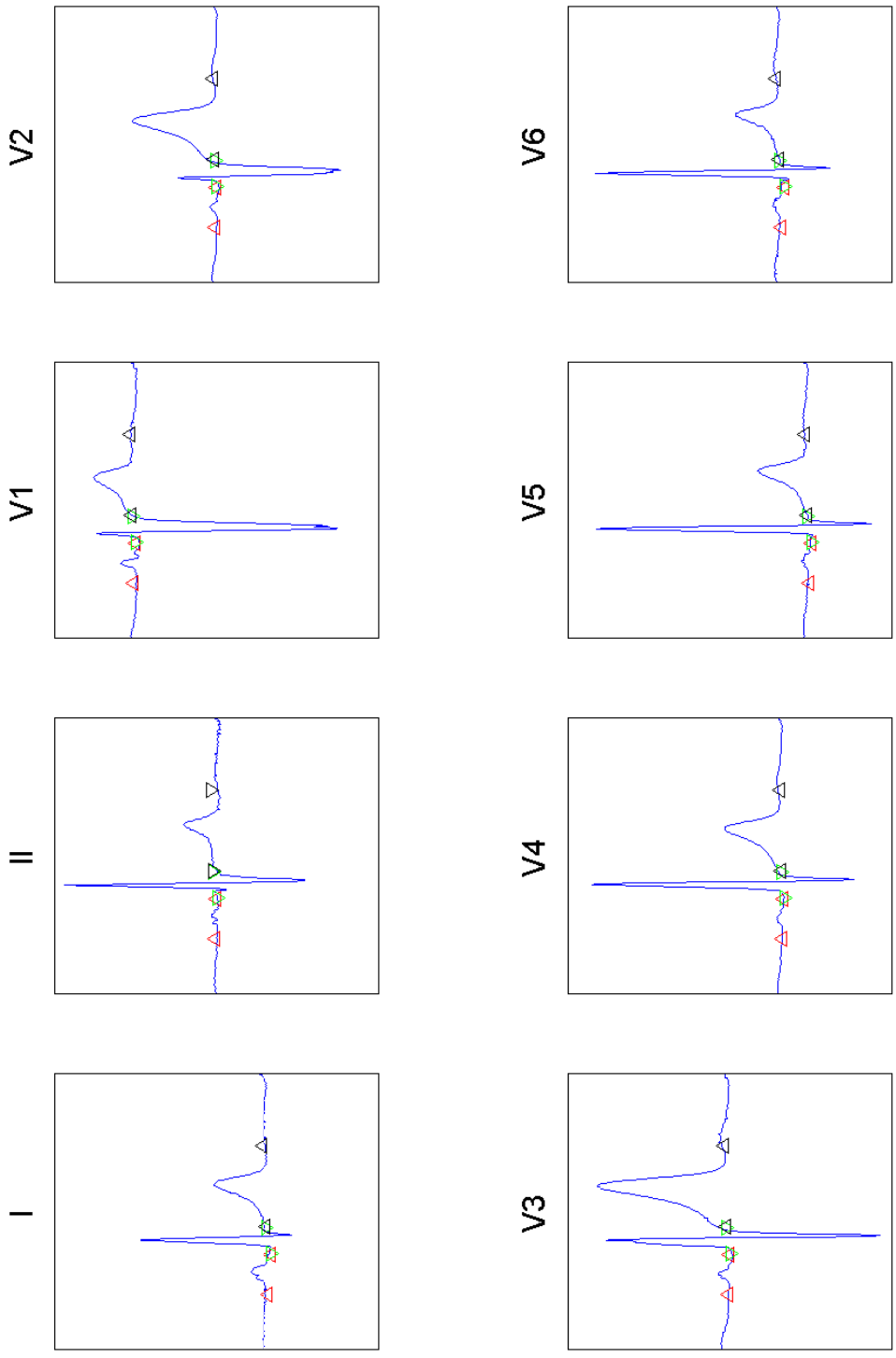

Figure 8.9: Figure shows an example of the segmentation of the independent leads. Red upward triangles indicate the P-segment, green downward triangles indicate the QRS-segment and the black upward triangles indicate the ST-T-segment.

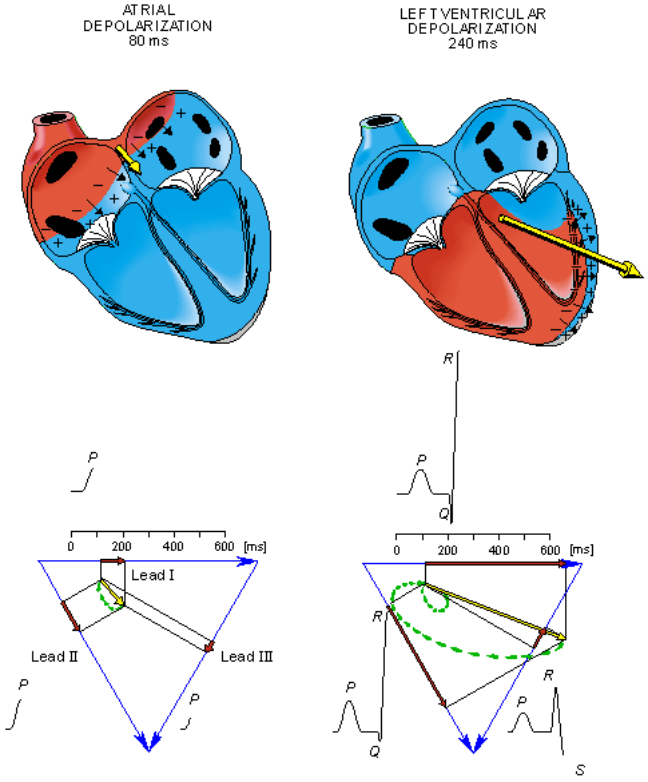

Figure 8.10: *Schematic illustration of projection of the electrical resultant vector of the heart on the lead vector. [40]*

Chapter 9

Results

9.1 Analysis of correlation coefficient

This chapter contain an overview of the results obtained in the analysis of correlation of ECG data. The analysis is divided in a pooled and an individual analysis. The contain of this chapter is as follows:

- Analysis of correlation coefficient (CC), for pooled data
- Analysis of CC, individualized data
- Q-Q plots of CC,individualized data

9.2 Correlation coefficient, for pooled data

In this analysis all the data is pooled, and each observation is assumed as independent.
Figure 9.1 shows the CC for leads V7(blue circle), V8(red pentagram) and V9(gray rectangle). Further the CC of the posterior leads are also shown.

Figure 9.2 shows the CC for leads V10(blue circle), V11(red pentagram) and V12(gray rectangle). Further the CC of the posterior leads are also shown.

9.3 Correlation coefficient, for individualized data

The ECG data is arranged in a (time x leads x subject) matrix. The CC's are determined for the posterior leads on both sides.
Figure 9.3 shows the CC for leads V7(blue circle), V8(red pentagram) and V9(gray rectangle), as an average. The 95 % standard deviation is given by the error bars.

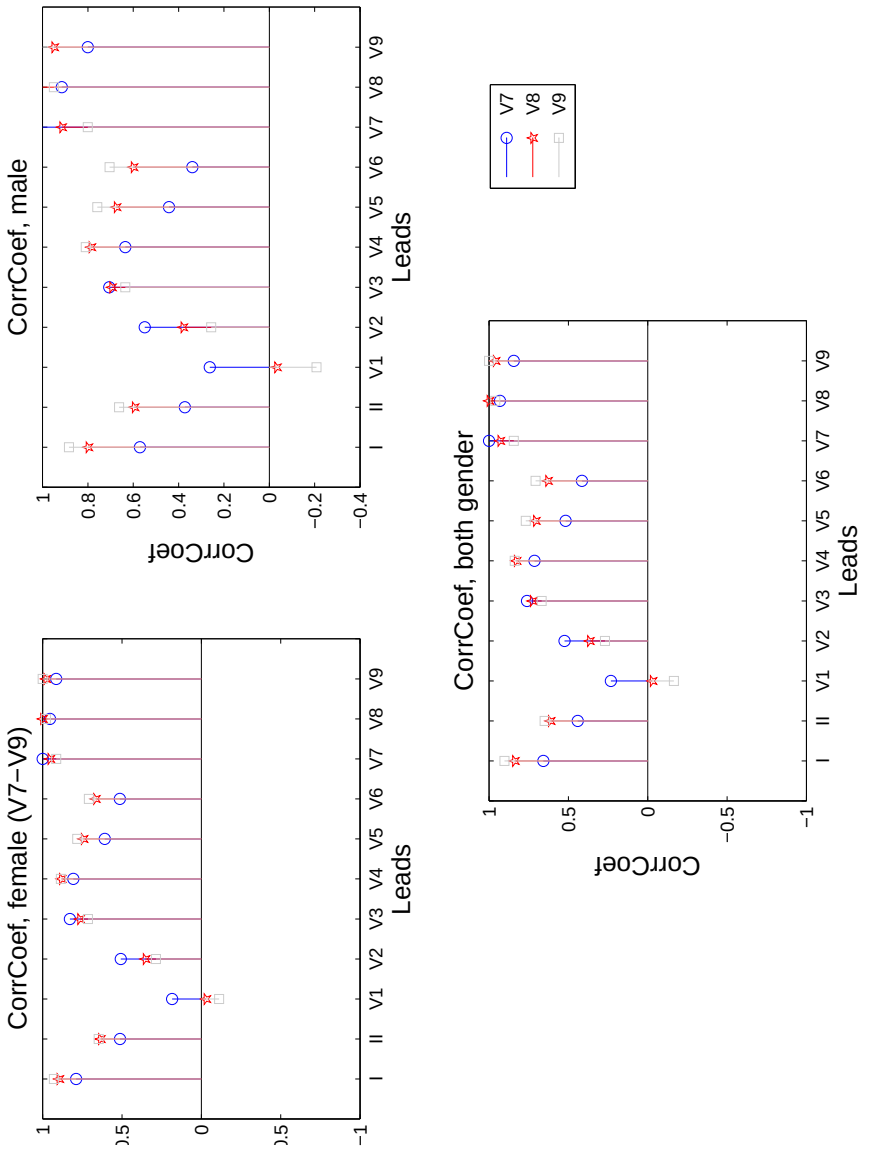

Figure 9.1: *CC of the posterior leads V7, V8 and V9. The data is pooled.*

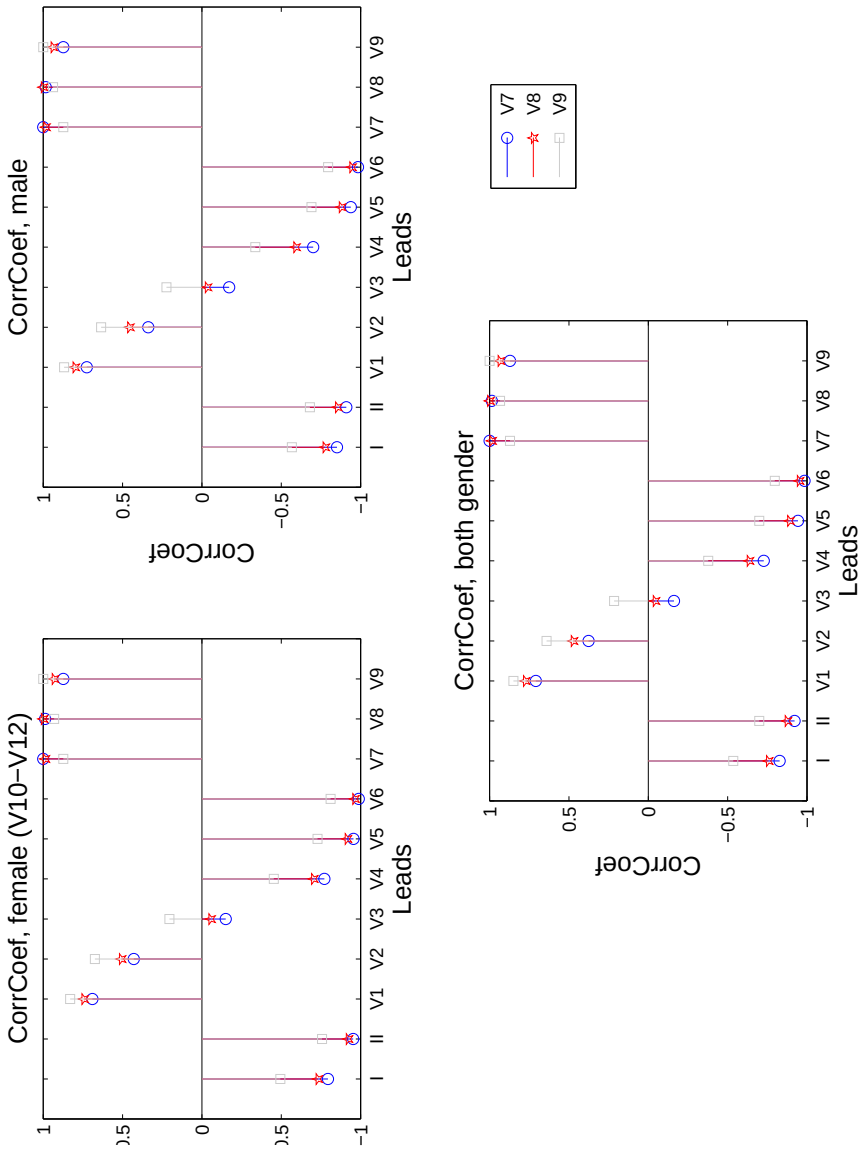

Figure 9.2: *CC of the posterior leads V10, V11 and V12. The data is pooled.*

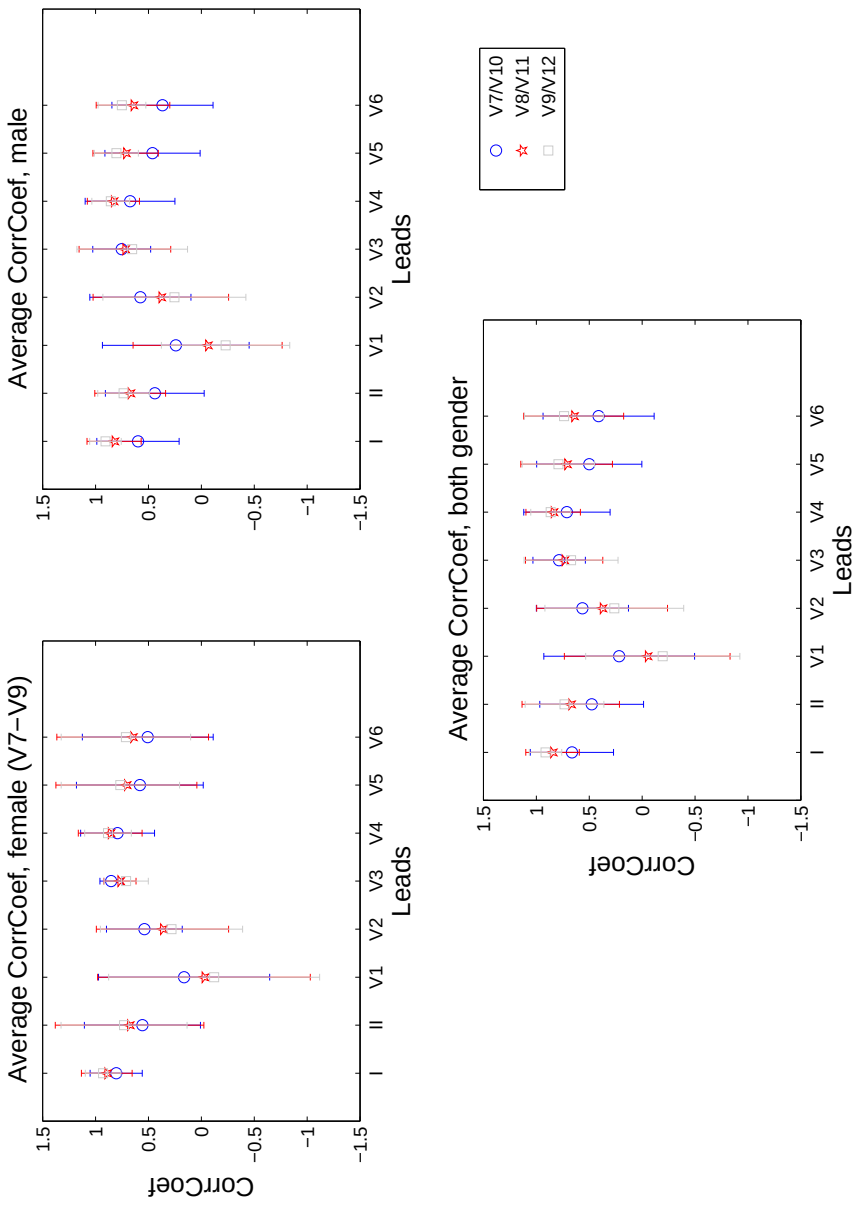

Figure 9.3: *Average CC of the posterior leads V7, V8 and V9. The data is individualized.*

Figure 9.4 shows the CC for leads V10(blue circle), V11(red pentagram) and V12(gray rectangle), as an average. The 95 % standard deviation is given by the error bars.

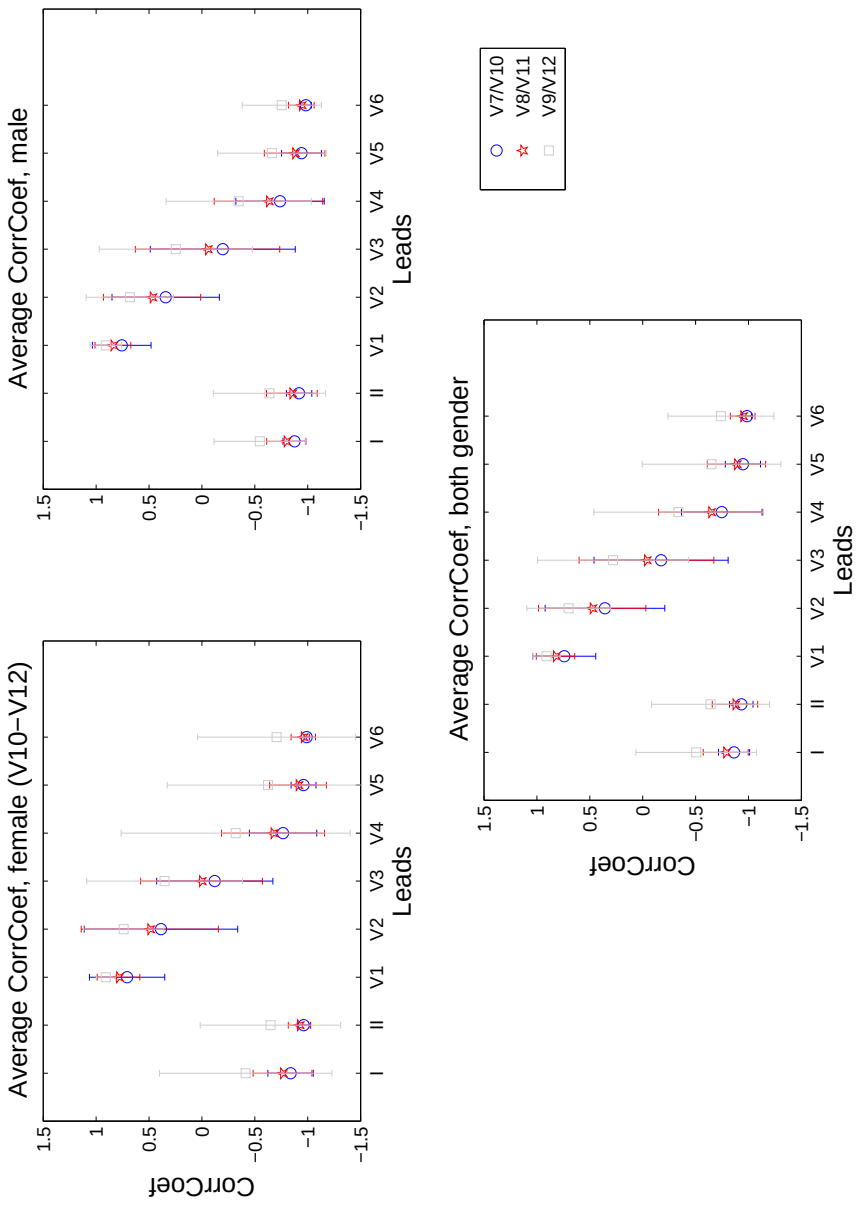

Figure 9.4: *Average CC of the posterior leads V10, V11 and V12. The data is individualized.*

9.4 Q-Q plots of CC,individualized data

The is Q-Q plots are used to determined whether the underlying distribution of the individual CC's are normal distributed. The following six figures 9.5-9.10 show the Q-Q plot of V7, V8, V9, V10, V11 and V12 in the mentioned

order.

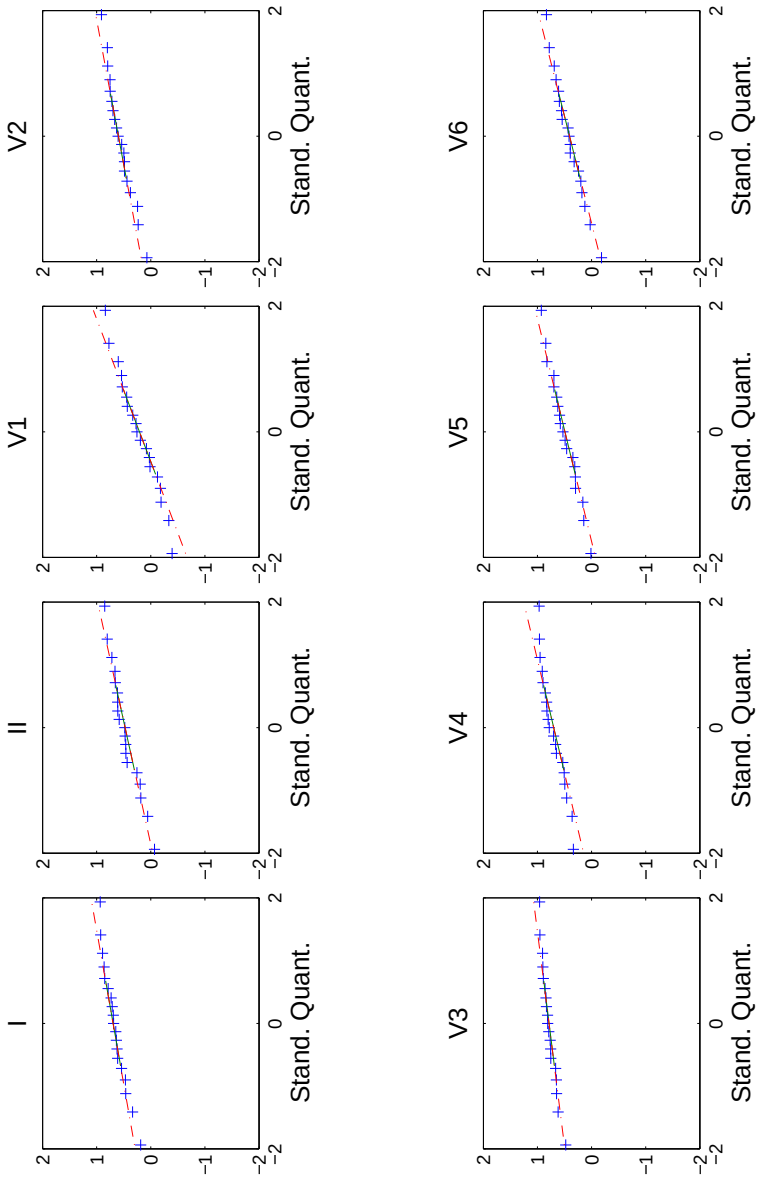

Figure 9.5: *Q-Q plot of the CC's of the lead V7 and the standard leads.*

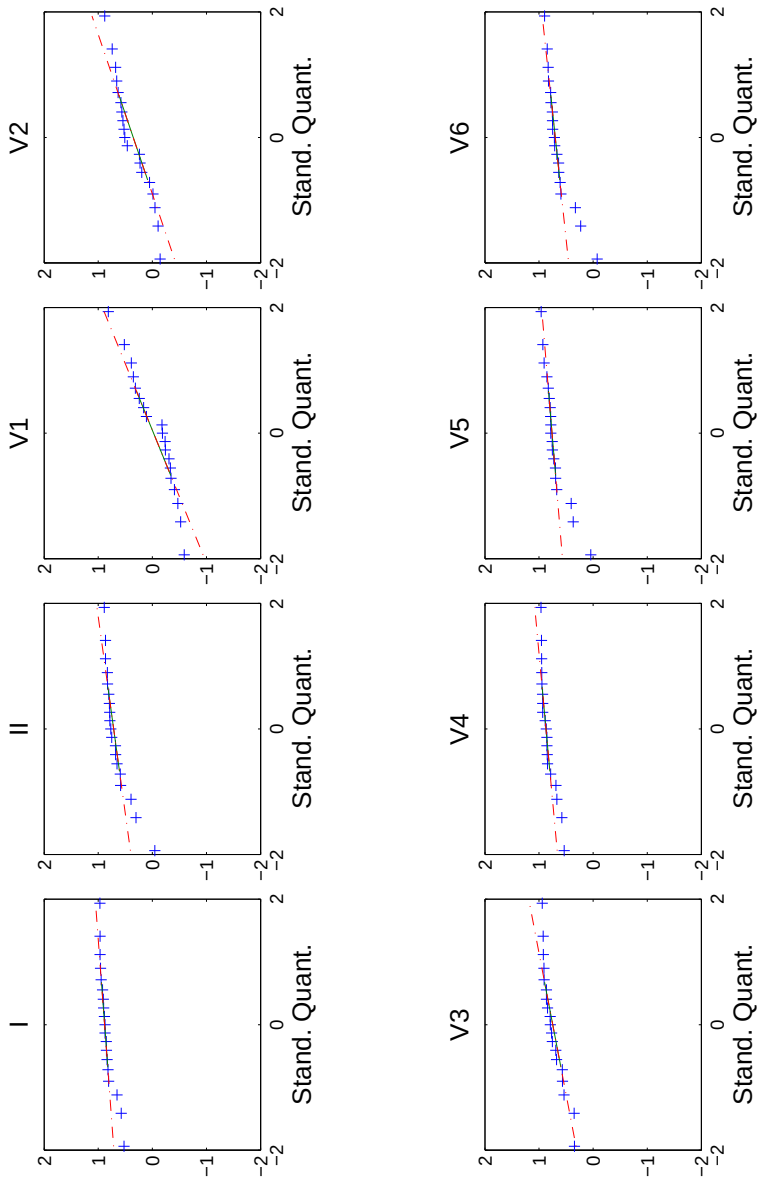

Figure 9.6: *Q-Q plot of the CC's of the lead V8 and the standard leads.*

9.5 Characteristics of study group

In each sub-group 19 subjects were allocated, 6 females and 13 males. The median age in the training group was 26 years and the median age in test group was 24 years. The average height was equal in both group, while the average weight was higher in test group then in the training group, 79 kg

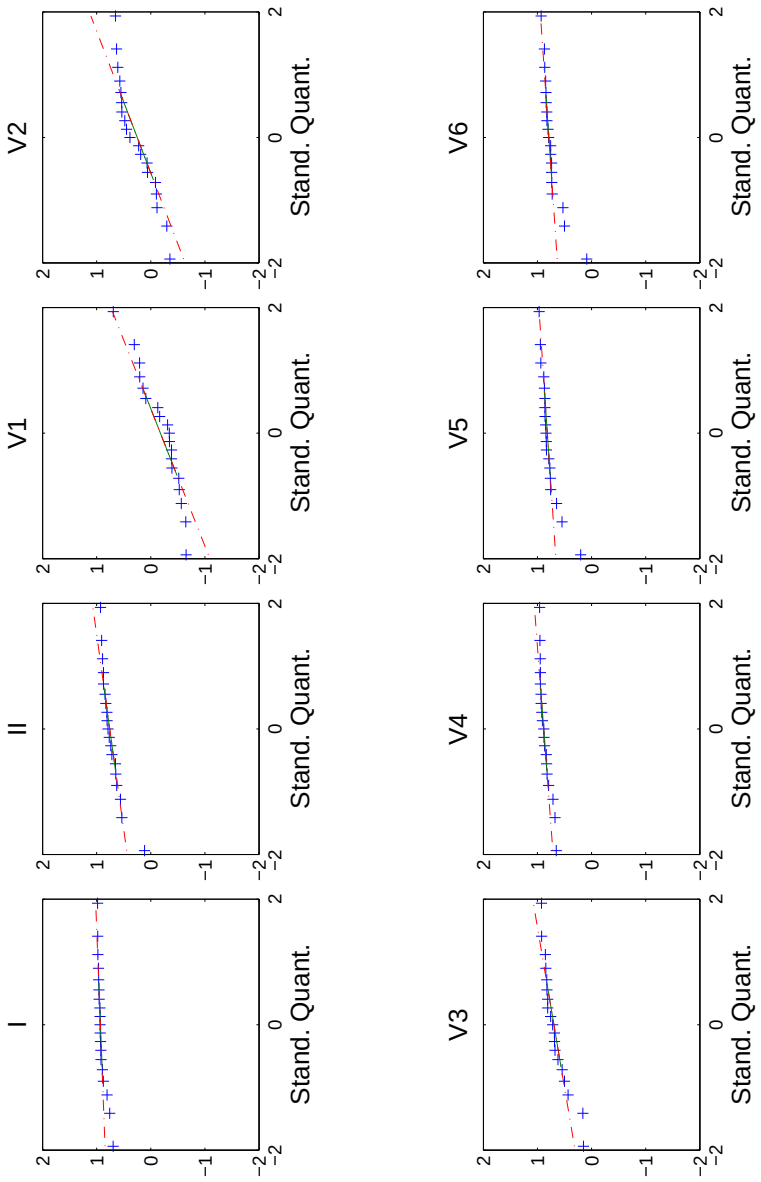

Figure 9.7: *Q-Q plot of the CC's of the lead V9 and the standard leads.*

and 76.84 kg, respectively. The higher average weight in the test group is reflected in the body mass index (BMI), 24.17 $\frac{kg}{m^2}$ for the test group and 23.53 $\frac{kg}{m^2}$ for the training group, see table 9.1.

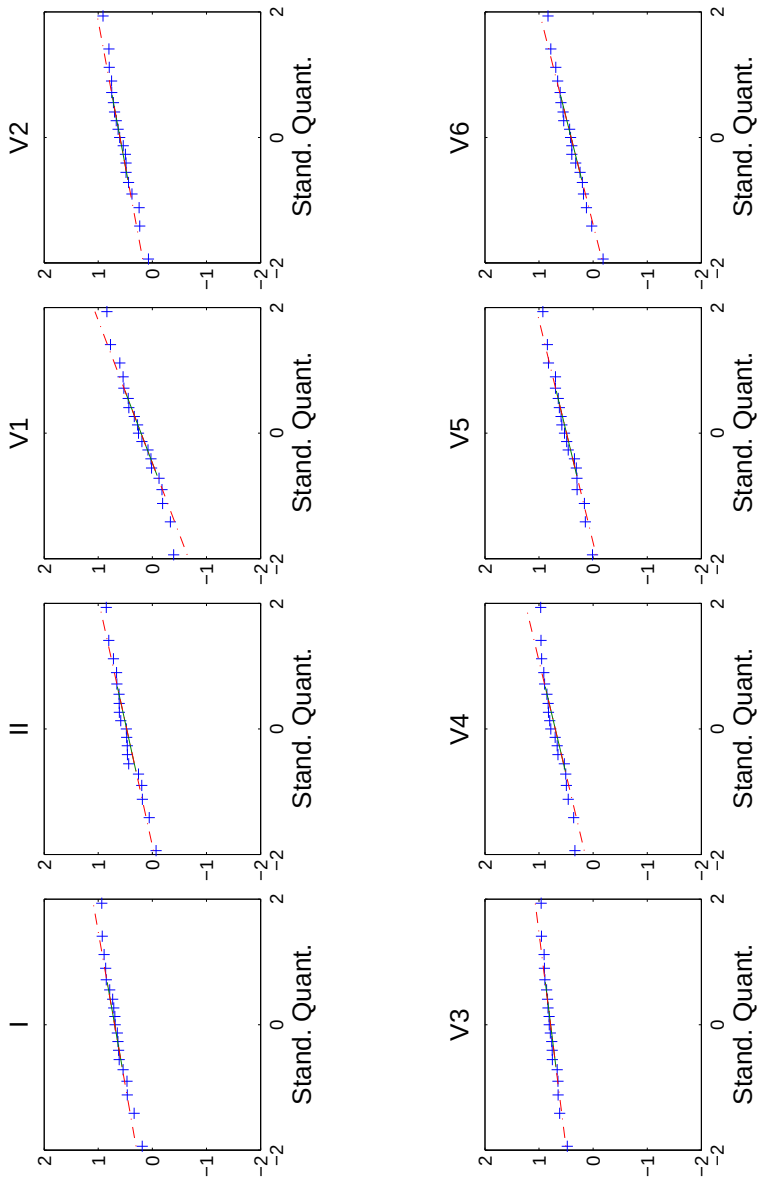

Figure 9.8: *Q-Q plot of the CC's of the lead V10 and the standard leads.*

9.6 Multiple regression model

Table 9.2 shows the coefficients of the transformation matrix for the multiple regression model. Each coefficients in the columns describes the weighting of the specific independent lead in the regression model to obtain the dependent leads (shown in the rows). To obtain the posterior leads $V7$-$V9$, the

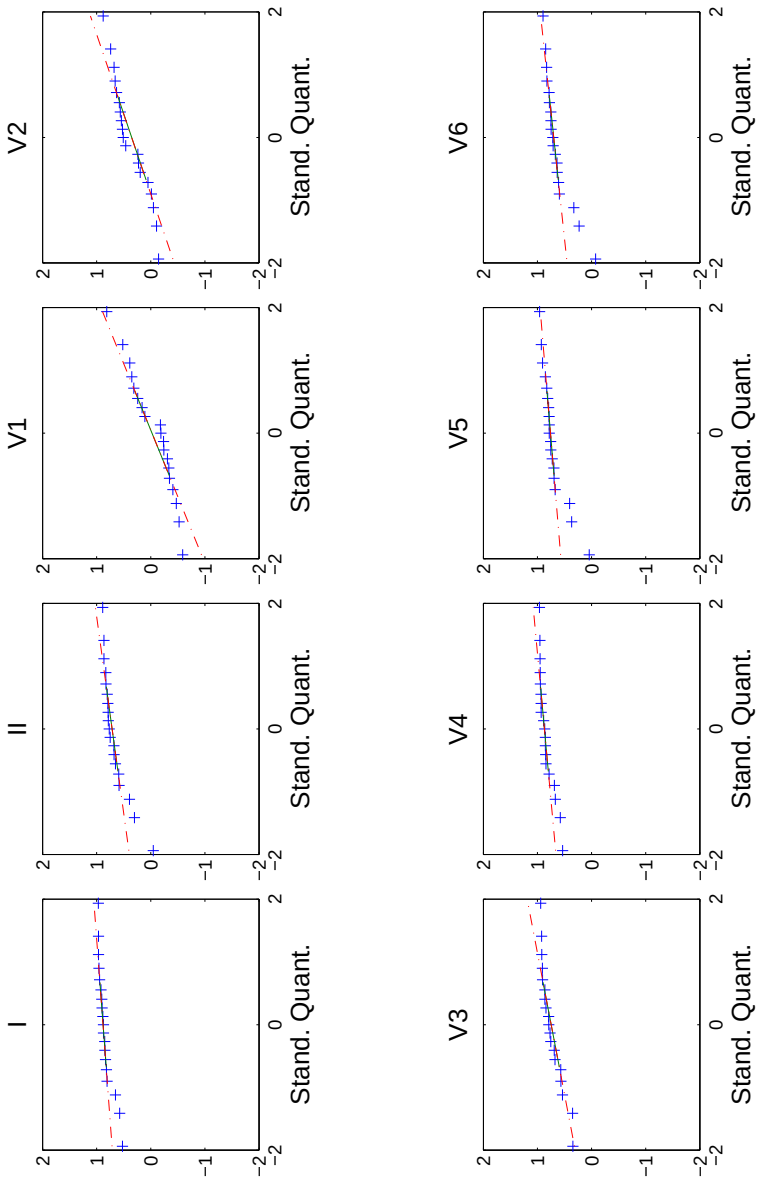

Figure 9.9: *Q-Q plot of the CC's of the lead V11 and the standard leads.*

information from lead $V6$ and to a certain extent also lead $V5$ are of great importance, while all other independent leads I-$V4$, have modest contribution to the model. In determination of the dependent leads $V10$-$V12$ the most influential independent leads were I, $V5$ and $V6$. The coefficients of the transformation matrix are also plotted in figure 9.11 for better graphical overview.

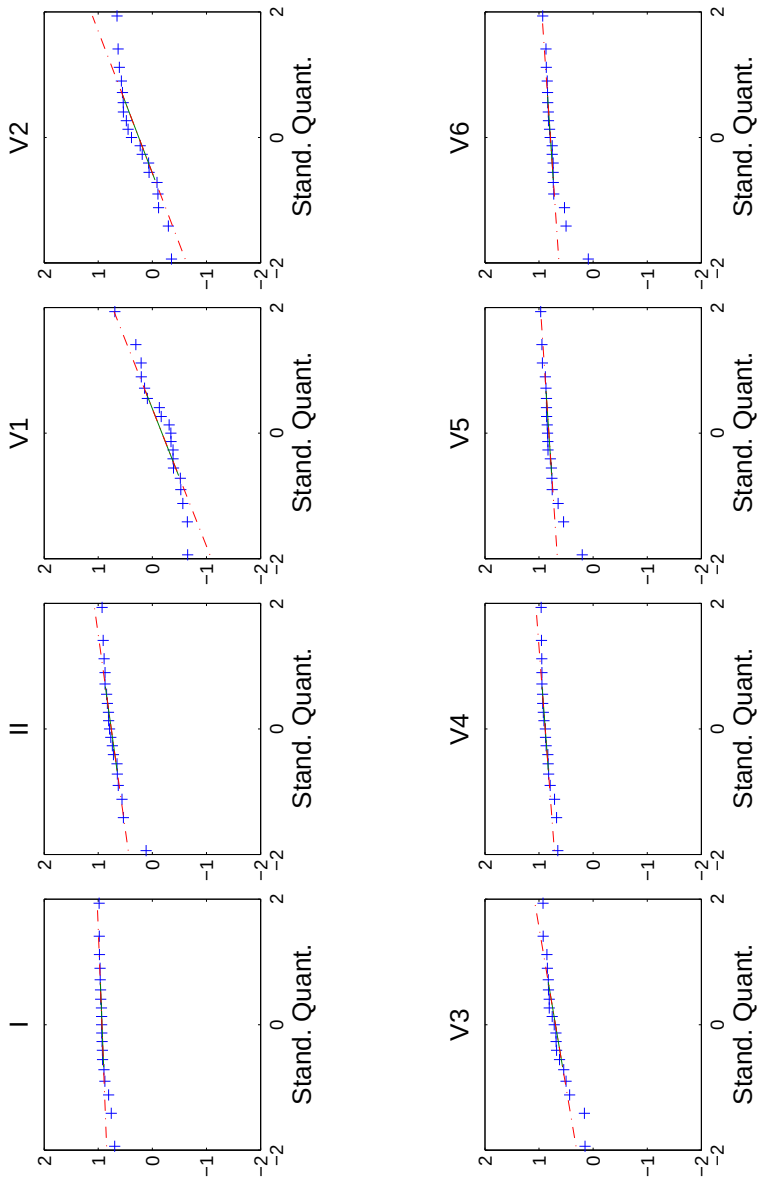

Figure 9.10: *Q-Q plot of the CC's of the lead V12 and the standard leads.*

The median coefficients of determination R^2 of the six dependent leads are given in table 9.3. In column two and three the median and the range of R^2 for the training group are listed. In column four and five the same information is given for the test group. In both groups the highest R^2 is obtained for $V7$. R^2=0.98 for the training group and R^2=0.96 for the test group, respectively. R^2 is decreasing toward $V9$ in both group. For the leads

Table 9.1: Summarization of subjects characteristics. * = Median/range

	Training		Test	
Parameter	**Mean**	**SD**	**Mean**	**SD**
Female	n = 6		n = 6	
Male	n = 13		n = 13	
Age	26*	21-37*	24*	21-36*
Height	1.80 m	± 0.08	1.80 m	± 0.10
Weight	76.84 kg	± 11.69	79 kg	± 16.49
BMI	23.53 $\frac{kg}{m^2}$	± 2.40	24.17 $\frac{kg}{m^2}$	± 3.88

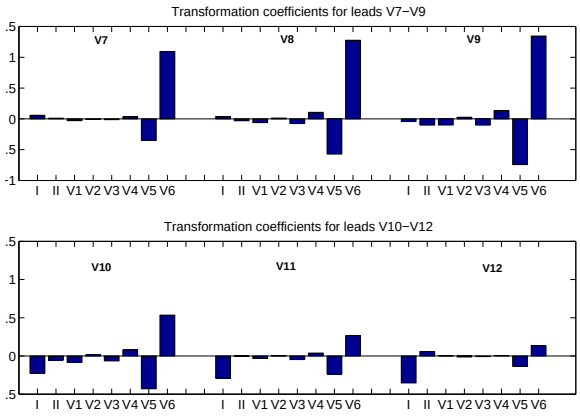

Figure 9.11: Graphical presentation of the coefficients of transformation matrix.

Table 9.2: Transformation matrix, multiple regression model

	I	II	V1	V2	V3	V4	V5	V6
V7	0.058	0.0121	-0.0289	-0.0092	-0.0126	0.0344	-0.35	1.0947
V8	0.0387	-0.0304	-0.0608	0.0123	-0.0755	0.106	-0.5717	1.2764
V9	-0.0423	-0.1009	-0.0999	0.0271	-0.1008	0.1345	-0.7423	1.3453
V10	-0.2257	-0.0542	-0.0812	0.0139	-0.0647	0.0794	-0.4287	0.5339
V11	-0.2916	-0.0008	-0.0323	0.0046	-0.0469	0.038	-0.2363	0.2661
V12	-0.3527	0.0582	0.0038	-0.0131	-0.0086	0.0061	-0.1355	0.1342

$V10$-$V12$, R^2 is almost equal between the leads and also between the groups. The values given in the table are truncated values.

9.7 Simple regression model

Simple regression of the standard leads and the posterior leads yielded the coefficients of determination r^2, and are given in table 9.4. The transformation coefficients are not shown. In reconstruction of the posterior leads $V7$-$V9$ the standard leads II, $V2$, $V5$ and $V6$ contribute with information, while e.g. lead $V3$ explains less than 15 % of the variance in the model. In reconstruction of leads $V10$-$V12$, the standard leads I, $V3$ and $V4$ performs well, while $V1$ does not contribute with significant amount of information.

The coefficients in the table given in graphical presentation, for better overview.

Table 9.3: Coefficients of determination, multiple regression model

	Training		Test	
Lead	**Median**	**(Range)**	**Median**	**(Range)**
V7	0.98	(1-0.34)	0.96	(1-0.08)
V8	0.95	(1-0.59)	0.93	(0.99-0.06)
V9	0.88	(0.98-0.14)	0.87	(0.99-0.28)
V10	0.90	(1-0.25)	0.89	(1-0.03)
V11	0.91	(0.99-0.36)	0.91	(0.99-0.18)
V12	0.90	(0.98-0.17)	0.89	(0.98-0.06)

Table 9.4: Coefficient of determination, simple regression model

	I	**II**	**V1**	**V2**	**V3**	**V4**	**V5**	**V6**
V7	0.75 (0.91 -0.20)	0.90 (0.99- 0.56)	0.56 (0.90- 0.11)	0.13 (0.63- 0.00)	0.14 (0.65- 0.00)	0.59 (0.99- 0.40)	0.92 (1- 0.81)	0.98 (1- 0.81)
V8	0.60 (0.84- 0.07)	0.80 (0.97- 0.26)	0.69 (0.94- 0.04)	0.22 (0.72- 0.00)	0.09 (0.58- 0.00)	0.49 (0.88- 0.01)	0.79 (0.97- 0.18)	0.89 (0.99- 0.00)
V9	0.23 (0.69- 0.00)	0.48 (0.87- 0.00)	0.84 (0.96- 0.02)	0.46 (0.88- 0.00)	0.09 (0.78- 0.00)	0.16 (0.75- 0.01)	0.40 (0.90- 0.00)	0.59 (0.95- 0.00)
V10	0.50 (0.89- 0.03)	0.22 (0.72- 0.00)	0.17 (0.86- 0.00)	0.50 (0.84- 0.01)	0.72 (0.92- 0.12)	0.66 (0.94- 0.01)	0.31 (0.86- 0.01)	0.17 (0.71- 0.00)
V11	0.77 (0.95- 0.18)	0.50 (0.79- 0.00)	0.10 (0.74- 0.01)	0.31 (0.84- 0.00)	0.70 (0.93- 0.12)	0.83 (0.94- 0.25)	0.61 (0.92- 0.00)	0.48 (0.86- 0.01)
V12	0.86 (0.98- 0.15)	0.54 (0.88- 0.00)	0.13 (0.74- 0.01)	0.24 (0.81- 0.00)	0.62 (0.91- 0.02)	0.79 (0.92- 0.00)	0.68 (0.94- 0.04)	0.55 (0.90- 0.01)

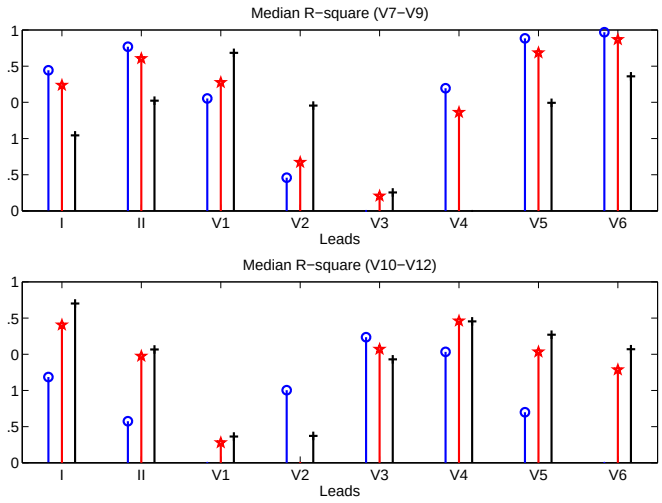

Figure 9.12: *The coefficients in table 9.4 shown as stem plots.*

9.8 Beta coefficients with interception

The figure 9.13 below shows the beta coefficient when the regression is made with interception. In this study, we constrained the model and let the interception be 0. $\beta_0 \neq 0$ do not make nay sense.

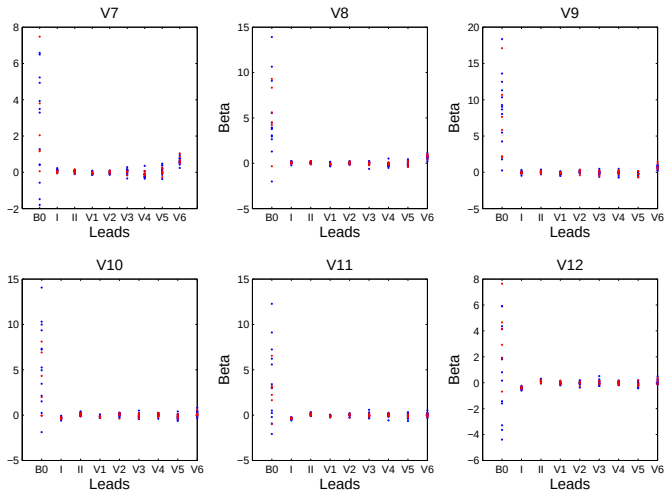

Figure 9.13: *The coefficients of the regression model with interception is shown.*

9.9 Test of the independent variables

The aim of this test is to determine the statistical probability of the information contribution of the independent leads. The test was conducted on the

Subset	R^2	F-stat	F-stat Param.	P-value
V6	0.978	$1.24*10^9$		
V5 V6	0.988	$1.55*10^9$	$4.87*10^5$	$\leq$0.01
V1, V5, V6	0.990	$1.39*10^9$	$1.13*10^5$	$\leq$0.01
V1, V4, V5, V6	0.990	$1.12*10^9$	$0.52*10^4$	$\leq$0.01
V1, V2, V4,V5, V6	0.990	$0.95*10^9$	$1.06*10^4$	$\leq$0.01
V1, V2, V3 V4,V5, V6	0.990	$0.82*10^9$	8.13	$\leq$0.01
II, V1, V2, V3 V4,V5, V6	0.990	$0.71*10^9$	-0.85	$\geq$0.01
I, II, V1, V2, V3 V4,V5, V6	0.990	$0.63*10^9$	-1.49	$\geq$0.01

Table 9.5: Summary of statistics of lead V7

Subset	R^2	F-stat	F-stat Param.	P-value
V6	0.936	$4.13*10^6$		
V5, V6	0.965	$5.20*10^6$	$4.73*10^5$	$\leq$0.01
V1, V5, V6	0.974	$5.34*10^6$	$2.02*10^5$	$\leq$0.01
II, V1, V5,V6	0.974	$4.35*10^6$	$9.50*10^6$	$\leq$0.01
V1, V3, V4,V5, V6	0.975	$3.66*10^6$	$6.68*10^3$	$\leq$0.01
II, V1, V3 V4,V5, V6	0.975	$3.24*10^6$	$1.61*10^4$	$\leq$0.01
II, V1, V2, V3 V4,V5, V6	0.975	$2.83*10^6$	$2.9*10^2$	$\leq$0.01
I, II, V1, V2, V3 V4,V5, V6	0.975	$2.51*10^6$	-1.04	$\geq$0.01

Table 9.6: Summary of statistics of lead V8

six posterior leads. The combination of leads which contributed to the final model with significant amount of information, was found iterative. First the best subset of one independent variable was found. In next step the best subset of two independent variables was found and so on to the end where the model contained all independent variables. For each step the SSE (mean square error in Matlab) was calculated.
The F-statistics was calculated for each time a new variable was added to the model. If the $F - statistics > F_{K1,n-K-1,\alpha}$, then the statistical probability of adding the new independent variable do not contribute with significant more information then the previous model is ≤ 0.01.

9.10 Stability

The aim this analysis was to investigate the stability of the regression coefficients of the linear regression model. The expectation is that at a certain

Subset	R^2	F-stat	F-stat Param.	P-value
V6	0.770	95376.976		
V1, V6	0.867	$1.23*10^6$	$4.13*10^6$	≤0.01
V1, V5, V6	0.903	$1.32*10^6$	$2.10*10^5$	≤0.01
II, V1, V5, V6	0.910	$1.15*10^6$	$4.63*10^4$	≤0.01
II, V1, V4,V5, V6	0.911	$9.75*10^5$	$8.29*10^3$	≤0.01
II, V1, V3 V4,V5, V6	0.912	$8.47*10^5$	$7.03*10^3$	≤0.01
II, V1, V2, V3 V4,V5, V6	0.913	$7.43*10^5$	$1.14*10^3$	≤0.01
I, II, V1, V2, V3 V4,V5, V6	0.913	$6.60*10^5$	-1.40	≥0.01

Table 9.7: Summary of statistics of lead V9

Subset	R^2	F-stat	F-stat Param.	P-value
V1	0.750	$8.52*10^5$		
V1, V4	0.763	$6.11*10^5$	$3.18*10^4$	≤0.01
V1, V5, V6	0.785	$5.19*10^5$	$5.81*10^4$	≤0.01
II, V1, V5, V6	0.793	$4.36*10^6$	$2.26*10^4$	≤0.01
II, V1, V2,V5, V6	0.793	$3.64*10^6$	$9.17*10^2$	≤0.01
II, V1, V3 V4,V5, V6	0.795	$3.15*10^6$	$4.87*10^3$	≤0.01
II, V1, V2, V3 V4,V5, V6	0.795	$2.76*10^6$	$2.73*10^2$	≤0.01
I, II, V1, V2, V3 V4,V5, V6	0.795	$2.45*10^6$	-1.15	≥0.01

Table 9.8: Summary of statistics of lead V10

Subset	R^2	F-stat	F-stat Param.	P-value
V1	0.845	$1.55*10^6$		
V1, V4	0.852	$1.09*10^6$	$2.86*10^4$	≤0.01
V1, V5, V6	0.858	$8.63*10^5$	$2.49*10^4$	≤0.01
V1, V3, V5, V6	0.861	$7.08*10^5$	$1.27*10^4$	≤0.01
V1, V3, V4, V5, V6	0.862	$5.92*10^6$	$1.25*10^3$	≤0.01
II , V1, V3, V4, V5, V6	0.862	$5.09*10^5$	$1.64*10^3$	≤0.01
II, V1, V2, V3, V4, V5, V6	0.862	$4.45*10^5$	-0.98	≥0.01
I, II, V1, V2,V3, V4,V5, V6	0.862	$3.96*10^6$	-1.00	≥0.01

Table 9.9: Summary of statistics of lead V11

Subset	R^2	F-stat	F-stat Param.	P-value
V2	0.869	$1.88*10^6$		
II, V3	0.878	$1.36*10^6$	$4.27*10^4$	$\leq$0.01
II, V1, V4	0.882	$1.06*10^6$	$18.20*10^4$	$\leq$0.01
II, V2, V5, V6	0.885	$7.31*10^5$	$1.66*10^4$	$\leq$0.01
II, V1, V2, V5, V6	0.885	$5.92*10^5$	4.57	$\geq$0.01
II, V1, V2, V3, V5, V6	0.885	$6.26*10^5$	-0.99	$\geq$0.01
II, V1, V2, V3, V4, V5, V6	0.885	$5.48*10^5$	-1.00	$\geq$0.01
I, II, V1, V2, V3,V4,V5 V6	0.885	$4.87*10^5$	-1.00	$\geq$0.01

Table 9.10: Summary of statistics of lead V12

point, the beta coefficients will stabilize. Behind the number of patients, the model is stable, and the small variations in the coefficients can be attributed to random variation. When the coefficients are stabilized the one of the numerous solutions to the problem is obtained [99]. Small fluctuations will always appear, but it do not mean that a larger populations is needed to obtain statistical stability [99].

The analysis was conducted for the six posterior leads. The analysis was based step wise addition of more ECG data. For each step a new subject was added and the regression coefficient for the six posterior leads were determined. The first 19 subjects were subject included in the training group and subjects 20-37 were subjects included in the test group.

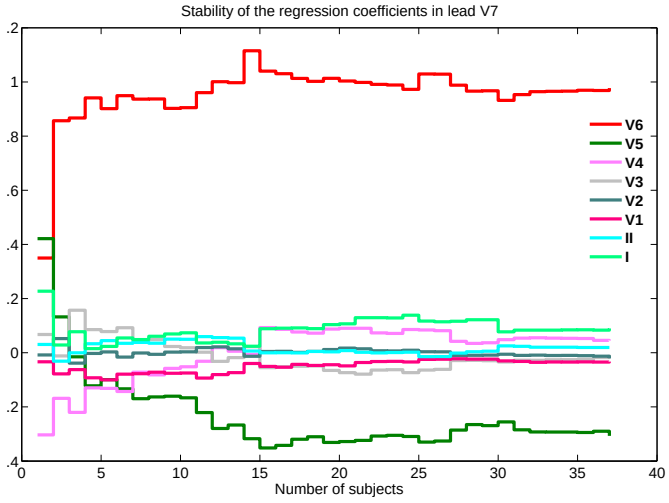

Figure 9.14: Development of regression coefficients for predicting posterior lead V7.

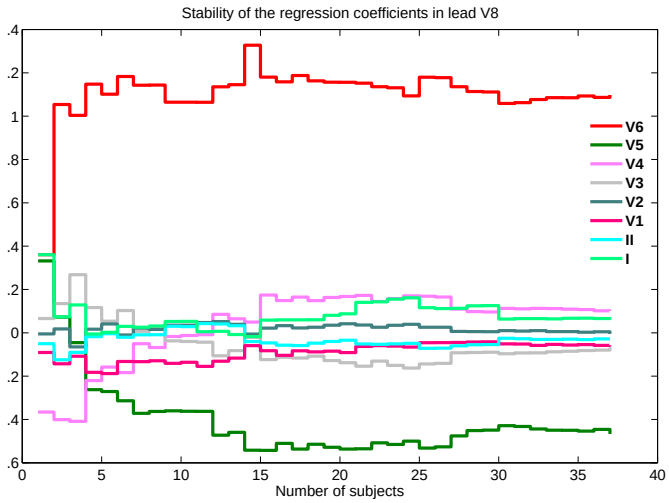

Figure 9.15: Development of regression coefficients for predicting posterior lead V8.

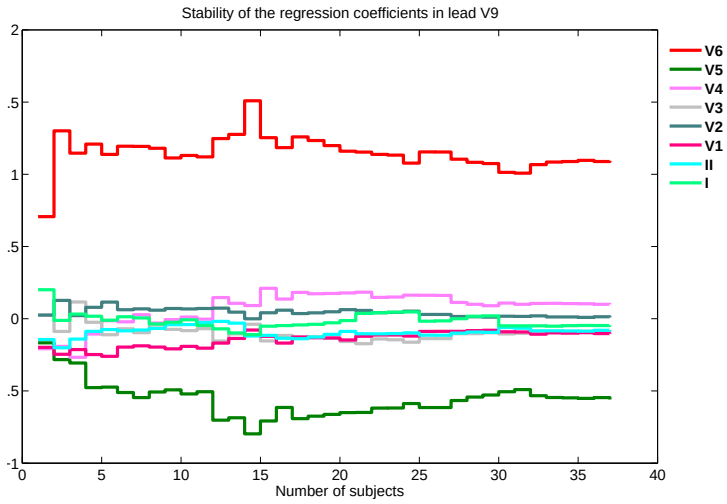

Figure 9.16: Development of regression coefficients for predicting posterior lead V9.

9.11 Results of the average regression model

In table 9.11, the regression coefficients for the average regression model is given.

In figure 9.20, the regression coefficients are given as bars for better graphical overview.

In figures 9.21-9.23, the 19 different coefficients for the independent variables for predicting the posterior leads V7-V12 are given.

In table 9.12, the performance of the pooled and the average method are given.

In figures 9.24-9.26, the results of the reduced average models are shown.

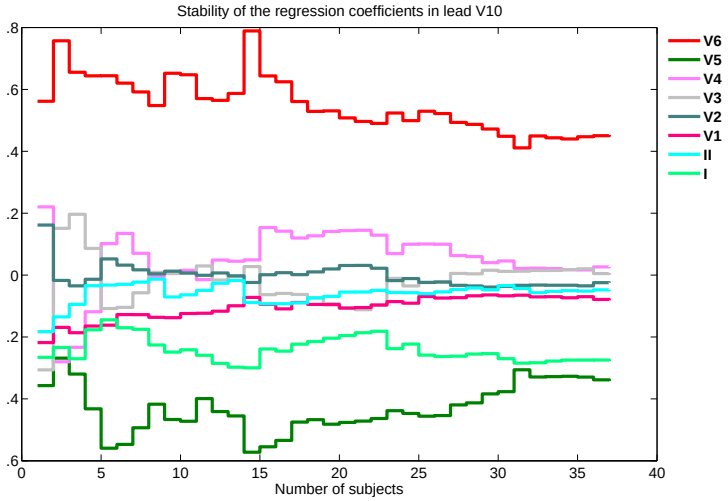

Figure 9.17: Development of regression coefficients for predicting posterior lead V10.

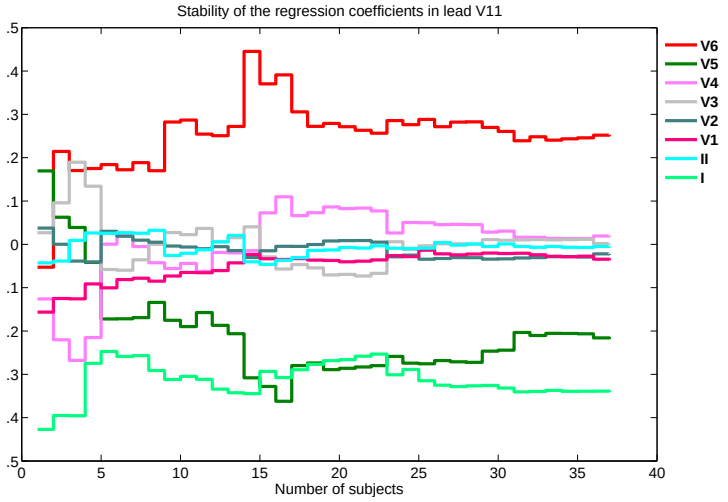

Figure 9.18: Development of regression coefficients for predicting posterior lead V11.

	β_I	β_{II}	β_{V1}	β_{V2}	β_{V3}	β_{V4}	β_{V5}	β_{V6}
V7	0.0811	0.0453	-0.0517	-0.0015	0.0128	-0.1048	0.0785	0.6580
V8	0.0797	0.0591	-0.0969	0.0345	-0.0416	-0.0999	-0.0489	0.7151
V9	0.0072	0.0643	-0.1438	0.0738	-0.1129	-0.0509	-0.2547	0.7611
V10	-0.2850	-0.1304	-0.1396	0.0712	-0.1280	0.0364	-0.2427	0.5339
V11	-0.3370	0.1343	-0.0774	0.0185	-0.0493	0.0081	-0.1512	0.0684
V12	-0.3936	0.1463	-0.0273	-0.0151	-0.0008	0.0037	-0.1411	0.0652

Table 9.11: Regression matrix, average regression model

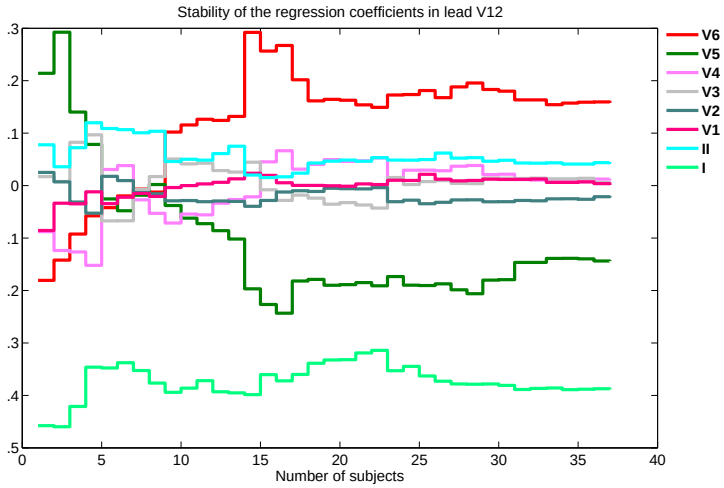

Figure 9.19: Development of regression coefficients for predicting posterior lead V12.

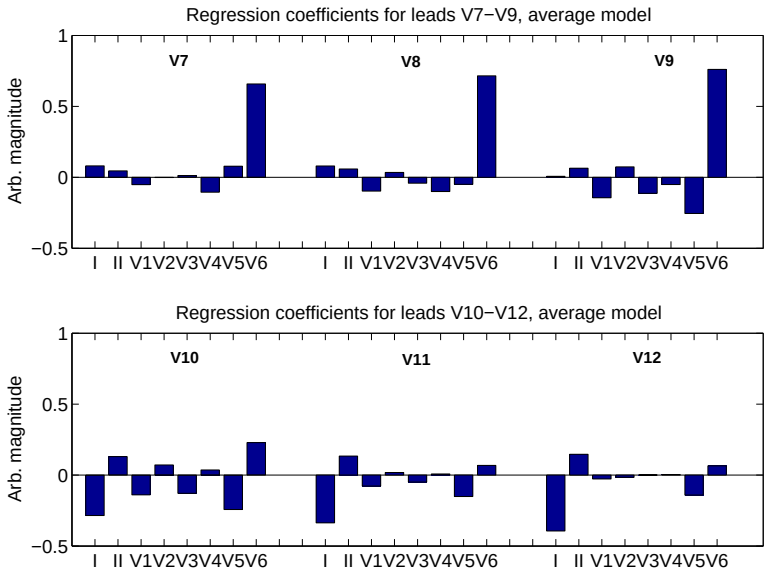

Figure 9.20: Graphical presentation of the coefficients of regression matrix.

9.12 Results of the analysis of the global model vs. partial models

In figure 9.27 and 9.28, the results of the simple regression of the leads V5 and V7/V12 are given.

The results of table 9.13 are given in figure 9.29 for better graphical overview. The median residuals of the partial models (solid lines) and the median residuals for the global model (given as dashed lines).

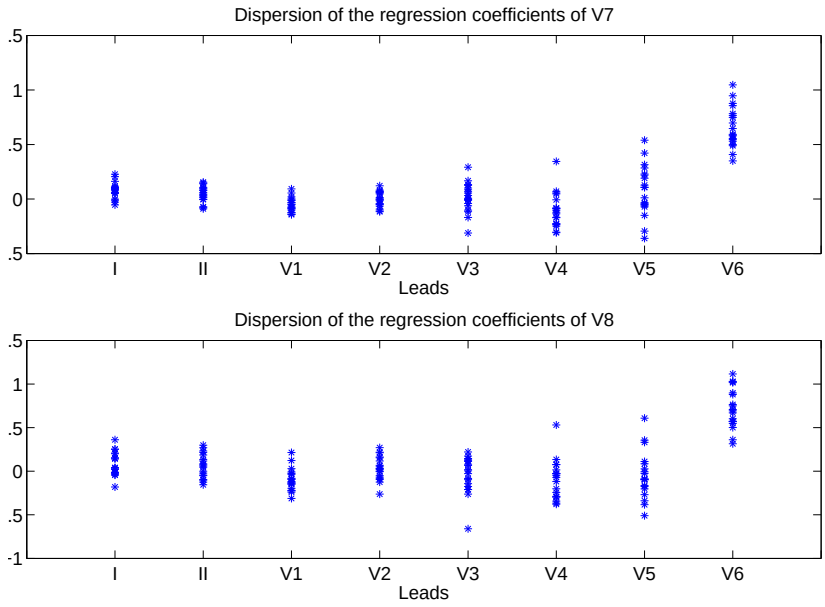

Figure 9.21: Dispersion of the regression coefficients of leads V7 and V8.

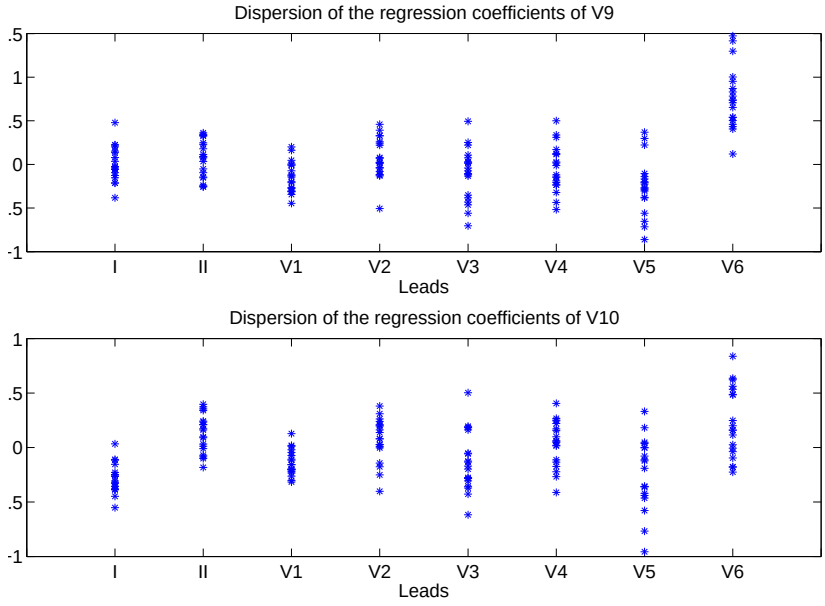

Figure 9.22: Dispersion of the regression coefficients of leads V9 and V10.

9.13 Standardized beta coefficients

Range of the magnitude

In figure 9.30, the ranges of the magnitudes of all measured leads are given. The magnitudes are given in an arbitrary unit. The largest ranges are found in the standard leads V2-V4 and the smallest ranges are observed in the

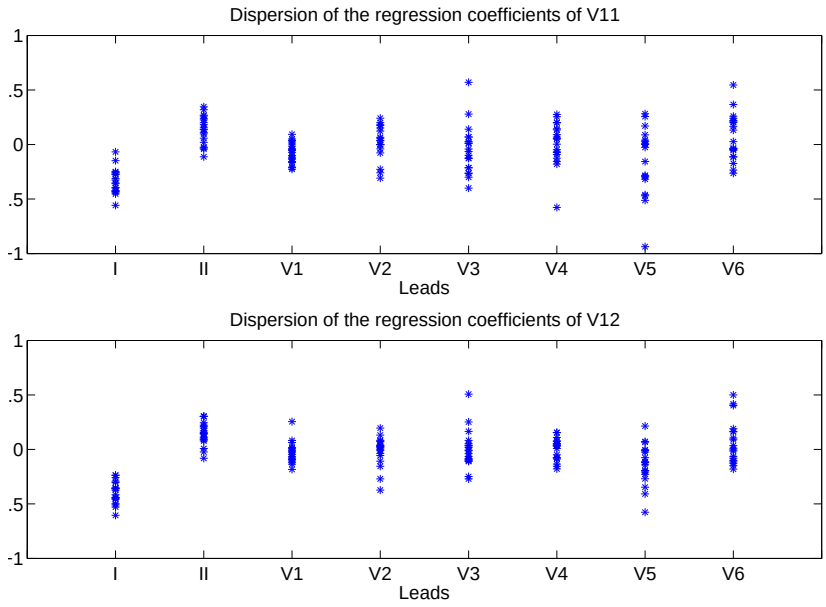

Figure 9.23: Dispersion of the regression coefficients of leads V11 and V12.

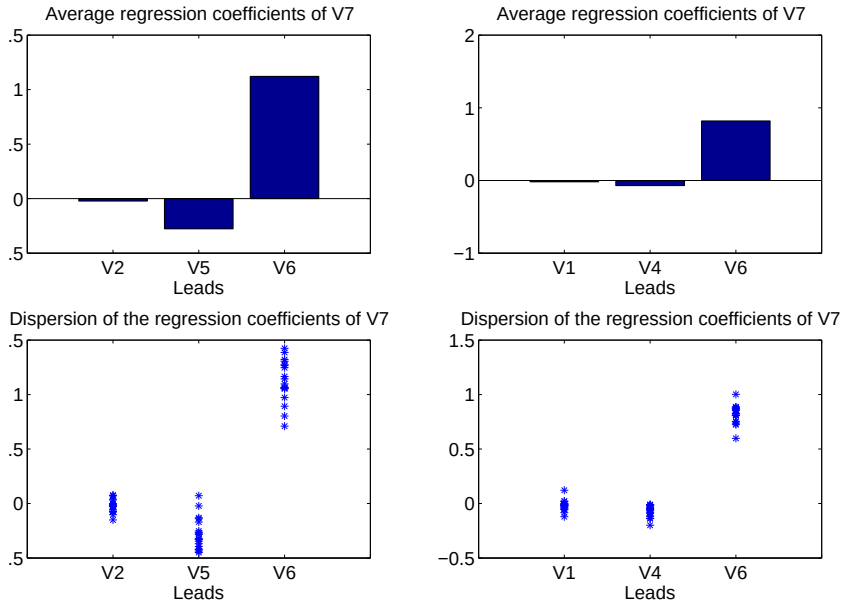

Figure 9.24: The average regression coefficients and the dispersion of the regression coefficients of leads V7.

posterior leads V10-V12. The displacement of the ranges with respect to zero indicates the upward or downward direction of the QRS-complex.

In figure 9.31 left subplot, the data points of the standard lead V6 are plotted against the data points of the posterior lead V7. These two leads are neighbouring leads and measure almost the same signal and are therefore highly correlated [90]. We can assume the ratio of their output spans (out-

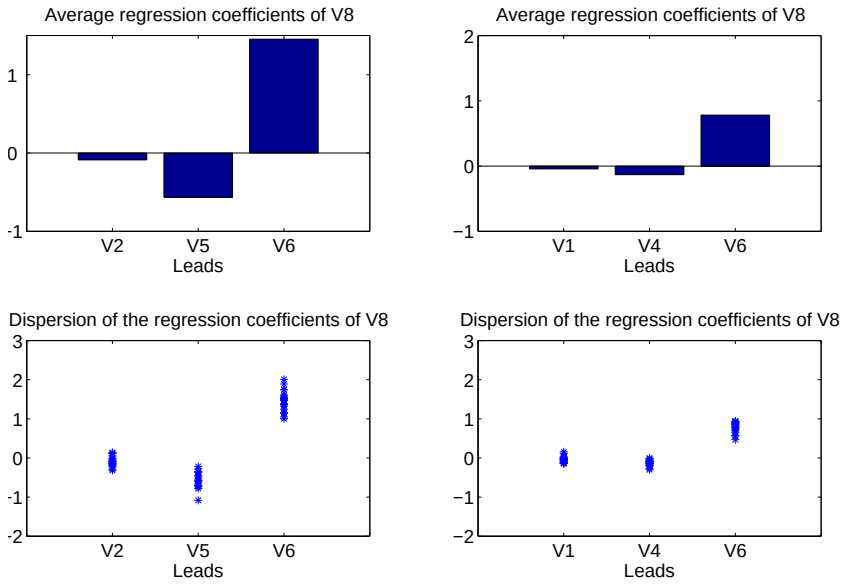

Figure 9.25: The average regression coefficients and the dispersion of the regression coefficients of leads V8.

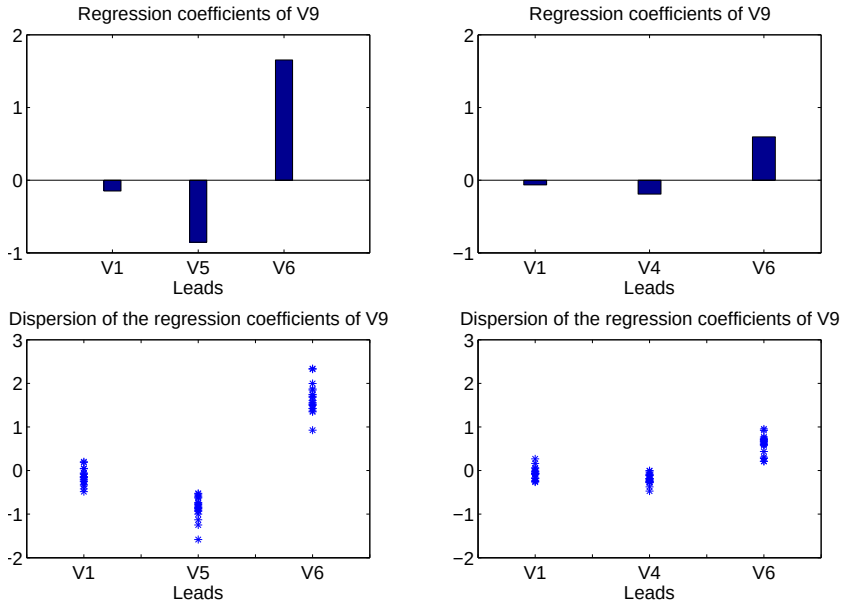

Figure 9.26: The average regression coefficients and the dispersion of the regression coefficients of leads V9.

put ratio) to be one. In right subplot, the data points of the standard lead V4 are plotted against the data points of the posterior lead V10. These leads are measuring the electrical potential on opposite sites of the heart. They can truly be highly correlated [90], however the output ratio is $\ll 1$. The data points of the three segments P (red), QRS (blue) and T (yellow) are colour coded in the figure.

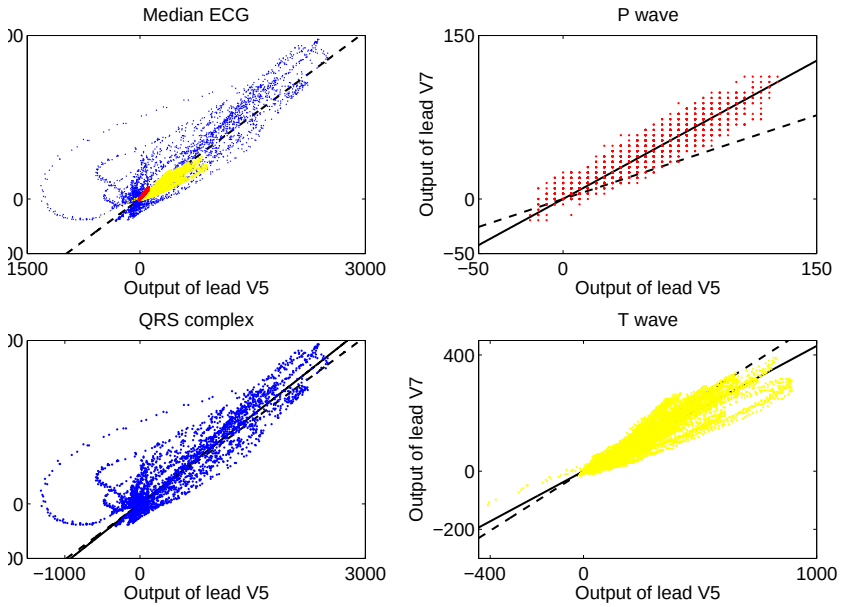

Figure 9.27: The figure shows the results of the simple regression of the leads V5 and V7.

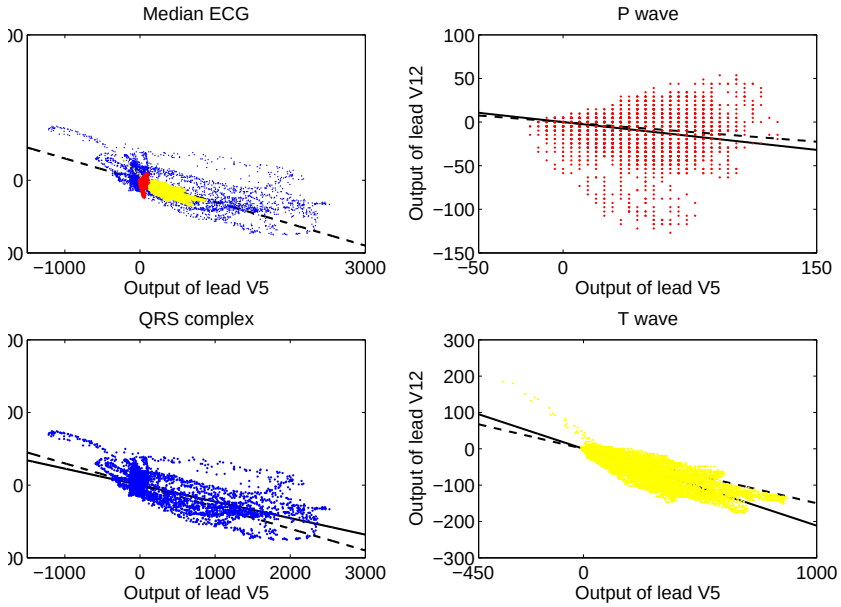

Figure 9.28: The figure shows the results of the simple regression of the leads V5 and V12.

Standardized regression coefficients

Figure 9.32 shows examples of the Q-Q plots of un-segmented ECG and segmented ECG. First column shows an example of Q-Q plots of the un-segmented ECG of the standard leads; I, II and V4. From column one, we see a highly tailed distribution of the three standard leads. And the Q-Q

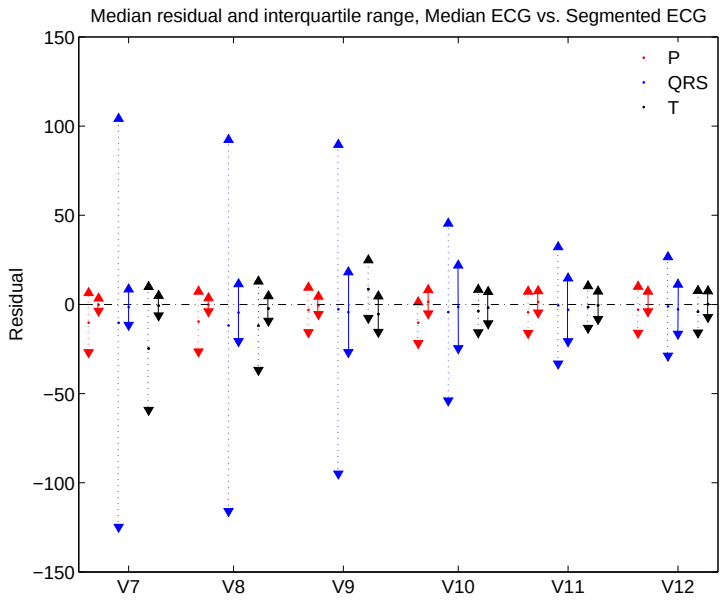

Figure 9.29: The figure shows the results of the simple regression of the leads V5 and V12.

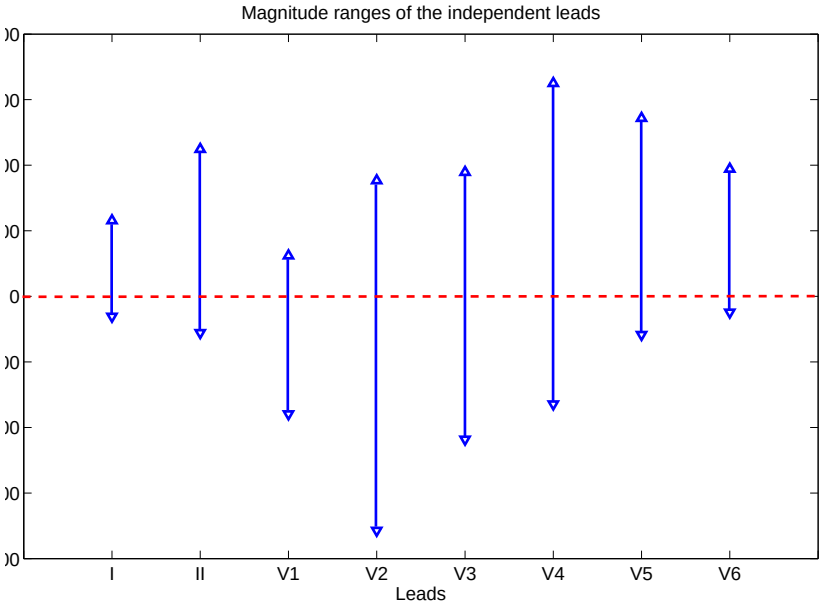

Figure 9.30: The figure shows the ranges of the magnitudes of all measured leads.

plots may suggest that the un-segmented ECG's are piece wise normally distributed. In columns 2-4 Q-Q plots of the segments P, QRS and T of leads I, II and V4 are given. Only a limited range of data is shown.

Figure 9.35 and 9.36 shows the magnitude of the SBC as bars for the three segments for predicting the posterior leads V7-V12. To obtain the posterior leads V7-V9, the absolute values of the SBC of leads V5 and V6 are of

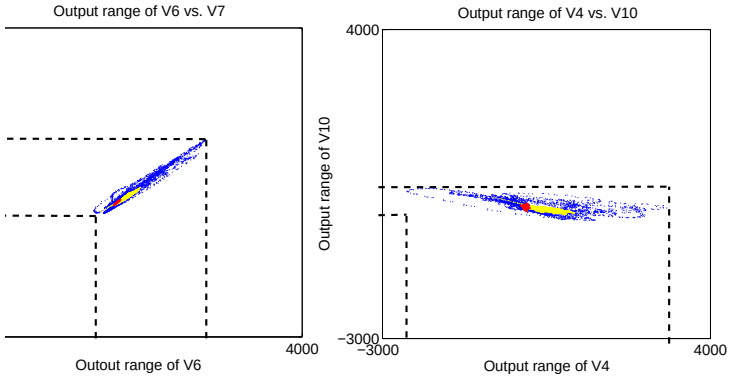

Figure 9.31: In the left subplot, the data points of V6 are plotted against the data points of V7 and in right subplot, the data points of V4 are plotted against the data points of V10. In the left subplot the output ratio is ? 1 and in the right subplot the output ratio is « 1. The colours indicate data points of P (red), QRS (blue) and T (yellow).

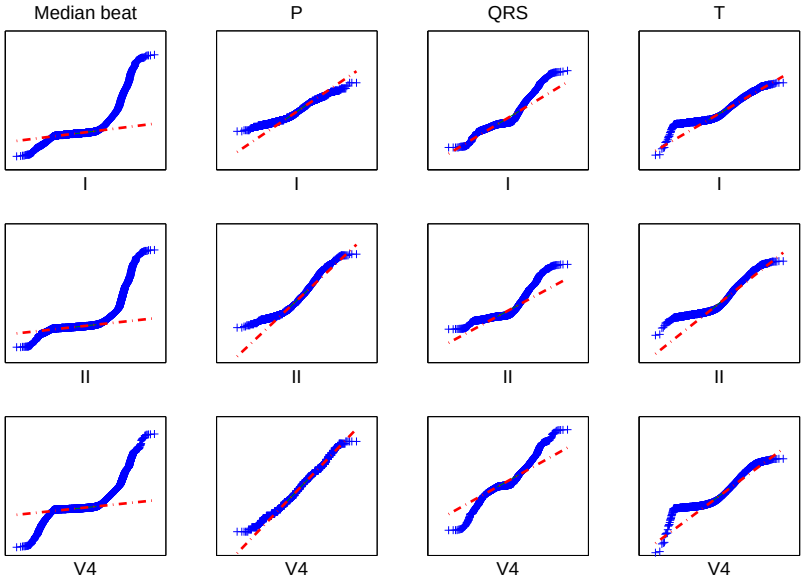

Figure 9.32: The figure shows the Q-Q plot of the standard leads; I, II and V4. First column shows the Q-Q plot of un-segmented ECG's. Columns 2-4 show the Q-Q plot of the three segments P, QRS and T, respectively.

greatest magnitude. In the determination of the posterior leads V10-V12, the absolute values of the SBC of leads I, V 5 and V 6 are of greatest magnitude.

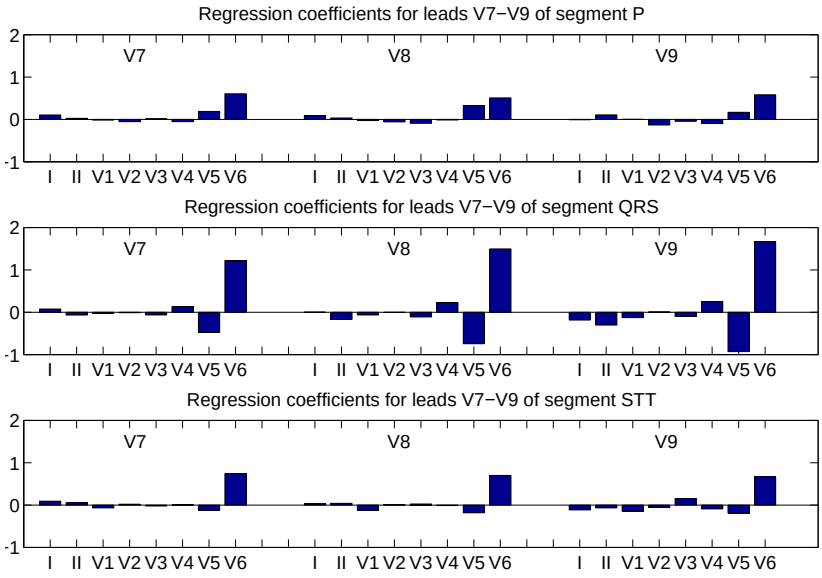

Figure 9.33: The figure shows the magnitude of the SBC of the partial regression models for leads V7-V9, plotted as bars.

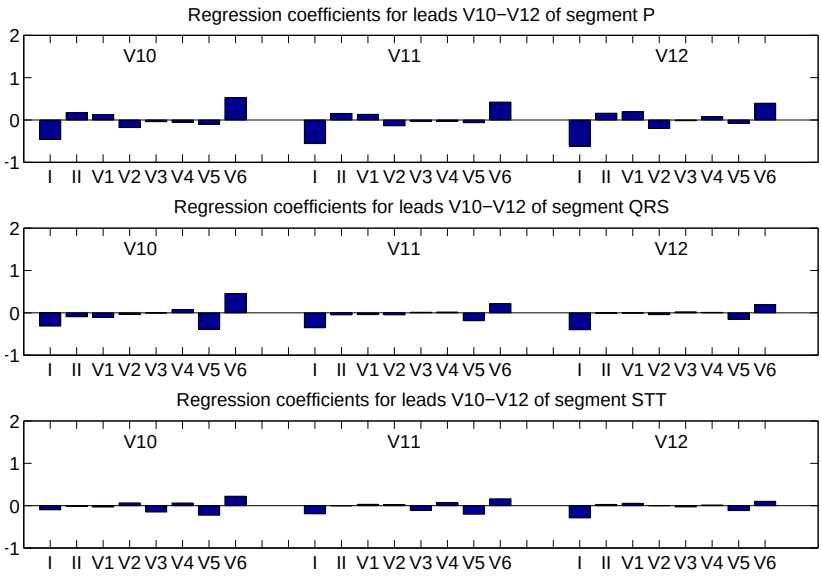

Figure 9.34: The figure shows the magnitude of the SBC of the partial regression models for leads V10-V12, plotted as bars.

9.14 Results of regression of the P-, QRS- and ST-T- segments

A graphical plot of the regression coefficients are shown in figure 9.35 and figure 9.36

The results of the segment wise regression do not differ form the regression

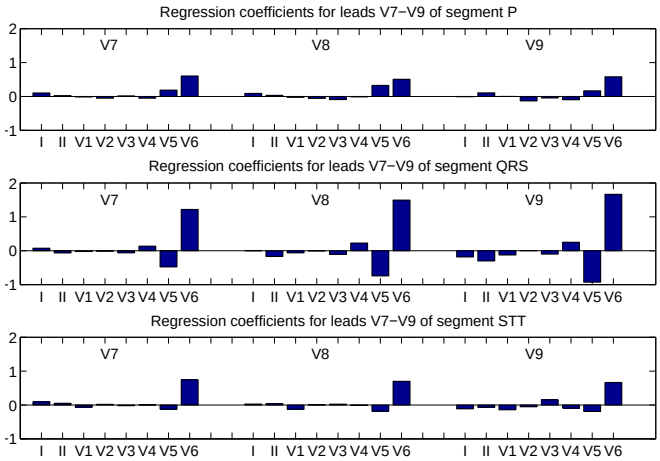

Figure 9.35: Figure shows the regression coefficients of the segments P, QRS and ST-T in the posterior leads V7-V9.

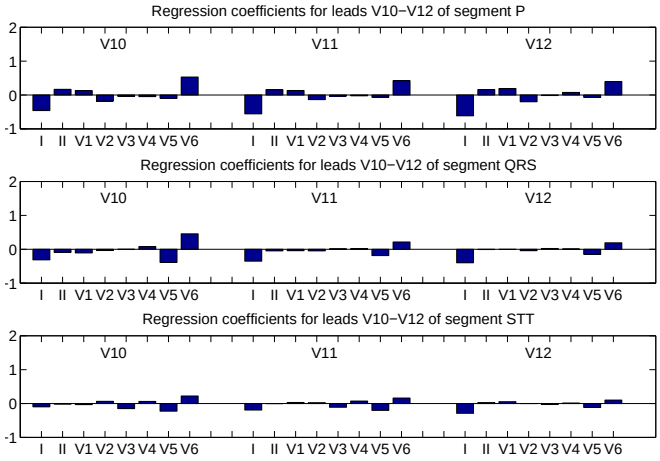

Figure 9.36: Figure shows the regression coefficients of the segments P, QRS and ST-T in the posterior leads V10-V12.

of the entire signal. The most dominating leads are still $V5$ and $V6$ in the posterior leads $V7$-$V9$ and in the posterior leads $V10$-$V12$ the dominating independent leads are I, $V5$ and $V6$.

	Pooled method		Average method	
Lead	**Median**	**(Interq. range)**	**Median**	**(Interq. range)**
V7	0.98	(1.00-0.95)	0.58	(0.97-0.19)
V8	0.96	(0.99-0.92)	0.52	(0.91-0.14)
V9	0.95	(0.99-0.91)	0.40	(0.75-0.05)
V10	0.81	(0.90-0.71)	0.32	(0.68-0.00)
V11	0.82	(0.92-0.73)	0.31	(0.66-0.00)
V12	0.85	(0.93-0.77)	0.30	(0.61-0.00)

Table 9.12: Coefficients of determination R^2 of the pooled and the average method.

		Pooled		Average		
Lead		**Median(Range)**		**Median(Range)**		***p*-value**
	P	-10.24	(-26.91-6.43)	-0.13	(-3.67-3.40)	$p < 0.05$
V7	**QRS**	-10.32	(-124.79-104.14)	-1.54	(-11.55-8.48)	$p < 0.05$
	T	-24.68	(-59.23-9.85)	-0.68	(-6.24-4.88)	$p < 0.05$
	P	-9.61	(-26.48-7.25)	-0.20	(-3.98-3.58)	$p < 0.05$
V8	**QRS**	-11.82	(-115.96-92.31)	-4.60	(-20.63-11.43)	$p < 0.05$
	T	-11.91	(-36.77-12.93)	-2.29	(-9.28-4.69)	$p < 0.05$
	P	-3.07	(-15.65-9.50)	-0.54	(-5.54-4.46)	$p < 0.05$
V9	**QRS**	-2.68	(-94.96-89.59)	-4.34	(-26.81-18.13)	$p < 0.05$
	T	8.59	(-7.66-24.85)	-5.44	(-15.49-4.59)	$p < 0.05$
	P	-10.24	(-21.79-1.30)	1.49	(-5.14-8.14)	$p < 0.05$
V10	**QRS**	-4.27	(-53.94-45.39)	-1.38	(-24.67-21.90)	$p < 0.05$
	T	-3.70	(-15.75-8.35)	-1.82	(-10.71-7.06)	$p < 0.05$
	P	-4.42	(-16.11-7.27)	1.43	(-4.67-7.54)	$p < 0.05$
V11	**QRS**	-0.52	(-33.22-32.17)	-3.03	(-20.74-14.68)	$p < 0.05$
	T	-1.47	(-13.26-10.30)	-0.47	(-8.25-7.31)	$p < 0.05$
	P	-2.96	(-15.96-10.03)	-2.68	(-3.97-7.28)	$p < 0.05$
V12	**QRS**	-1.12	(-28.82-26.56)	-2.75	(-16.53-11.16)	$p < 0.05$
	T	-4.09	(-15.88-7.69)	-0.14	(-7.16-7.46)	$p < 0.05$

Table 9.13: Residuals of the global model and the partial models.

Bibliography

[1] German Institute of Medical Documentation and Information and WHO. International statistical classification of diseases and related health problems 10th revisionversion for 2007. Internet, September 2007.

[2] Niels Holm-Nielsen (Editor). *Klinisk ordbog*, chapter *. Munksgaard, 11th edition, 2001.

[3] Tim Evans, Robert Beaglehole, Jim Kim, and Paulo Teixeira. *The world health report 2004*, chapter *. World Health Organization, UN, 2004.

[4] W D Rosamond, L E Chambless, A R Folsom, L S Cooper, D E Conwill, L Clegg, C H Wang, and G Heiss. Trends in the incidence of myocardial infarction and in mortality due to coronary heart disease, 1987 to 1994. *N Engl J Med*, 339(13):861–7, 1998.

[5] Ahmet Ergin, Paul Muntner, Roger Sherwin, and Jiang He. Secular trends in cardiovascular disease mortality, incidence, and case fatality rates in adults in the United States. *Am J Med*, 117(4):219–27, 2004.

[6] G Pérez, A Pena, J Sala, P Roset, R Masiá, J Marrugat, and the REGICOR Investigators. Acute myocardial infarction case fatality, incidence and mortality rates in a population registry in Gerona, Spain, 1990-1992. *Int. J. Epidemiol.*, 27(4):599–604, 1998.

[7] Miguel Gil, Helena Marti, Roberto Elosua, Maria Grau, Joan Sala, Rafael Masia, Gloria Perez, Pere Roset, Oscar Bielsa, Joan Vila, and Jaume Marrugat. [Analysis of trends in myocardial infarction case-fatality, incidence and mortality rates in Girona, Spain, 1990-1999]. *Rev Esp Cardiol*, 60(4):349–56, 2007.

[8] S Z Abildstrom, S Rasmussen, M Rosen, and M Madsen. Trends in incidence and case fatality rates of acute myocardial infarction in Denmark and Sweden. *Heart*, 89(5):507–511, 2003.

[9] M Rosen, L Alfredsson, N Hammar, T Kahan, C L Spetz, and A S Ysberg. Attack rate, mortality and case fatality for acute myocardial infarction in Sweden during 1987-95. Results from the national AMI register in Sweden. *J Intern Med*, 248(2):159–64, 2000.

[10] Kjell C Nikus, Markku J Eskola, Vesa K Virtanen, Jarkko Harju, Heini Huhtala, Jussi Mikkelsson, Pekka J Karhunen, and Kari O Niemela. Mortality of patients with acute coronary syndromes still remains high: a follow-up study of 1188 consecutive patients admitted to a university hospital. *Ann Med*, 39(1):63–71, 2007.

[11] Kaes Al-Anee, Ahmed Al-Ani, Magne Henriksen, Bjorn Arild Halvorsen, and Per Anton Sirnes. [Mortality after acute coronary syndrome]. *Tidsskr Nor Laegeforen*, 127(12):1628–30, 2007.

[12] C Sarti, D Rastenyte, Z Cepaitis, and J Tuomilehto. International trends in mortality from stroke, 1968 to 1994. *Stroke*, 31(7):1588–601, 2000.

[13] Michiaki Yoshida, Yoshikuni Kita, Yasuyuki Nakamura, Akihiko Nozaki, Akira Okayama, Hideki Sugihara, Takayuki Kasamatsu, Kunihiko Hirose, Masahiko Kinoshita, and Hirotsugu Ueshima. Incidence of acute myocardial infarction in Takashima, Shiga, Japan. *Circ J*, 69(4):404–8, 2005.

[14] Tunstall-Pedoe H, Kuulasmaa K, Tolonen H, Davidson M, and Mendis S with 64 other contributors for The WHO MONICA Project. *MONICA Monograph and Multimedia Sourcebook.*, chapter *. World Health Organization, UN, 2003.

[15] S Capewell, B M Livingston, K MacIntyre, J W Chalmers, J Boyd, A Finlayson, A Redpath, J P Pell, C J Evans, and J J McMurray. Trends in case-fatality in 117 718 patients admitted with acute myocardial infarction in Scotland. *Eur Heart J*, 21(22):1833–40, 2000.

[16] Soren Rasmussen, Steen Z Abildstrom, Mans Rosen, and Mette Madsen. Case-fatality rates for myocardial infarction declined in Denmark and Sweden during 1987-1999. *J Clin Epidemiol*, 57(6):638–46, 2004.

[17] P Buch, S Rasmussen, G H Gislason, J N Rasmussen, L Kober, N Gadsboll, S Stender, M Madsen, C Torp-Pedersen, and S Z Abildstrom. Temporal decline in the prognostic impact of a recurrent acute myocardial infarction 1985 to 2002. *Heart*, 93(2):210–5, 2007.

[18] J. Videbaek and M. Madsen (Editors). *Hjertestatistik 2004*, chapter *. Hjerteforeningen, 2004.

[19] M Osler, T I Sorensen, S Sorensen, K Rostgaard, G Jensen, L Iversen, T S Kristensen, and M Madsen. Trends in mortality, incidence and case fatality of ischaemic heart disease in Denmark, 1982-1992. *Int J Epidemiol*, 25(6):1154–61, 1996.

[20] J. Videbæk, S. Rasmussen, and M. Madsen (Editors). *Hjertestatistik for de nye regioner 2006*, chapter *. Hjerteforeningen, 2007.

[21] J L Y Liu, N Maniadakis, A Gray, and M Rayner. The economic burden of coronary heart disease in the UK. *Heart*, 88(6):597–603, 2002.

[22] Matthew J Taylor, Paul A Scuffham, Patrick L McCollam, and David E Newby. Acute coronary syndromes in Europe: 1-year costs and outcomes. *Curr Med Res Opin*, 23(3):495–503, 2007.

[23] Michael Dickson and Stéphane Jacobzone. *Pharmaceutical Use and Expenditure for Cardiovascular Disease and Stroke: A Study of 12 OECD Countries*, chapter *. OECD, 2003.

[24] F. Martini (Editor). *Fundamentals of anatomy and physiology*, chapter 20. Benjamin Cummings, 2004.

[25] R. A. Rhoadea and G. A Tanner (Editor). *Medical physiology*, chapter 10. Lippincott Williams & Wilkins, 2003.

[26] J. Malmivuo and R. Plonsey. *Bioelectromagnetism*, chapter 6. Oxford University Press, 1995.

[27] F. Martini (Editor). *Fundamentals of anatomy and physiology*, chapter 12. Benjamin Cummings, 2004.

[28] M. C. Kim, A. S. Kini, and V. Fuster. *Hurst's The Heart*, chapter 48. McGRAW-HILL, 11th edition, 2004.

[29] R. A. O'Rourke. *Hurst's The Heart*, chapter 51. McGRAW-HILL, 11th edition, 2004.

[30] R. Virmani and A. P. Burke. *Hurst's The Heart*, chapter 49. McGRAW-HILL, 11th edition, 2004.

[31] G. A. Lanza, S. Coli, D. Cianflone, and A. Maseri. *Hurst's The Heart*, chapter 46. McGRAW-HILL, 11th edition, 2004.

[32] J. R. Hampton. *The ECG made easy*, chapter *. Churchill Livingstone, 6'st edition, 2003.

[33] R. Wayne Alexander, Craig M. Pratt, Thomas J. Ryan, and Robert Roberts. *Hurst's The Heart*, chapter 52. McGRAW-HILL, 11th edition, 2004.

[34] R Roberts, K S Gowda, P A Ludbrook, and B E Sobel. Specificity of elevated serum MB creatine phosphokinase activity in the diagnosis of acute myocardial infarction. *Am J Cardiol*, 36(4):433–7, 1975.

[35] Y Ishikawa, J E Saffitz, T L Mealman, A M Grace, and R Roberts. Reversible myocardial ischemic injury is not associated with increased creatine kinase activity in plasma. *Clin Chem*, 43(3):467–75, 1997.

[36] E M Antman, M J Tanasijevic, B Thompson, M Schactman, C H McCabe, C P Cannon, G A Fischer, A Y Fung, C Thompson, D Wybenga, and E Braunwald. Cardiac-specific troponin I levels to predict the risk of mortality in patients with acute coronary syndromes. *N Engl J Med*, 335(18):1342–9, 1996.

[37] W. L. Duvall, D. A. Vorchheimer, and V. Fuster. *Hurst's The Heart*, chapter 54. McGRAW-HILL, 11th edition, 2004.

[38] J. S. Douglas and S. B. King III. *Hurst's The Heart*, chapter 55. McGRAW-HILL, 11th edition, 2004.

[39] B. W. Lytle. *Hurst's The Heart*, chapter 58. McGRAW-HILL, 11th edition, 2004.

[40] J. Malmivuo and R. Plonsey. *Bioelectromagnetism*, chapter 15. Oxford University Press, 1995.

[41] J. Boutkan. *Vectorcardiography, physical bases and clinical practice*, chapter *. Centrex publishing company, Eindhoven, 1965.

[42] T. C. Chou, R. A. Helm, and S. Kaplan. *Clinical Vectorcardiography*, chapter *. Grune & Stratton, 1974.

[43] G E Dower, H B Machado, and J A Osborne. On deriving the electrocardiogram from vectoradiographic leads. *Clin Cardiol*, 3(2):87–95, 1980.

[44] Anton P. Gorgles, Domien J. Engelen, and Hein J. J. Wellens. *Hurst's The Heart*, chapter 53. McGRAW-HILL, 11th edition, 2004.

[45] *. Guidelines 2000 for Cardiopulmonary Resuscitation and Emergency Cardiovascular Care. Part 7: the era of reperfusion: section 1: acute coronary syndromes (acute myocardial infarction). The American Heart Association in collaboration with the International Liaison Committee on Resuscitation. *Circulation*, 102(8 Suppl):I172–203, 2000.

[46] Antman EM, Anbe DT, Armstrong PW, Bates ER, Green LA, Hand M, Hochman JS, Krumholz HM, Kushner FG, Lamas GA, Mullany CJ, Ornato JP, Pearle DL, Sloan MA, and Smith SC Jr. Acc/aha guidelines for the management ĺ 2004 by the american college of cardiology foundation and the american heart association, inc. of patients with st-elevation myocardial infarction: a report of the american college

of cardiology/american heart association task force on practice guidelines (committee to revise the 1999 guidelines for the management of patients with acute myocardial infarction). *Available at www.acc.org/clinical/guidelines/stemi/index.pdf.*, 2004.

[47] Todd J Crocco, Michael R Sayre, and Tom P Aufderheide. Prehospital triage of chest pain patients. *Prehosp Emerg Care*, 6(2):224–8, 2002.

[48] M Whitbread, V Leah, T Bell, and T J Coats. Recognition of ST elevation by paramedics. *Emerg Med J*, 19(1):66–7, 2002.

[49] D B Foster, J H Dufendach, C M Barkdoll, and B K Mitchell. Prehospital recognition of AMI using independent nurse/paramedic 12-lead ECG evaluation: impact on in-hospital times to thrombolysis in a rural community hospital. *Am J Emerg Med*, 12(1):25–31, 1994.

[50] Jan Kyst Madsen. Hjerteanfald- blodprop i hjertet. only in danish! *Dit laegemagasin*, 12(2):22–25, 2005.

[51] P Grim, T Feldman, M Martin, R Donovan, V Nevins, and R W Childers. Cellular telephone transmission of 12-lead electrocardiograms from ambulance to hospital. *Am J Cardiol*, 60(8):715–20, 1987.

[52] J P Ioannidis, D Salem, P W Chew, and J Lau. Accuracy and clinical effect of out-of-hospital electrocardiography in the diagnosis of acute cardiac ischemia: a meta-analysis. *Ann Emerg Med*, 37(5):461–70, 2001.

[53] J Lau, J P Ioannidis, E M Balk, C Milch, N Terrin, P W Chew, and D Salem. Diagnosing acute cardiac ischemia in the emergency department: a systematic review of the accuracy and clinical effect of current technologies. *Ann Emerg Med*, 37(5):453–60, 2001.

[54] *. Emergency department: rapid identification and treatment of patients with acute myocardial infarction. National Heart Attack Alert Program Coordinating Committee, 60 Minutes to Treatment Working Group. *Ann Emerg Med*, 23(2):311–29, 1994.

[55] S Johnston, R Brightwell, and M Ziman. Paramedics and pre-hospital management of acute myocardial infarction: diagnosis and reperfusion. *Emerg Med J*, 23(5):331–4, 2006.

[56] David G Strauss, Paula Quintal Sprague, Kevin Underhill, Charles Maynard, George L Adams, Amy Kessenich, Michael H Jr Sketch, Peter B Berger, David Marcozzi, Christopher B Granger, and Galen S Wagner. Paramedic transtelephonic communication to cardiologist of clinical and electrocardiographic assessment for rapid reperfusion of ST-elevation myocardial infarction. *J Electrocardiol*, 40(3):265–70, 2007.

[57] Brian W Gross, Kent W Dauterman, Mark G Moran, Todd S Kotler, Stephen J Schnugg, Paul S Rostykus, Amy M Ross, and W Douglas Weaver. An approach to shorten time to infarct artery patency in patients with ST-segment elevation myocardial infarction. *Am J Cardiol*, 99(10):1360–3, 2007.

[58] E Boersma, A C Maas, J W Deckers, and M L Simoons. Early thrombolytic treatment in acute myocardial infarction: reappraisal of the golden hour. *Lancet*, 348(9030):771–5, 1996.

[59] Giuseppe De Luca, Harry Suryapranata, Jan Paul Ottervanger, and Elliott M Antman. Time delay to treatment and mortality in primary angioplasty for acute myocardial infarction: every minute of delay counts. *Circulation*, 109(10):1223–5, 2004.

[60] Paul W. Armstrong, Desire Collen, and Elliott Antman. Fibrinolysis for Acute Myocardial Infarction: The Future Is Here and Now. *Circulation*, 107(20):2533–2537, 2003.

[61] Joel Xue, Tom Aufderheide, R Scott Wright, John Klein, Robert Farrell, Ian Rowlandson, and Brian Young. Added value of new acute coronary syndrome computer algorithm for interpretation of prehospital electrocardiograms. *J Electrocardiol*, 37 Suppl(NIL):233–9, 2004.

[62] Kai M Eggers, Johan Ellenius, Mikael Dellborg, Torgny Groth, Jonas Oldgren, Eva Swahn, and Bertil Lindahl. Artificial neural network algorithms for early diagnosis of acute myocardial infarction and prediction of infarct size in chest pain patients. *Int J Cardiol*, 114(3):366–74, 2007.

[63] Thomas D Sequist, David W Bates, E Francis Cook, Steven Lampert, Mary Schaefer, Jenny Wright, Luke Sato, and Thomas H Lee. Prediction of missed myocardial infarction among symptomatic outpatients without coronary heart disease. *Am Heart J*, 149(1):74–81, 2005.

[64] R L Kennedy, A M Burton, H S Fraser, L N McStay, and R F Harrison. Early diagnosis of acute myocardial infarction using clinical and electrocardiographic data at presentation: derivation and evaluation of logistic regression models. *Eur Heart J*, 17(8):1181–91, 1996.

[65] Colum Owens, Cesar Navarro, Anthony McClelland, John Riddell, Omar Escalona, John McC Anderson, and Jennifer Adgey. Improved detection of acute myocardial infarction using a diagnostic algorithm based on calculated epicardial potentials. *Int J Cardiol*, 111(2):292–301, 2006.

[66] I B Menown, R S Patterson, G MacKenzie, and A A Adgey. Body-surface map models for early diagnosis of acute myocardial infarction. *J Electrocardiol*, 31 Suppl(NIL):180–8, 1998.

[67] Cesar Navarro, Colum Owens, John Riddell, Anthony McClelland, John McC Anderson, Omar Escalona, Colin Turner, and Jennifer Adgey. The use of calculated epicardial potentials improves significantly the sensitivity of a diagnostic algorithm in the detection of acute myocardial infarction. *J Electrocardiol*, 36 Suppl(NIL):127–32, 2003.

[68] Anthony J J McClelland, Colum G Owens, Ian B A Menown, Mark Lown, and A A Jennifer Adgey. Comparison of the 80-lead body surface map to physician and to 12-lead electrocardiogram in detection of acute myocardial infarction. *Am J Cardiol*, 92(3):252–7, 2003.

[69] R E Casas, H J Marriott, and D L Glancy. Value of leads V7-V9 in diagnosing posterior wall acute myocardial infarction and other causes of tall R waves in V1-V2. *Am J Cardiol*, 80(4):508–9, 1997.

[70] R F Veldkamp, S Sawchak, J E Pope, R M Califf, and M W Krucoff. Performance of an automated real-time ST-segment analysis program to detect coronary occlusion and reperfusion. *J Electrocardiol*, 29(4):257–63, 1996.

[71] R F Veldkamp, J R Bengtson, S T Sawchak, J E Pope, J R Mertens, D W Mortara, R M Califf, and M W Krucoff. Evolution of an automated ST-segment analysis program for dynamic real-time, noninvasive detection of coronary occlusion and reperfusion. *J Electrocardiol*, 25 Suppl(NIL):182–7, 1992.

[72] Miquel Fiol, Iwona Cygankiewicz, Andres Carrillo, Antoni Bayes-Genis, Omar Santoyo, Alfredo Gomez, Armando Bethencourt, and Antoni Bayes de Luna. Value of electrocardiographic algorithm based on "ups and downs" of ST in assessment of a culprit artery in evolving inferior wall acute myocardial infarction. *Am J Cardiol*, 94(6):709–14, 2004.

[73] Gunter Lehmann, Claus Schmitt, Victoria Kehl, Sebastian Schmieder, and Albert Schomig. Electrocardiographic algorithm for assignment of occluded vessel in acute myocardial infarction. *International Journal of Cardiology*, 89(1):79–85, 2003.

[74] Domien J. Engelen, Anton P. Gorgels, Emile C. Cheriex, Ebo D. De Muinck, Anton J. Oude Ophuis, Willem R. Dassen, Jindra Vainer, Vincent G. van Ommen, and Hein J. Wellens. Value of the electrocardiogram in localizing the occlusion site in the left anterior descending coronary artery in acute anterior myocardial infarction. *Journal of the American College of Cardiology*, 34(2):389–395, 1999.

[75] S Matetzky, D Freimark, M S Feinberg, I Novikov, S Rath, B Rabinowitz, E Kaplinsky, and H Hod. Acute myocardial infarction with

isolated ST-segment elevation in posterior chest leads V7-9: "hidden" ST-segment elevations revealing acute posterior infarction. *J Am Coll Cardiol*, 34(3):748–53, 1999.

[76] Shlomi Matetzky, Dov Freimarkm, Pierre Chouraqui, Babeth Rabinowitz, Shmuel Rath, Elieser Kaplinsky, and Hanoch Hod. Significance of st segment elevations in posterior chest leads (v7 to v9) in patients with acute inferior myocardial infarction: Application for thrombolytic therapy. *Journal of the American College of Cardiology*, 31(3):506–511, 1998.

[77] Yochai Birnbaum, Galen S. Wagner, Gabriel I. Barbash, Kathy Gates, Douglas A. Criger, Samuel Sclarovsky, Robert J. Siegel, Christopher B. Granger, Jonathan S. Reiner, and Allan M. Ross. Correlation of angiographic findings and right (v1 to v3) versus left (v4 to v6) precordial st-segment depression in inferior wall acute myocardial infarction. *The American Journal of Cardiology*, 83(2):143–148, 1999.

[78] Abid R. Assali, Samuel Sclarovsky, Itzhak Herz, Yehuda Adler, Avital Porter, Alejandro Solodky, and Boris Strasberg. Comparison of patients with inferior wall acute myocardial infarction with versus without st-segment elevation in leads v5 and v6. *The American Journal of Cardiology*, 81(1):81–83, 1998.

[79] Michael C. Kontos, MD, MD Pratik V. Desai, MD Robert L. Jesse, and MD Joseph P. Ornato. Usefulness of the admission electrocardiogram for identifying the infarct-related artery in inferior wall acute myocardial infarction. *The American Journal of Cardiology*, 79(2):182–184, 1997.

[80] M W Rich, M Imburgia, T R King, K C Fischer, and K L Kovach. Electrocardiographic diagnosis of remote posterior wall myocardial infarction using unipolar posterior lead V9. *Chest*, 96(3):489–93, 1989.

[81] Kian-Keong Poh, Boon-Lock Chia, Huay-Cheem Tan, Tiong-Cheng Yeo, and Yean-Teng Lim. Absence of st elevation in ecg leads v7, v8, v9 in ischaemia of non-occlusive aetiologies. *International Journal of Cardiology*, 97(3):389–392, 2004.

[82] J B Agarwal, K Khaw, F Aurignac, and A LoCurto. Importance of posterior chest leads in patients with suspected myocardial infarction, but nondiagnostic, routine 12-lead electrocardiogram. *Am J Cardiol*, 83(3):323–6, 1999.

[83] L J Melendez, D T Jones, and J R Salcedo. Usefulness of three additional electrocardiographic chest leads (V7, V8, and V9) in the diagnosis of acute myocardial infarction. *Can Med Assoc J*, 119(7):745–8, 1978.

[84] A U Kulkarni, R Brown, M Ayoubi, and V S Banka. Clinical use of posterior electrocardiographic leads: a prospective electrocardiographic analysis during coronary occlusion. *Am Heart J*, 131(4):736–41, 1996.

[85] Shu-Fen Wung and David Y. Kahn. A quantitative evaluation of st-segment changes on the 18-lead electrocardiogram during acute coronary occlusions. *Journal of Electrocardiology*, 39(3):275–281, 2006.

[86] MA Robert J. Zalenski MD, Robert J. Rydman PhD, MPH Edward P. Sloan MD, Kenneth H. Hahn MD, MPH David Cooke MD, Joanne Fagan RN, Denise J. Fligner MD, William Hessions MD, David Justis MD, RRA Linda M. Kampe BS, Shirish Shah MD, John Tucker MD, and Diane Zwicke MD. Value of posterior and right ventricular leads in comparison to the standard 12-lead electrocardiogram in evaluation of st-segment elevation in suspected acute myocardial infarction. *The American Journal of Cardiology*, 79(12):1579–1585, 1997.

[87] J. Malmivuo and R. Plonsey. *Bioelectromagnetism*, chapter 7. Oxford University Press, 1995.

[88] S. M. Ross. *Probability and statistics for engineers and scientists*, chapter 9. Elsevier, 2004.

[89] K. S. Shanmugan. *Random signals*, chapter 7. Wiley, 1998.

[90] Kartheeban Nagenthiraja. Linear model for predicting the posterior ecg leads v7-v12 in healthy subjects: Part 1. Master's thesis, Department of Health Science and Technology, Aalborg University, 2007.

[91] P Schweitzer. The electrocardiographic diagnosis of acute myocardial infarction in the thrombolytic era. *Am Heart J*, 119(3 Pt 1):642–54, 1990.

[92] H Blanke, M Cohen, G U Schlueter, K R Karsch, and K P Rentrop. Electrocardiographic and coronary arteriographic correlations during acute myocardial infarction. *Am J Cardiol*, 54(3):249–55, 1984.

[93] C H Croft, W Woodward, P Nicod, J R Corbett, S E Lewis, J T Willerson, and R E Rude. Clinical implications of anterior S-T segment depression in patients with acute inferior myocardial infarction. *Am J Cardiol*, 50(3):428–36, 1982.

[94] R S Gibson, R S Crampton, D D Watson, G J Taylor, B A Carabello, N D Holt, and G A Beller. Precordial ST-segment depression during acute inferior myocardial infarction: clinical, scintigraphic and angiographic correlations. *Circulation*, 66(4):732–41, 1982.

[95] M A Hlatky, R M Califf, K L Lee, D B Pryor, G S Wagner, and R A Rosati. Prognostic significance of precordial ST-segment depression during inferior acute myocardial infarction. *Am J Cardiol*, 55(4):325–9, 1985.

[96] R J Zalenski, D Cooke, R Rydman, E P Sloan, and D G Murphy. Assessing the diagnostic value of an ECG containing leads V4R, V8, and V9: the 15-lead ECG. *Ann Emerg Med*, 22(5):786–93, 1993.

[97] Michael P Somers, William J Brady, Devin C Bateman, Amal Mattu, and Andrew D Perron. Additional electrocardiographic leads in the ED chest pain patient: right ventricular and posterior leads. *Am J Emerg Med*, 21(7):563–73, 2003.

[98] C. J. Therkelsen. Personal communication with a cardiologist, October 2007.

[99] C L Levkov. Orthogonal electrocardiogram derived from the limb and chest electrodes of the conventional 12-lead system. *Med Biol Eng Comput*, 25(2):155–64, 1987.